A p53 score derived from TP53 CRISPR/Cas9 HMCLs predicts survival and reveals major role of BAX in BH3 mimetics response

Romane Durand, Géraldine Descamps, Christelle Dousset, Céline Bellanger, Sophie Maïga, Jean-Baptiste Alberge, Jennifer Derrien, Jonathan Cruard, Stéphane Minvielle, Nicoletta Libera Lilli, et al.

A p53 score derived from *TP53* CRISPR/Cas9 HMCLs predicts survival and reveals major role of BAX in BH3 mimetics response

Romane Durand[1,2], Géraldine Descamps[1,2]*, Céline Bellanger [1,2]*, Christelle Dousset[2,3]*, Sophie Maïga[2,3]*, Jean-Baptiste Alberge[1,2], Jennifer Derrien[1,2], Jonathan Cruard[1,2], Stéphane Minvielle[1,2], Nicoletta Libera Lilli[4], Catherine Godon[4], Yannick Le Bris[3], Benoit Tessoulin[2,3], Martine Amiot[1,2], Patricia Gomez-Bougie[2,3], Cyrille Touzeau[2,3], Philippe Moreau[2,3], David Chiron[1,2], Agnès Moreau-Aubry[1,2], Catherine Pellat-Deceunynck[1,2]

[1] Nantes Université, CNRS, INSERM, CRCI[2]NA, F-44000 Nantes, France.
[2] SIRIC ILIAD
[3] Nantes Université, CHU de Nantes, CNRS, INSERM, CRCI[2]NA, F-44000 Nantes, France.
[4] CHU de Nantes, F-44000 Nantes, France

*** Equal contributions**

Correspondence: Catherine Pellat-Deceunynck
Centre de Recherches en Cancérologie et Immunologie Intégré Nantes Angers, INSERM, CNRS, IRS-UN, 8, quai Moncousu, Nantes, BP70721 F-44007 France. Ph 33 2 28 08 02 98
catherine.pellat-deceunynck@univ-nantes.fr

Key words: *TP53*, *BAX*, p53 score, BH3 mimetic, scRNASeq

Running title

p53-dependent BAX governs response to BH3 mimetics

Counts

Abstract: 249 words

Text: 4357 words

Figures: 6

Tables: 2

References: 45

Supplemental Figures: 12

Supplemental Tables: 10

Key points:

a functional p53 score identifies cells with biallelic *TP53* invalidation and predicts survival in myeloma

p53-regulated BAX, but not BAK, expression governs the death response to MCL1 BH3 mimetic

Abstract

To establish a strict p53-dependent gene expression profile, p53 negative clones were derived from *TP53*$^{+/+}$ and *TP53*$^{-/mut}$ t(4;14) human myeloma cell lines (HMCLs) using CRISPR/Cas9 technology. From the 17 dysregulated genes shared between the 6 clones from the two *TP53*$^{+/+}$ myeloma cell lines, we established a functional p53 score, involving 13 genes specifically downregulated on p53 silencing. This functional score segregated clones and myeloma cell lines, as well as other cancer cell lines according to their *TP53* status. The score was efficient to identify myeloma patient samples with biallelic *TP53* inactivation and was predictive of overall survival in MMRF-coMMpass and CASSIOPEA cohorts. At the functional level, we showed that among the 13 genes, p53-regulated BAX expression correlated to, and directly impacted, the MCL1 BH3 mimetic S63845 sensitivity of myeloma cells by decreasing MCL1-BAX complexes. Resistance to S63845 was however overcome by combining MCL1 and BCL2 BH3 mimetic which displayed synergistic efficacy. BH3 mimetic combination was efficient in 97% of patient samples with or without del17p. Nevertheless, scRNAseq analysis showed that myeloma cells surviving to the combination had lower p53 score, confirming that myeloma cells with higher p53 score were more sensitive to BH3 mimetics. Taken together, we established a functional p53 score that identifies myeloma cells with biallelic *TP53* invalidation, demonstrated that p53-regulated BAX is critical for optimal cell response to BH3 mimetics, and showed that BH3 mimetic combination is efficient in vitro for patients with biallelic *TP53* invalidation, for whom there is still an unmet medical need.

Introduction

Over the last decade, significant progress has been made in the treatment of patients with Multiple Myeloma (MM) mainly thanks to the introduction of antibody or cell-based therapies[1–5]. Although most patients have an excellent response to treatment, patients with known high-risk features, like del17p or 1q gain, still have an insufficient response rate[6–8]. These chromosomal abnormalities involve at least two genes renowned in cancer resistance, respectively *TP53* and *MCL1*. Loss of p53 function induced by gene deletion and/or mutation is not directly druggable, although it induces targetable neo- vulnerabilities like viral permissiveness or loss of cell cycle control[9,10]. In contrast, 1q gain induces overexpression of MCL1 that can be targeted with MCL1-specific BH3 mimetics[11,12]. The role of p53 loss of function in cancer initiation/development is related to genome guardianship, as the silencing of p53 target genes involved in cell death or cell cycle does not recapitulate p53 loss, contrary to silencing genes involved in DNA repair and integrity[13]. In MM, hits in *TP53* are not primary events compared to 14q32 translocations, but they greatly impair PFS and OS[14,15]. This reduced response rate to treatment is instead thought to be related to resistance to tumor death and the loss of cell cycle control. The most frequent hit is monoallelic chromosomal deletion, although biallelic hits are more frequent in very advanced disease like secondary plasma cell leukemia. Moreover, whole genome sequencing of about 400 patients recently identified *TP53* biallelic losses in relapsed/refractory patients emphasizing that complete p53 inactivation plays a major role in resistance to treatment[16]. Loss of p53 or mutant-p53 expression might differently impair gene- expression profiling allowing “de novo” expression of genes not directly transactivated by p53[17,18]. To assess the direct and specific impact of p53 loss of expression on transcriptome in myeloma cells expressing wildtype p53 protein, we used CRISPR/Cas9 technology to silence p53 in myeloma cell lines having a homogeneous myeloma genomic background: we selected cell lines with t(4;14) translocation, another high-risk hallmark in myeloma.

Materials and Methods

Human myeloma cell lines (HMCLs) and patient samples

Samples from patients with MM came from the MYRACLE cohort (NCT03807128)[19]. Isolation of mononuclear cells, myeloma cells, assessment of chromosomal 1q gain or 17p loss, cDNA *TP53*-sequencing and characterization of human myeloma cell lines (HMCLs) was reported previously[12,20–23].

Generation of CRISPR/cas9 clones

NCI-H929, XG7, NAN3 and JIM3 HMCLs were stably transduced with lentivirus expressing mCherry-Cas9 (FUCas9Cherry gifted from Marco Herold-Addgene plasmid # 70182), prior to second infection with lentivirus containing *GFP* and doxycycline-inducible sgRNA (FgH1tUTG gifted from Marco Herold-Addgene plasmid # 70183). The sgRNA sequences were (5'-AGATGGCCATGGCGCGGACG(CGG)-3' for *TP53*, (5'-GCCATGCTGGTAGACGTGTA-3') for *BAK1*, and (5'- AGTAGAAAAGGGCGACAACC-3') for *BAX*[24]. GFP positive cells were sorted, sgRNA expression was induced with doxycycline and cells were cloned (0.3 cell/well). Control cells and clones were obtained from $mCherry^{+}GFP^{+}$ cells (containing sg*TP53*) not treated with doxycycline. To increase proportion of $TP53^{-/-}$ clones, mCherry+GFP+ NCI-H929 and XG7 were additionally treated 48h with Nutlin3a (10μM) prior to cloning. $TP53^{-/-}$, $BAK1^{-/-}$ or $BAX^{-/-}$ clones were selected based on the lack of protein expression and gene sequencing.

Cell death and BH3 profiling assays

Cell death was assessed by Annexin V staining (HMCLs) or loss of CD138 staining (patient samples) using flow cytometry[12,20,25]. BH3 profiling was performed as previously reported[26].

RNAseq and scRNAseq

Genomic profiling of HMCLs, clones or purified myeloma cells was determined with RNA sequencing (3'-Digital gene expression sequencing, DGE-Seq, GSE245163). For scRNASeq, MM bone marrow mononuclear cells were cultured overnight in RPMI1640, containing 7%FCS and 3 ng/ml IL6, with or without a combination of BH3 mimetics prior to scRNASeq analysis (10X, Chromium), as described in supplemental methods. Bulk RNA-seq, DGE-Seq or GEP p53 score was calculated via a rank-based gene set scoring method with the singscore package in R[27]. scRNASeq p53 score was calculated using the AddModuleScore function of Seurat package in R.

Additional materials and methods are detailed in the supplemental Materials and Methods section

Results

Silencing *TP53* identifies shared p53-regulated genes that provide a functional p53 score

To assess direct p53 impact in myeloma cells, $TP53^{-/-}$ cells were derived after CRISPR/Cas9 genome editing from t(4;14) HMCL, 2 $TP53^{+/+}$ NCI-H929 and XG7 and 2 $TP53^{-/mut}$ JIM3 $TP53^{-/R273C}$ and NAN3 $TP53^{-/R248Q}$). Three $TP53^{-/-}$ clones ($TP53^{-/-}$#1,2,3) were selected for each cell line and their expression profiling was compared to control cells ($mCherry^{+}GFP^{+}$ $TP53^{+/+}$ or $TP53^{-/mut}$ bulk cells) and/or control clones ($TP53^{+/+}$#1,2,3 or $TP53^{-/mut}$#1,2,3, Figure 1A, Table S1). Including *TP53*, 83 and 77 genes were differentially expressed between $TP53^{+/+}$ and $TP53^{-/-}$ cells in NCI-H929 and XG7, respectively (FDR<0.05, Table S2): 58% and 68% of these genes have been characterized elsewhere as p53-regulated genes[28] i.e., early-direct, late p53 targets, with or without proximal p53 binding, or translational, in response to nutlin3a in cell lines[29], Figure 1B. Several genes were differentially expressed between $TP53^{-/mut}$ and $TP53^{-/-}$ cells, but none, excepting *TP53* itself, was shared between the HMCLs. We next focused on the genes whose regulation was shared between the two $TP53^{+/+}$ HMCLs: 16 genes (including *TP53)* were downregulated in $TP53^{-/-}$ clones and 1 was upregulated, Table S2, Figure S1. We selected 13 genes with decreased expression in $TP53^{-/-}$ clones and known as "early direct" for creating a functional p53 score (Figure 1C, Table S3)[29]. Notably, only five of these genes were found differentially expressed between 16 $TP53^{wt}$ and 27 $TP53^{abnormal}$ HMCLs using microarray profiling (Table S2). The 13 genes are located on 12 different chromosome arms, excluding direct impact of myeloma-recurrent chromosomal abnormalities on expression (Table S3). The score discriminated $TP53^{-/-}$ and $TP53^{+/+}$ clones from NCI-H929 and XG7 but not $TP53^{-/-}$ and $TP53^{-/mut}$ cells from JIM3 and NAN3 (Figure 1D left panel). We also characterized the genes differentially expressed between $TP53^{+/+}$ and $TP53^{-/-}$ clones after nutlin3a treatment: excluding genes with Nutlin3a-induced modification of expression in $TP53^{-/-}$ clones (i.e., MDM2-dependent and p53-independent regulation), 825 genes (397 up, 428 down in $TP53^{+/+}$ versus $TP53^{-/-}$ cells) were commonly regulated in NCI-H929 and XG7, including the 16 downregulated genes (Figure S1 and Table S4). As expected, nutlin3a increased p53 score only in $TP53^{+/+}$ clones (Figure 1D, right panel). The score did not discriminate 8 HMCLs expressing a mutated p53 protein from 4 expressing no p53 protein, underscoring that it identifies p53 loss-of-function whatever its origin (Figure 1E). In HMCLs profiled using microarray, the score segregated 16 $TP53^{wt}$ from 27 $TP53^{abnormal}$ HMCLs ($p<0.0001$), whatever their myeloma-specific 14q32 translocation background (Figure S2A-B, Table S5). Moreover, in 1,105 cancer cell lines, the score was significantly associated with *TP53* deletion, mutation or both (Figure 1F left panel), cell lines with biallelic hits having the lowest score (Figure 1F right panel, Table S6), whatever the cell ontology and the gender (Figure S2C-D, Table S6).

The 13-gene functional p53 score is prognostic for myeloma patients' survival

In 38 samples from MYRACLE patients characterized for both del17p (FISH) and *TP53* mutation (Sanger sequencing), the p53 score significantly discriminated samples with del17p and *TP53* mutation (n=7) from samples without *TP53* hit (n=25, p=0.0009, Figure 2A, Table 1). Since *TP53* hits are known to impair overall survival[7], the p53 score was calculated in two cohorts of patients at diagnosis, with RNAseq expression at baseline and overall survival, with 139 patients from the CASSIOPEA trial and 764 from the MMRF-CoMMpass cohort (https://themmrf.org)[30]. In both cohorts, K-means method segregated patient samples into 4 groups (Figure S3A-B left panels). Overall survival analysis showed that the groups 1 with the lowest values (n=8 and 24 for CASSIOPEA and MMRF-CoMMpass, respectively) had significantly reduced overall survival, p=0.0138 and p=0.015, Figure 2B-C left panel. In CASSIOPEA patients, group 1 patients contained 75% of patients classified as high risk (HR) and 62.5% patients with del17p, respectively (Figure 2B middle and right panels): group 1, HR and del17p patients have all significant reduced overall survival (Figure S3A).

In the MMRF-CoMMpass cohort, *TP53* mutation and 17p deletion were available for 684 patients: 19 displayed deletion and mutation, 34 deletion and 5 mutation (deletion or mutation was considered when LOH or VAF was inferior to -0.5 or superior to 0.3, respectively). Samples with del17p and mutation had the lowest score ($p<0.0001$) and a lower score than samples with only del17p (p=0.0002, Figure 2C, middle panel). Noteworthy, 90% of samples with biallelic hit were in groups 1 (53%) and 2 (37%) while samples with del17p only were more equally distributed among the 4 groups (p=0.003, Figure S3B middle panel). Samples with *TP53* hit(s) constituted 74% of group 1 and only 5% to 10% of groups 2,3 and 4 (Figure S3B right panel). Patients with *TP53* mutation and del17p, and not with del17p only, had lower overall survival, the median was 870 days versus not reached in the other groups (Figure 2C right panel, p=0.004).

These results collectively showed that this score identified samples with double hit in *TP53* and provided prognosis in two independent cohorts. We further compared this score to another p53 functional score, used for the clinical interpretation of germline *TP53* variants in Li-Fraumeni syndrome, that assesses the increased expression of 10 p53 target genes (none shared with our 13-gene score, Figure S4) in doxorubicin-treated PBMCs. This score did not distinguish XG7 or NCI-H929 $TP53^{-/-}$ clones from $TP53^{+/+}$ clones in the absence of nutlin3a (Figure S5A-B). It also didn't segregate cell lines or patient samples according to their *TP53* status (Figure S5C-D).

_TP53_-silencing impairs mitochondrial MCL1 priming

As expected, p53-silencing in $TP53^{+/+}$ cells, but not in $TP53^{-/mut}$ cells, increased resistance to melphalan (LD_{50} values increased from 11.3 to 16.6 μM, p=0.0011 and from 18.7 to 28.3 μM, p=0.004 in NCI-H929 and XG7, respectively), and to nutlin3a (LD_{50} values were around 2 μM in $TP53^{+/+}$ clones, while no cell death was induced at 10 μM in $TP53^{-/-}$ clones), Table S7 [31,32]. The 13 genes involved in the p53 score

are known to be involved in the cell cycle, DNA duplication and repair (*CDKN1A*, *DDB2*, *RRM2B*), defense against viruses or ROS (*APOBEC3C, APOBEC3H*, *RPS27L*, *TIGAR*), apoptosis and mitochondrial metabolism (*BAX*, *TNFRSF10B*, *FDXR*), signaling pathways (*PHLDA3*, *EDA2R*), and in p53 regulation (*MDM2*). Given the major role of BAX in apoptosis, we focused on the impact of its expression on mitochondrial fitness. We confirmed that BAX expression was decreased in *TP53*$^{-/-}$ clones derived from *TP53*$^{+/+}$ HMCLs and unchanged in those derived from *TP53*$^{-/mut}$ HMCLs (Figure S6A). As previously reported, *TP53*$^{-/mut}$ HMCLs also under expressed BAX when compared to *TP53*^{wt} HMCLs (Figure S6B)[22,25,31]. Noteworthy, BAX was the only BCL2-family protein displaying modified expression in both NCI-H929 and XG7 *TP53*$^{-/-}$ clones. To assess the mitochondrial impact of p53 loss, we used BH3 mimetics specific to MCL1 (S63845), BCL2 (venetoclax) and BCLXL (A1155463), and performed BH3 profiling[12,33].

Silencing p53^{wt} in NCI-H929 and XG7 (but not p53^{mut} in JIM3 and NAN3) induced a resistance to S63845: LD_{50} mean values in clones increased from 6 to 40 nM (p=0.0002) and from 29 to 138nM, (p<0.0001), in NCI-H929 and XG7, respectively, Figure 3A, Table S7. Impact of p53 on response to venetoclax or A1155463 could not be assessed, cell lines being resistant to both. Global mitochondrial priming, i.e., response to BIM or BMF peptides, was unchanged for both NCI-H929 and XG7 *TP53*$^{-/-}$ clones (Figure S7), whereas cytochrome-C release in response to MS1 peptide specific to MCL1 was significantly decreased in both NCI-H929 and XG7 *TP53*$^{-/-}$ clones (Figure 3B), in keeping with reduced sensitivity to S63845. In 31 HMCLs, S63845, but not venetoclax or A1155463, LD_{50} values were also significantly lower in 11 *TP53*^{wt} HMCLs compared to 20 *TP53*^{Abn} HMCLs (median value was 12.5 nM versus 77.50 nM, p=0.026, Figure 3C, Table S8). These data collectively showed that *TP53* status strongly impacted priming to MCL1 in HMCLs.

BAX expression controls response to MCL1-specific BH3 mimetic

To determine the respective role of BAX and BAK in the response to S63845, we transiently silenced *BAK1*, *BAX* or both in *TP53*$^{+/+}$ and *TP53*$^{-/-}$ XG7 cells (Figure S8A). By contrast to *BAK1* silencing that did not significantly impaired response to S63845, *BAX* silencing (with or without *BAK1* silencing) strongly inhibited cell death: death inhibition was 87%±5% (p<0.0001) and 91%±4% (p=0.0385) in *TP53*$^{+/+}$ and *TP53*$^{-/-}$ cells treated with 25 nM S63845, respectively. CRISPR/Cas9-mediated inactivation of *BAX* or *BAK1* in NCI-H929 cells confirmed that BAX, but not BAK, expression was essential for response to low doses of S63845 (Figure 4B, S8B and Table S9): compared with control clones, *BAX* inactivation induced 10-fold increase in LD_{50} (mean values 64 nM versus 6nM, p<0.0001) whereas *BAK1* inactivation did not induce significant LD_{50} changes (6.7 nM versus 6nM). Of note, *BAX*$^{-/-}$ clones appeared slightly more resistant to S63845 than *TP53*$^{-/-}$ clones (mean values 64nM versus 40nM, p=0.015), the latter having heterogeneous LD_{50} values and BAX expression, Figures 4B, S6.

We next assessed the impact of *BAX* expression on S63845 sensitivity. *BAX* expression inversely correlated with S63845 LD_{50} values in $TP53^{+/+}$ and $TP53^{-/-}$ clones (r=-0.8521, p=0.0009, Spearman test), while *BAK1* expression demonstrated no significant correlation (Figure 4C). In 30 HMCLs, S63845 LD_{50} values also displayed an inverse correlation with *BAX* expression (r=-0.5011, p=0.0048), but not with *BAK1* (p=0.6, Figure 4D). None other BCL2 family members displayed significant correlation with S63845 LD_{50} values in both clones and HMCLs (Figure S9).

These results prompted us to directly assess the amount of MCL1 complexed with BAX and BAK. MCL1 immunoprecipitation showed that $TP53^{-/-}$ clones displayed strong decreased amount of MCL1/BAX complexes (median reduction 3.07, p=0.008) and slight increased amount of MCL1/BAK (median increase 1.32, p=0.026) when compared to $TP53^{+/+}$ clones, Figure 4E. S63845 induced the disruption of MCL1-BAX and MCL1-BAK complexes, and BAX-MCL1 complexes were disrupted at lower S63845 concentrations than BAK-MCL1 complexes (Figure S8C). These data showed that p53 loss reduced the amount of MCL1-BAX complexes.

_TP53_ deletion impaired response to BH3 mimetics combination

Because combination of the BH3 mimetics S63845 with venetoclax was reported to be synergistic in myeloma cells, we wondered how p53 loss would impact its efficacy[33]. Combination was indeed synergistic at high doses in $TP53^{+/+}$ and $TP53^{-/-}$ clones, BLISS scores were 11.7±2.1 and 16.3±1.9 in $TP53^{+/+}$#1 and $TP53^{-/-}$#2 NCI-H929 clones and 13.6±6.1 and 14.6±2.8 in $TP53^{+/+}$#1 and $TP53^{-/-}$#1 XG7 clones, respectively (Figure 5A). However, at the same doses, maximum cell death induced by combination was significantly lower in $TP53^{-/-}$ clones versus $TP53^{+/+}$ clones (mean values 59% ±15% versus 79%±3.2% in NCI-H929, p<0.0001, and 28%±6.5% versus 61%±11% in XG7 cells, p<0.01, Figure 5B). Noteworthy, combination was more efficient in NCI-H929 cells than in XG7 cells, which have very low BCL2 expression, Figure S6.

We next assessed death response to S63845, venetoclax and their combination in myeloma cells from 71 consecutive patients at diagnosis, progression or relapse. Median values of cell death induced by 25 nM S63845, 300 nM venetoclax or combination were 21%, 18% and 81%, respectively (Table 2).

Presence of 1q gain positively impacted response to S63845 (cell death was 13% in 33 no 1q samples versus 28.5% in 38 1q samples, p=0.0152), as previously reported, but did not impact response to venetoclax or to the combination, and presence of del17p did not impact responses to BH3 mimetics (Figure 5C-D)[11,34]. Whatever the presence of 1q21 or del17p, combination was effective in 97% of the samples i.e., additive (-10%< observed death minus expected death <10%) in 10 samples (14%) and supra additive to synergistic (observed death minus expected death> 10%) in 59 samples (83%). Supra additivity to synergy of combination was mainly found in samples without t(11;14), t(11;14) samples having a high response rate to venetoclax alone (Figure S10A-B).

As observed in NCI-H929 and XG7 clones, combination had a trend to be less efficient in the del17p samples when compared to the no del17p samples: median of observed minus expected value was 11% (range -10 to 55) versus 23.5% (range -14 to 85), respectively, p=0.09, Figure 5D. Of note, the del17p impact on BH3 combination efficacy was rather restricted to samples without t(11;14), median of observed minus expected value was 13% (range -10 to 55) in 10 samples del17p versus 34% (range -12 to 85) in 32 samples with no del17p, p=0.0457, Figure S10A.

Myeloma cells resistant to BH3 mimetics displayed a lower p53 score at single-cell level

Given the p53 impact on the response to BH3 mimetics and the heterogeneity of myeloma cells in patients, we used scRNAseq to determine whether cells surviving to BH3 mimetics would have a lower p53 score. Bone marrow (n=23) or pleural effusion (n=1) mononuclear cells from 24 patients (Table S10) were cultured overnight with or without BH3 mimetics combination, and 15,000 living cells were separated and profiled using 10XChromium. Myeloma cells were identified as described in Supplemental materials and methods section. Figure 6A shows the 83,191 myeloma cells from the 24 control (55,114 control cells) and BH3-mimetics treated samples (28,077 treated cells) and their molecular classification: 21 samples were classified as CD-1, CD-2, HY, LB, MF, MS and samples belonging to the same molecular subgroup were grouped together (Figure S11)[35]. The median myeloma number analyzed per sample was 2,284 cells and 643 cells in control and BH3 mimetics-treated conditions, respectively (Figure S12). In 15 of 24 samples, proportion of cells in paired clusters was significantly modified upon BH3 mimetics treatment as illustrated for sample #3 in Figure 6B, p<0.0001 (all samples are shown in Figure S12). Del17p status of clusters was determined using InferCNV, clusters with del17p being shown in red, Figure 6B. The p53 score median value in clusters was compared between paired control and treated samples (when cluster contained at least 10 cells in both conditions): in BH3 mimetics treated samples, the score was unchanged in 51 clusters (66.2%), inferior in 25 clusters (32.5%), and superior in 1 cluster (1.3%). Change in score was not similar in clusters with or without del17p (p=0.035, Chi-2 test), i.e., it decreased in 35.4 % of clusters with no del17p (23 out of 65) versus 16.7% of clusters with del17p (2 out of 12), Figure S12. The p53 score value was compared between control and treated cells: the p53 score was 3.13-fold inferior in treated cells versus control cells (median values were -0.009612 and -0.03004, respectively p<0.0001, Figure 6C-D).

Discussion

In our work, we performed CRISPR/Cas9 *TP53*-silencing to study the direct genomic and functional impact of p53 silencing in myeloma cells. Given the myeloma genomic heterogeneity, we chose 2 HMCLs belonging to the same subgroup, the t(4;14) group. Using RNAseq, 17 genes were significantly regulated upon p53 silencing in both *TP53*$^{+/+}$ HMCLs, 16 down (including *TP53*) and 1 up. Using microarray, only 5 genes were under expressed (*MDM2, CDKN1A, DDB2, FDXR*, and *PHLDA3*) and 1 overexpressed (*CDKN2A*) in *TP53*^{abn} HMCLs when compared with *TP53*^{wt} HMCLs: by contrast to the 5 under expressed genes, *CDKN2A* expression was not modified in isogenic clones. *CDKN2A* has never been reported as regulated by p53 and its overexpression in *TP53*^{abn} HMCLs is, in fact, related to *CDKN2A/ARF* locus loss in some *TP53*^{wt} HMCLs[21], which is a common hit in *TP53*^{wt} cancer cells. This difference illustrates the major interest of isogenic cells for providing a specific p53 transcriptome. As expected, none of the genes impacted by p53-silencing in both NCI-H929 and XG7 were found modified in JIM3 or NAN3 *TP53*$^{-/-}$ clones, excepting *TP53*, showing that R273C or R248Q mutation had no residual p53 transcriptomic activity. Although the expression of several genes was found modified in either JIM3 or NAN3 *TP53*$^{-/-}$ clones, the modest changes instead suggested non-specific regulation.

To establish a functional p53 score, we kept the under expressed genes in both NCI-H929 and XG7 *TP53*$^{-/-}$ clones, known as p53 target: these 13 genes were identified as early-transactivated upon p53 activation, highlighting their high sensitivity to the amount of p53[29]. This score segregated *TP53*$^{+/+}$ from *TP53*$^{-/-}$ or *TP53*$^{-/m}$ cells, underscoring its efficacy for identifying p53 loss-of-function whatever its origin i.e., lack of expression or mutation, and whatever the genomic background. In 1,105 cancer cell lines, the score also distinguished cells with mono- or bi-allelic *TP53* hit (deletion and/or mutation) from cells without any *TP53* abnormalities. Monoallelic deletion or mutation was associated with a low score, and cells displaying biallelic hit had an even lower score. In patient cells, samples with low score were mostly del17p in CASSIOPEA (*TP53* sequence was not assessed) or del17p and *TP53* mutated in MYRACLE and MMRF-coMMpass. Indeed, in MMRF-coMMpass cohort, *TP53* deletion alone had only a trend to impact the score (p=0.18). This discrepancy between patient cells and cell lines might be explained by the low number of del17p samples in patient cohorts and/or by the clonal proportion (100% of cells in cell lines but not in patient samples) or by the bi- versus mono-allelic deletion, the biallelic deletion being more frequent in cell lines than in patient cells. Taken together, this functional p53 score is highly efficient in identifying samples with biallelic inactivation both in cell lines and patient samples.

Although the score will not identify samples with *TP53* hit in minor subpopulations by contrast to FISH or NGS, it could define the functional impact of mutation. Nevertheless, the score also identified few samples lacking any *TP53* hit suggesting the existence of other p53 pathway dysregulations that merit

further investigation. Of interest, the score was also heterogeneous at single cell level, suggesting that it identified cells with low to high activation of p53 pathway.

Interestingly, the score was predictive of overall survival in two cohorts of patient: it indeed identified 3 to 5% of patients with a low p53 score which is consistent with the low occurrence of mutation/bi-allelic hit in *TP53* gene[16,36]. In 139 patients from the CASSIOPEA trial (VTD and daratumumab versus VTD), 75% of patients with a low score were classified as High-Risk (R-ISS) and 62.5% had del17p: del17p was associated with reduced survival but impact of mono- versus bi-allelic hit was not assessed. In the MMRF-coMMpass cohort, which is like MYRACLE a real-life cohort, only del17p and mutation was predictive of overall survival and p53 score indeed identified patients with biallelic hit (53% of biallelic samples were in group 1). Deletion alone was not associated with significant lower overall survival, in good agreement with its lack of impact on the score.

The p53 score involves a combination of genes that has not been used in other p53 score either derived from sh*TP53* HMCLs or from MMRF-CoMMpass study[34,37,38]. Our p53 functional score did also not share any gene with the "Li-Fraumeni" functional p53 score that was unable to discriminate 1,105 cell lines, 12 clones and 38 patient samples according to their respective *TP53* status.

As expected, *TP53* silencing in XG7 and NCI-H929 HMCLs increased resistance to melphalan and nutlin3a. We didn't assess functional impact of one allele deletion in isogenic cell lines because both alleles were inactivated in all clones. However, Munawar and collaborators previously demonstrated that the loss of one allele significantly impaired drug sensitivity in isogenic AMO1 cells[39]. To investigate the functional impact of p53-dependent BAX decrease in CRISPR/Cas9 *TP53*$^{-/-}$ cells, we focused on mitochondrial fitness. Regarding BCL2-family proteins, only the expression of BAX was found significantly modified in *TP53*$^{-/-}$ clones: expression of two other known p53 target genes i.e., *PMAIP1* (NOXA) and *BBC3* (PUMA), was not decreased in *TP53*$^{-/-}$ clones in the absence of stress. Indeed, transactivation of these genes requires a higher amount of p53, as illustrated by their activation by nutlin3a that induced p53 accumulation[29,31,32]. Although BAX and BAK are considered as redundant, only *BAX* expression is directly regulated by p53. To decipher its role we used BH3 mimetics that directly target mitochondria without inducing genomic or signaling stress, in contrast to DNA-damaging drugs like melphalan. In MM, sensitivity to BH3 mimetics is primarily associated with genomic heterogeneity, t(11;14) cells being sensitive to BCL2 BH3 mimetics, t(4;14) to MCL1 BH3 mimetics[12]. NCI-H929 and XG7 were sensitive to S63845 but resistant to venetoclax, and removal of p53 induced about 5-fold increase in S63845 LD_{50} values. Transient or permanent silencing of *BAX* or *BAK1* in XG7 or NCI-H929 demonstrated that BAX (not BAK) expression was essential for the death response to low doses of S63845, whatever the level of BAK expression. These results clearly demonstrated that BAX decrease in *TP53*$^{-/-}$ clones greatly impacted mitochondrial fitness, in spite of a slight increase in the amount of MCL1/BAK complexes: indeed MCL1 IP assays showed that the amount

of MCL1-BAX was greatly decreased in *TP53*$^{-/-}$ clones, and that low concentrations of S63845 totally disrupted MCL1-BAX, and partly MCL1-BAK complexes. Although BAX and BAK affinity for MCL1 is quite similar, BAK has been reported to display a higher affinity than BAX that could favor the release of BAX under low concentrations of S63845[40,41]. These results showed that BAK is not requisite for a response to low or intermediate doses of S63845. Moreover, the impact of p53 and BAX (but not BAK) on MCL1-sensitivity was also found in HMCLs: S63845 LD_{50} values were correlated with *TP53* status and with *BAX* expression level. Overall, these results show that BAK and BAX are not completely redundant, and that p53-induced BAX expression is a limiting factor in mitochondrial apoptosis. Most *TP53*^{wt} HMCLs being resistant to BCL2 or BCLXL inhibitors, p53/BAX impact on other BH3 mimetics response could not be assessed in myeloma. Nonetheless, in other hematological malignancies loss of *TP53* was also reported to impair response to BCL2 or MCL1 BH3 mimetic[42–44]. In CLL, efficacy of venetoclax with obinutuzumab was efficient but reported inferior in patients with *TP53* hit compared with patients without *TP53* hit[45]. Although BCL2 and MCL1 BH3 mimetics combination was more efficient in *TP53*$^{+/+}$ clones, it overcame the resistance induced by p53 loss in both NCI-H929 and XG7 *TP53*$^{-/-}$ clones and was highly efficient in 69% of del17p patient samples (9 of 13). At single cell level, we showed in 24 paired control and treated samples that the 13-gene p53 score was heterogeneous: cells surviving to BH3 mimetics combination in vitro mainly displayed either a decreased or unchanged p53 score, suggesting again that cells with high p53 score were more sensitive to BH3 mimetics.

In summary, we established a functional p53 score that identifies myeloma cells with biallelic *TP53* invalidation, demonstrated that p53-regulated BAX is critical for optimal cell response to BH3 mimetics, and showed that BH3 mimetic combination is efficient in vitro for patients with biallelic *TP53* invalidation, for whom there is still an unmet medical need.

Acknowledgments
This work was supported by grants from FFRMG, LNCC, INCA (INCa-DGOS-INSERM_12558, INCa-DGOS-INSERM-ITMO Cancer_18011), Action Cancer 44. The authors acknowledge the Cytocell-Flow Cytometry and FACS core facility (SFR Bonamy, BioCore, Inserm UMS 016, CNRS UAR 3556, Nantes, France) for its technical expertise and help, member of the Scientific Interest Group (GIS) Biogenouest and the Labex IGO program supported by the French National Research Agency (n°ANR-11-LABX-0016-01). The authors are grateful to the Genomics Core Facility GenoA, member of Biogenouest and France Genomique and to the Bioinformatics Core Facility BiRD, member of Biogenouest and Institut Français de Bioinformatique (IFB) (ANR-11-INBS-0013) for the use of their resources and their technical support. The authors thank Elise Douillard and Magali Devic for expert technical assistance. The authors thank Emma Leguedey for performing experiments. The coMMpass data was generated as part of the Multiple Myeloma Research Foundation (MMRF) Personalized Medicine Initiative (https://themmrf.org).
RD was supported by SIRIC ILIAD, NLL was supported by HEMA-NexT.

Authorship Contributions
RD participated in the design of the study, performed experiments, analyzed the results, and participated in the writing.
GD and CD derived, profiled CRISPR/Cas9 *TP53* cells, and performed experiments.
SMa managed the patients' cohort and performed experiments.
CB performed bioinformatic analysis and p53 scoring
JBA performed TP53 analysis in MMRF-coMMpass
JBA, JC and JD performed scRNAseq analysis
NLL managed the patients' cohort
BT, CT, PM participated in the design of the study and managed the patients' cohorts.
CG and YLB provided samples and supervised FISH experiments
SMi provided CASSIOPEA RNAseq data
DC and AMA designed CRISPR/Cas9 strategy and derived CRISPR/Cas9 clones
PGB, MA, DC, SMi participated in the design of scRNAseq study and supervised experiments
CPD designed the study, analyzed the results, and wrote the article.

Disclosure of conflict of interest
The authors have no conflict of interest to declare.

Legends to Tables and Figures

Table 1. p53 score in MYRACLE patients

CD138+ myeloma cells were purified from BM or PB of patient with myeloma and gene expression profiling was performed using DGE-Seq. The 13-gene p53 score was calculated using singscore package in R. Del17p and *TP53* sequencing were determined by FISH and Sanger sequencing in RT-PCR cDNA products. *TP53* hit was considered when deletion and/or mutation involved the majority of cells.

MM multiple myeloma, sPCL secondary plasma cell leukemia, pPCL primary plasma cell leukemia. D diagnosis, P progression, R relapse

Table 2. Cell death in MYRACLE samples induced by BH3 mimetics

Mononuclear cells from BM or PE of patient with myeloma were cultured for 24h with 25 nM S63845, 300 nM venetoclax or their combination and myeloma cell death was assessed using flow cytometry. 1q21 gain or 17p loss was considered when it involved more than 50% of cells.

MM multiple myeloma, BM bone marrow, PE pleural effusion, D diagnosis, P progression, R relapse, x not done.

Figure 1. A 13-gene functional p53 score established from isogenic *TP53* CRISPR/Cas9 HMCLs .

A_ Principal component analysis of $TP53^{+/+}$ or $TP53^{-/mut}$ and $TP53^{-/-}$ cells derived from NCI-H929, XG7, JIM3 and NAN3 HMCLs. PCA was performed on all cells profiled in triplicate wells using RNA sequencing (3'-Digital gene expression sequencing, DGE-Seq). RNA profiling was performed on $TP53^{+/+}$ control (bulk) cells and $TP53^{-/-}$ clones.

B_ Number of genes significantly differentially expressed between $TP53^{+/+}$ control cells and $TP53^{-/-}$ clones. The graph represents the number of genes significantly downregulated or upregulated in $TP53^{-/-}$ NCI-H929, XG7, JIM3 and NAN3 clones compared to their respective $TP53^{+/+}$ or $TP53^{-/mut}$ control cells (FDR<0.05). Genes were classified according to their unknown or known p53 transactivation: early-direct, late-direct, late-indirect and not regulated by p53[29]. Expression profiling was performed by DGE-Seq in triplicate wells (see Table S2 for complete gene listing).

C_ Schematic representation of the functional p53 score construction. Sixteen downregulated genes in $TP53^{-/-}$ clones were shared between NCI-H929 and XG7, and 13 known as early-direct p53 regulated genes were selected for establishing the p53 functional score.

D_ The p53 score segregates the clones according to their *TP53* status. The score was calculated in $TP53^{+/+}$ or $TP53^{-/mut}$ and $TP53^{-/-}$ NCI-H929, XG7, JIM3 and NAN3 cells under constitutive (left panel) or 24h-nutlin3a (2 μM for XG7 cells, 10 μM for all other clones) culture (right panel). Statistical analyses were performed using the Mann-Whitney test. Blue, red, and orange represent $TP53^{+/+}$, $TP53^{-/-}$ and $TP53^{-/\text{mutated}}$ cells, respectively.

E_ The p53 score segregates HMCLs according to their p53 status. The score was calculated in 18 HMCLs characterized by DGE-seq. *TP53* sequencing was performed on cDNA and p53 expression was determined by western blotting (Table S5). Statistical analyses were performed using the Kruskal-Wallis test with multiple comparisons.

F_ The p53 score is functional in 1,105 cancer cell lines with different *TP53* status. The score was calculated in 1,105 cancer cell lines from DepMap and analyzed according to the presence of *TP53* deletion and/or mutation (left panel) and to the number of *TP53* deletion or mutation (right panel). Statistical analyses were performed using the Kruskal-Wallis test with multiple comparisons.

**** p<0.0001, *** p<0.001, ** p<0.01, * p<0.05

Figure 2. The 13-gene p53 score is predictive of overall survival

A_ The score discriminates patient samples according to *TP53* status. The score was calculated in 38 patient samples characterized by DGE-seq (Table 1). Del17p and *TP53* sequencing were determined by FISH and Sanger in RT-PCR cDNA products, respectively[25]. Statistical analysis was performed using the Kruskal-Wallis test with multiple comparisons.

B_ The p53 score is predictive of overall survival (OS) of 139 CASSIOPEA patients. Groups of patients were determined according to score level using the K-means method (see Fig S3A). Left graph represents the OS of the 4 groups. Middle and right graphs represent the frequency of patients classified as high risk or with del17p in each K-means groups. Statistical significance was determined using the Log-rank (Mantel-Cox) test or Chi-2 test.

C_ Overall survival of 764 MMRF-coMMpass patients according to p53 score. Groups were determined using the K-means method (see Fig S3B). Left graph represents the OS of the 4 groups. Middle graph represents the p53 score in groups separated according to the presence of *TP53* deletion or/and mutation in 684 patients, and right graph represents their OS. VAF thresholds were set up at <-0.5 for deletion and >0.35 for mutation. Statistical significance was determined using the Log-rank (Mantel-Cox) test.

**** p<0.0001, *** p<0.001, ** p<0.01, * p<0.05

Figure 3. *TP53* loss impairs response to MCL1 BH3 mimetic S63845

A_ CRISPR/Cas9-mediated *TP53* inactivation increased resistance to BH3 mimetic specific to MCL1. Left panels: BH3 mimetic specific to MCL1 dose response in isogenic $TP53^{+/+}$ and $TP53^{-/-}$ NCI-H929 and XG7 clones. Graphs represent 3 independent experiments. Right panels: LD_{50} S63845 values in $TP53^{+/+}$ control cells (bulk), $TP53^{+/+}$ and $TP53^{-/-}$ clones in NCI-H929 (upper panel) and XG7 (lower panel), see Table S7. Statistical analysis was performed using the Mann-Whitney test.

B_ CRISPR/Cas9-mediated *TP53* inactivation decreased priming to MCL1. Priming to MCL1 was assessed by determining cytochrome C release induced by MS1 peptide. Cytochrome-C staining was performed using anti-cytochrome-C mAb and analyzed by flow cytometry. Graphs represent the mean ± SD of 3 to 4 independent experiments. Statistical analysis was performed using the Wilcoxon matched pairs signed-rank test.

C_ S63845 LD_{50} values were significantly lower in $TP53^{wt}$ HMCLs. S63845, Venetoclax and A1155463 LD_{50} values were analyzed in 11 $TP53^{wt}$ and 20 $TP53^{Abn}$ HMCLs (see Table S8). Each point represents one HMCL, median values are indicated. For A1155463 and Venetoclax, LD_{50} was arbitrarily set up at 20,000 nM and 10,000 nM when it did not reach 10,000nM or 5,000 nM, respectively. Statistical analyses were performed using the Mann-Whitney test.

**** p<0.0001, *** p<0.001, ** p<0.01, * p<0.05

Figure 4. BAX expression governs the response to MCL1 BH3-mimetic S63845

A_ *BAX* silencing inhibited S63845-induced cell death. XG7 $TP53^{+/+}$#1 and $TP53^{-/-}$#1 were transiently transfected with siCont, si*BAX*, si*BAK1*, or both, prior to treatment with increasing doses of S63845. The graph represents the mean ± SD of 3 independent experiments. Statistical analyses were performed using the unpaired t-test.

B_ CRISPR/Cas9-mediated *BAX*, but not *BAK1,* inactivation inhibited response to S63845 in NCI-H929 cells. Left panel: $TP53^{+/+}$#1, $TP53^{-/-}$#2, $BAX^{-/-}$ (n=3) and $BAK1^{-/-}$ (n=3) clones were treated with increasing doses of S63845 for 24h and cell death was determined using flow cytometry. The graph represents the mean ± SD of 3 experiments. Right panel: the graph represents the LD_{50} values of each clone (mean ± SD). Statistical analysis was performed using the Mann-Whitney test.

C_ *BAX*, but not *BAK1,* expression correlated with sensitivity to S63845 in NCI-H929 and XG7 clones. Expression of *BAX* and *BAK1* (mean DGE-Seq values) were plotted against LD_{50} S63845 values. Correlation was assessed using the Spearman test.

D_ *BAX*, but not *BAK1,* expression correlated with sensitivity to S63845 in HMCLs. Expression of *BAX* and *BAK1* (microarray) in 30 HMCLs was plotted against LD_{50} S63845 value. Correlation was assessed using the Spearman test.

E_ CRISPR/Cas9-mediated *TP53* inactivation increased MCL1/BAK and decreased MCL1/BAX complexes. For IP assays, cells were lysed in 1 % digitonin-containing buffer and lysates were pre-cleared with protein A conjugated to sepharose beads. For MCL1 IP assay, 700 μg of protein lysate was incubated overnight with an agarose-conjugated mAb anti-MCL1 from Santa Cruz Biotechnology. After immunoblotting, MCL1, BAK and BAX levels were determined in the immunoprecipitated fraction and BAX/MCL1 et BAK/MCL1 ratios were calculated to evaluate the abundance of both complexes.

One experiment out of 3 is represented. The graph represents the quantities of BAX and BAK bound to MCL1 in *TP53*$^{+/+}$ and *TP53*$^{-/-}$ NCI-H929 and XG7 cells (3 independent experiments). Statistical analyses were performed using the Mann-Whitney test.

**** p<0.0001, *** p<0.001, ** p<0.01, * p<0.05

Figure 5 p53-silencing impacts combination of S63845 and venetoclax

A_ Combination of S63845 and venetoclax was synergistic in *TP53*$^{+/+}$ and *TP53*$^{-/-}$ NCI-H929 and XG7 clones. Clones were cultured for 24h with increasing concentrations of S63845 and venetoclax clones as indicated in the figure. BLISS scores were calculated using https://synergyfinder.fimm.fi/. The figure represents the mean of 3 independent experiments.

B_ Combination of S63845 and venetoclax was efficient in *TP53*$^{+/+}$ and *TP53*$^{-/-}$ clones in both NCI-H929 and XG7 cell lines. The 12 clones were cultured for 24h with 10 nM (NCI-H929) or 20 nM (XG7) S63845 combined with 300 nM venetoclax. The graphs represent 3 independent experiments. Statistical analyses were performed using the Mann-Whitney or Wilcoxon matched pairs signed-rank tests.

C_ Gain of 1q21, but not del17p, impacted response to S63845. Response to 25 nM S63845 or 300 nM venetoclax was assessed in 71 myeloma samples, characterized by FISH for both 1q21 gain and del17p (see Table 2). The graphs represent cell death induced by each BH3 mimetic in function of 1q21 gain or del17p. Statistical analyses were performed using the Mann-Whitney test.

D_ Deletion of 17p had a trend to decrease the synergy between S63845 and venetoclax. The graphs represent cell death induced by 25 nM S63845 combined with 300 nM venetoclax depending on 1q gain or del17p (left, middle panels), and the difference between observed cell death (25 nM S63845 combined with 300 nM venetoclax) minus expected cell death (sum of cell death induced by 25 nM S63845 and by 300 nM venetoclax) depending on del17p. Cell death was assessed after 24h using flow cytometry. Statistical analyses were performed using the Mann-Whitney test.

**** p<0.0001, *** p<0.001, ** p<0.01, * p<0.05

Figure 6 scRNAseq analysis of response to BH3 mimetics

A_ UMAP representation of myeloma cells from 24 control and BH3 mimetics-treated patient samples using scRNAseq. Mononuclear cells from 23 bone marrow or 1 pleural effusion from patients with MM were cultured overnight with IL6 in the presence, or not, of 25nM S63845 and 300 nM Venetoclax (BH3 m). Cell processing and scRNASeq analysis were performed as described in supplemental materials and methods section. Each patient sample is numbered according to Table S10 and their molecular classification is indicated.

B_ Example of individual scRNAseq analysis of response to BH3 mimetics. Upper left: UMAP split representation of myeloma cells in merged control and treated samples from patient #3, cells are colored according to clusters. Upper right: Infer Copy Number Variation (InferCNV) of control and BH3 mimetics treated cells. InferCNV was calculated using broadinstitute/infercnv package in R in comparison with normal bone marrow plasma cells.

Lower left: the graphs represent the number of cells per cluster and their proportion in each condition. Right: statistical comparison of p53 score in paired clusters (Mann-Whitney test). Black and red violin indicate no del17p and del17p, respectively. All samples are shown in Figure S12.

C, D_ The p53 score is decreased in cells surviving to BH3 mimetic combination. C: UMAP representation of p53 score of myeloma cells split into control (left) and treated (right) samples (blue=low to red=high). The p53 score was calculated independently in each patient samples. D: the graph represents the violin representation of p53 score in 55,114 control cells and 28,077 BH3 mimetic-treated cells from the 24 samples. Statistical analysis was performed using the Mann-Whitney test.

**** $p<0.0001$, *** $p<0.001$, ** $p<0.01$, * $p<0.05$

References

1. Moreau P, Attal M, Hulin C, et al. Bortezomib, thalidomide, and dexamethasone with or without daratumumab before and after autologous stem-cell transplantation for newly diagnosed multiple myeloma (CASSIOPEIA): a randomised, open-label, phase 3 study. *The Lancet*. 2019;394(10192):29–38.
2. Facon T, Kumar SK, Plesner T, et al. Daratumumab, lenalidomide, and dexamethasone versus lenalidomide and dexamethasone alone in newly diagnosed multiple myeloma (MAIA): overall survival results from a randomised, open-label, phase 3 trial. *Lancet Oncol.* 2021;22(11):1582–1596.
3. Manier S, Ingegnere T, Escure G, et al. Current state and next-generation CAR-T cells in multiple myeloma. *Blood Rev.* 2022;54:100929.
4. Berdeja JG, Madduri D, Usmani SZ, et al. Ciltacabtagene autoleucel, a B-cell maturation antigen-directed chimeric antigen receptor T-cell therapy in patients with relapsed or refractory multiple myeloma (CARTITUDE-1): a phase 1b/2 open-label study. *The Lancet*. 2021;398(10297):314–324.
5. Munshi NC, Anderson LD, Shah N, et al. Idecabtagene Vicleucel in Relapsed and Refractory Multiple Myeloma. *N. Engl. J. Med.* 2021;384(8):705–716.
6. Thakurta A, Ortiz M, Blecua P, et al. High subclonal fraction of 17p deletion is associated with poor prognosis in multiple myeloma. *Blood*. 2019;133(11):1217–1221.
7. Corre J, Perrot A, Caillot D, et al. del(17p) without *TP53* mutation confers a poor prognosis in intensively treated newly diagnosed patients with multiple myeloma. *Blood*. 2021;137(9):1192–1195.
8. Rajkumar SV. Multiple myeloma: 2022 update on diagnosis, risk stratification, and management. *Am. J. Hematol.* 2022;97(8):1086–1107.
9. Lok A, Descamps G, Tessoulin B, et al. p53 regulates CD46 expression and measles virus infection in myeloma cells. *Blood Adv.* 2018;2(23):3492–3505.
10. Botrugno OA, Bianchessi S, Zambroni D, et al. ATR addiction in multiple myeloma: synthetic lethal approaches exploiting established therapies. *Haematologica*. 2019;
11. Slomp A, Moesbergen LM, Gong J, et al. Multiple myeloma with 1q21 amplification is highly sensitive to MCL-1 targeting. *Blood Adv.* 2019;3(24):4202–4214.
12. Gomez-Bougie P, Maiga S, Tessoulin B, et al. BH3-mimetic toolkit guides the respective use of BCL2 and MCL1 BH3-mimetics in myeloma treatment. *Blood*. 2018;132(25):2656–2669.
13. Janic A, Valente LJ, Wakefield MJ, et al. DNA repair processes are critical mediators of p53-dependent tumor suppression. *Nat. Med.* 2018;24(7):947–953.
14. Manier S, Salem KZ, Park J, et al. Genomic complexity of multiple myeloma and its clinical implications. *Nat. Rev. Clin. Oncol.* 2017;14(2):100–113.
15. Tessoulin B, Eveillard M, Lok A, et al. p53 dysregulation in B-cell malignancies: More than a single gene in the pathway to hell. *Blood Rev.* 2017;31(4):251–259.
16. Ansari-Pour N, Samur M, Flynt E, et al. Whole-genome analysis identifies novel drivers and high-risk double-hit events in relapsed/refractory myeloma. *Blood*. 2023;141(6):620–633.
17. Loizou E, Banito A, Livshits G, et al. A Gain-of-Function p53-Mutant Oncogene Promotes Cell Fate Plasticity and Myeloid Leukemia through the Pluripotency Factor FOXH1. *Cancer Discov.* 2019;9(7):962–979.
18. Boettcher S, Miller PG, Sharma R, et al. A dominant-negative effect drives selection of *TP53* missense mutations in myeloid malignancies. *Science*. 2019;365(6453):599–604.
19. Benaniba L, Tessoulin B, Trudel S, et al. The MYRACLE protocol study: a multicentric observational prospective cohort study of patients with multiple myeloma. *BMC Cancer*. 2019;19(1):855.
20. Tessoulin B, Descamps G, Moreau P, et al. PRIMA-1Met induces myeloma cell death independent of p53 by impairing the GSH/ROS balance. *Blood*. 2014;124(10):1626–1636.
21. Tessoulin B, Moreau-Aubry A, Descamps G, et al. Whole-exon sequencing of human myeloma cell lines shows mutations related to myeloma patients at relapse with major hits in the DNA regulation and repair pathways. *J. Hematol. Oncol.J Hematol Oncol*. 2018;11(1):137.

22. Moreaux J, Klein B, Bataille R, et al. A high-risk signature for patients with multiple myeloma established from the molecular classification of human myeloma cell lines. *Haematologica*. 2011;96(4):574–582.
23. Maïga S, Brosseau C, Descamps G, et al. A simple flow cytometry-based barcode for routine authentication of multiple myeloma and mantle cell lymphoma cell lines. *Cytom. Part J. Int. Soc. Anal. Cytol.* 2015;87(4):285–288.
24. Lopez J, Bessou M, Riley JS, et al. Mito-priming as a method to engineer Bcl-2 addiction. *Nat. Commun.* 2016;7(1):10538.
25. Surget S, Chiron D, Gomez-Bougie P, et al. Cell death via DR5, but not DR4, is regulated by p53 in myeloma cells. *Cancer Res.* 2012;72(17):4562–4573.
26. Dousset C, Maïga S, Gomez-Bougie P, et al. BH3 profiling as a tool to identify acquired resistance to venetoclax in multiple myeloma. *Br. J. Haematol.* 2017;179(4):684–688.
27. Foroutan M, Bhuva DD, Lyu R, et al. Single sample scoring of molecular phenotypes. *BMC Bioinformatics*. 2018;19(1):404.
28. Fischer M. Census and evaluation of p53 target genes. *Oncogene*. 2017;36(28):3943–3956.
29. Andrysik Z, Galbraith MD, Guarnieri AL, et al. Identification of a core TP53 transcriptional program with highly distributed tumor suppressive activity. *Genome Res.* 2017;27(10):1645–1657.
30. Alberge J-B, Kraeber-Bodéré F, Jamet B, et al. Molecular Signature of ^{18} F-FDG PET Biomarkers in Newly Diagnosed Multiple Myeloma Patients: A Genome-Wide Transcriptome Analysis from the CASSIOPET Study. *J. Nucl. Med.* 2022;63(7):1008–1013.
31. Surget S, Descamps G, Brosseau C, et al. RITA (Reactivating p53 and Inducing Tumor Apoptosis) is efficient against TP53abnormal myeloma cells independently of the p53 pathway. *BMC Cancer*. 2014;14:437.
32. Surget S, Lemieux-Blanchard E, Maïga S, et al. Bendamustine and melphalan kill myeloma cells similarly through reactive oxygen species production and activation of the p53 pathway and do not overcome resistance to each other. *Leuk. Lymphoma*. 2014;55(9):2165–2173.
33. Seiller C, Maiga S, Touzeau C, et al. Dual targeting of BCL2 and MCL1 rescues myeloma cells resistant to BCL2 and MCL1 inhibitors associated with the formation of BAX/BAK hetero-complexes. *Cell Death Dis.* 2020;11(5):316.
34. Ziccheddu B, Da Vià MC, Lionetti M, et al. Functional Impact of Genomic Complexity on the Transcriptome of Multiple Myeloma. *Clin. Cancer Res.* 2021;27(23):6479–6490.
35. Zhan F, Huang Y, Colla S, et al. The molecular classification of multiple myeloma. *Blood*. 2006;108(6):2020–2028.
36. Chng WJ, Price-Troska T, Gonzalez-Paz N, et al. Clinical significance of TP53 mutation in myeloma. *Leukemia*. 2007;21(3):582–584.
37. Teoh PJ, Chung TH, Sebastian S, et al. p53 haploinsufficiency and functional abnormalities in multiple myeloma. *Leukemia*. 2014;28(10):2066–2074.
38. De Ramón C, Rojas EA, Cardona-Benavides IJ, et al. Transcriptional signature of *TP53* biallelic inactivation identifies a group of multiple myeloma patients without this genetic condition but with dismal outcome. *Br. J. Haematol.* 2022;199(3):344–354.
39. Munawar U, Roth M, Barrio S, et al. Assessment of TP53 lesions for p53 system functionality and drug resistance in multiple myeloma using an isogenic cell line model. *Sci. Rep.* 2019;9(1):18062.
40. Chonghaile TN, Sarosiek KA, Vo T-T, et al. Pretreatment Mitochondrial Priming Correlates with Clinical Response to Cytotoxic Chemotherapy. *Science*. 2011;334(6059):1129–1133.
41. Kale J, Osterlund EJ, Andrews DW. BCL-2 family proteins: changing partners in the dance towards death. *Cell Death Differ.* 2018;25(1):65–80.
42. Thijssen R, Diepstraten ST, Moujalled D, et al. Intact TP-53 function is essential for sustaining durable responses to BH3-mimetic drugs in leukemias. *Blood*. 2021;137(20):2721–2735.
43. Liu T, Lam V, Thieme E, et al. Pharmacologic Targeting of Mcl-1 Induces Mitochondrial Dysfunction and Apoptosis in B-Cell Lymphoma Cells in a *TP53*- and *BAX*- Dependent Manner. *Clin. Cancer Res.* 2021;27(17):4910–4922.
44. Carter BZ, Mak PY, Tao W, et al. Combined inhibition of BCL-2 and MCL-1 overcomes BAX

deficiency-mediated resistance of TP53-mutant acute myeloid leukemia to individual BH3 mimetics. *Blood Cancer J.* 2023;13(1):57.
45. Brem EA, O'Brien S. Is a BTKi or BCL2i preferable for first "novel" therapy in CLL? The case for BTKis. *Blood Adv.* 2022;6(4):1361–1364.

Table 1. Genes of the p53 score

Gene symbol	Gene name	Cytogenetic location
APOBEC3C	Apolipoprotein B MRNA Editing Enzyme Catalytic Subunit 3C	22q13.1
APOBEC3H	Apolipoprotein B MRNA Editing Enzyme Catalytic Subunit 3H	22q13.1
BAX	BCL2 Associated X	19q13.33
CDKN1A	Cyclin Dependent Kinase Inhibitor 1A	6p21.2
DDB2	Damage Specific DNA Binding Protein 2	11p11.2
EDA2R	Ectodysplasin A2 Receptor	Xq12
FDXR	Ferredoxin Reductase	17q25.1
MDM2	MDM2 Proto-Oncogene	12q15
PHLDA3	Pleckstrin Homology Like Domain Family A Member 3	1q32.1
RPS27L	Ribosomal Protein S27 Like	15q22.2
RRM2B	Ribonucleotide Reductase Regulatory TP53 Inducible Subunit M2B	8q22.3
TIGAR	TP53 Induced Glycolysis Regulatory Phosphatase	12p13.32
TNFRSF10B	TNF Receptor Superfamily Member 10b	8p21.3

Table 2. Cell death in MYRACLE samples induced by BH3 mimetics

Characteristics of patients' samples								Myeloma cell death (%)		
Number	Disease	Sample	Stage	1q21, 17p	t(4 ;14)	t(11 ;14)	*TP53*	S63845	venetoclax	S63845+ venetoclax
1	MM	BM	D			x	x	0	31	78
2	MM	BM	D	1q21			x	4	5	94
3	MM	BM	D		t(4 ;14)	x		5	9	73
4	MM	BM	D	1q21		x	x	33	33	81
5	MM	BM	D	1q21		t(11 ;14)		98	12	99
6	MM	BM	D	1q21	t(4 ;14)		x	21	44	100
7	MM	BM	D			x	x	0	25	58
8	MM	BM	D	del17p			x	5	15	44
9	MM	BM	D			t(11 ;14)		63	60	98
10	MM	BM	D	del17p			x	13	6	74
11	MM	BM	D		x		x	18	0	32
12	MM	BM	D	1q21		x	x	23	8	72
13	MM	BM	D	del17p				5	1	2
14	MM	BM	D	1q21, del17p		t(11 ;14)		14	85	90
15	MM	BM	D	1q21		t(11 ;14)		19	1	59
16	MM	BM	D				x	31	38	73
17	MM	BM	D					16	53	83
18	MM	BM	D	del17p			H193R	0	51	95
19	MM	BM	D				x	0	0	3
20	MM	BM	D				x	17	12	73
21	MM	BM	D			t(11 ;14)	x	38	95	94
22	MM	BM	D	1q21	x	x	x	30	12	44
23	MM	BM	D			t(11 ;14)	x	15	79	85
24	MM	BM	D	1q21		x	x	81	47	88
25	MM	BM	D				x	0	21	66
26	MM	BM	D	1q21			x	0	3	34
27	MM	BM	D		x	x	x	44	11	100
28	MM	BM	D				x	0	24	70
29	MM	BM	D	1q21			x	37	29	71
30	MM	BM	D	1q21, del17p	t(4 ;14)		x	73	10	96
31	MM	BM	D	1q21		t(11 ;14)		33	19	95
32	MM	BM	D	1q21	t(4 ;14)		x	72	0	84
33	MM	BM	P	1q21				12	0	38
34	MM	BM	P	1q21	t(4 ;14)			28	10	98
35	MM	BM	R			t(11 ;14)		56	57	98
36	MM	BM	R	1q21, del17p		x	x	24	86	90
37	MM	BM	R			t(11 ;14)	x	37	35	79
38	MM	BM	R					0	0	83
39	MM	BM	R		t(4 ;14)			39	12	64
40	MM	BM	R	1q21		t(11 ;14)	x	66	45	98
41	MM	BM	R	1q21, del17p	t(4 ;14)			21	5	26
42	MM	BM	R	1q21				30	0	70
43	MM	BM	R	1q21	t(4 ;14)			0	0	65
44	MM	BM	R				x	38	7	77
45	MM	BM	R	1q21	x		x	1	0	22
46	MM	BM	R	1q21		t(11 ;14)	x	15	40	65
47	MM	BM	R	1q21			x	49	25	91
48	MM	BM	R	1q21			x	41	0	73
49	MM	BM	R	del17p			x	1	24	29
50	MM	BM	R	1q21			x	6	17	59
51	MM	BM	R	1q21		t(11 ;14)		75	73	100
52	MM	BM	R	1q21			x	9	0	53
53	MM	BM	R	del17p		t(11 ;14)	x	61	81	96
54	MM	BM	R	1q21	t(4 ;14)		x	29	27	92
55	MM	PE	R	1q21	t(4 ;14)		x	12	0	57
56	MM	BM	R					44	41	74
57	MM	BM	R		x		x	0	18	83
58	MM	BM	R	1q21				2	87	96
59	MM	BM	R		x	t(11 ;14)	x	2	8	63
60	MM	BM	R		x		x	13	24	98
61	MM	BM	R	1q21	x		x	32	18	92
62	MM	BM	R	1q21, del17p	x			70	16	97
63	MM	BM	R	1q21	t(4 ;14)			10	4	87
64	MM	BM	R	1q21		t(11 ;14)		54	56	86
65	MM	BM	R	1q21, del17p				55	24	98
66	MM	BM	R			t(11 ;14)	x	0	92	94
67	MM	BM	R	1q21, del17p			x	74	0	91
68	MM	BM	R			t(11 ;14)	x	26	87	92
69	MM	BM	R	1q21		t(11 ;14)	x	6	93	99
70	MM	BM	R		x	x	x	0	0	21
71	MM	BM	R			x	x	40	28	71

Figure 1

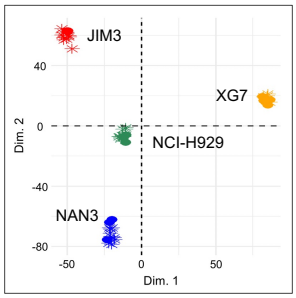

● *TP53*$^{+/+}$ & *TP53*$^{-/m}$ cells
* *TP53*$^{-/-}$ clones

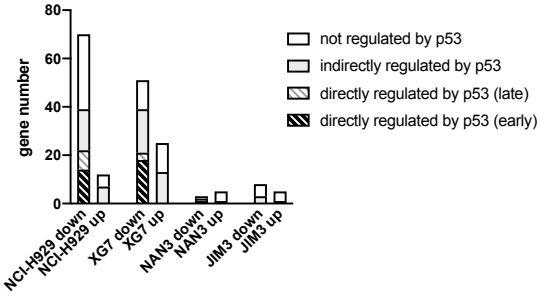

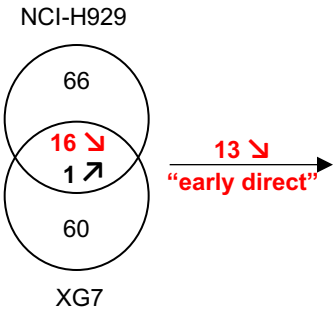

APOBEC3C *MDM2*
APOBEC3H *PHLDA3*
BAX *RPS27L*
CDKN1A *RRM2B*
DDB2 *TIGAR*
EDA2R *TNFRSF10B*
FDXR

genes with modified expression

functional p53 score

TP53$^{+/+}$, *TP53*$^{-/m}$ and *TP53*$^{-/-}$ cells (RNA-Seq)

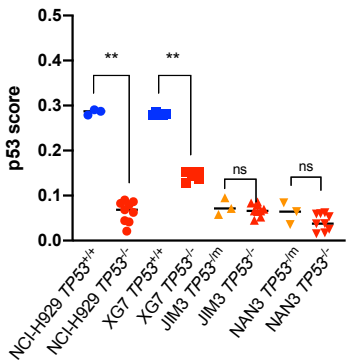

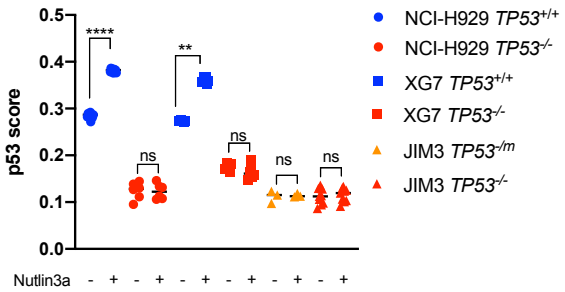

HMCLs (RNA-Seq, n=18)

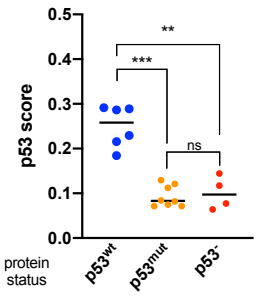

Cancer cell lines (n=1,105)

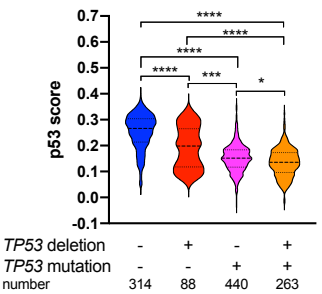

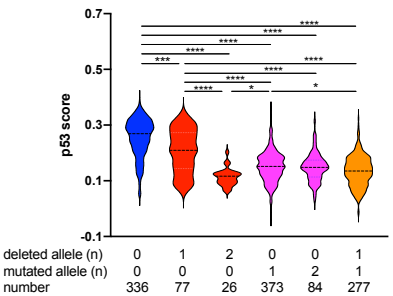

Figure 2

A

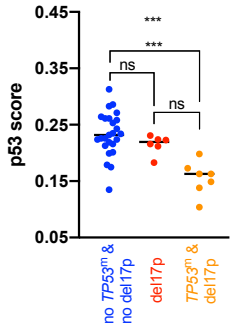
p53 score
0.45
0.35
0.25
0.15
0.05
***
***
ns
ns
no TP53m & no del17p
del17p
TP53m & del17p

B

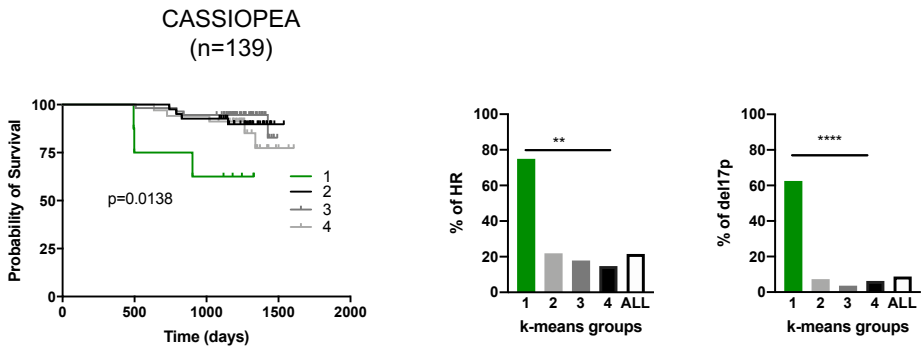
CASSIOPEA
(n=139)
Probability of Survival
p=0.0138
1
2
3
4
Time (days)
% of HR
**
k-means groups
% of del17p
****
k-means groups
1 2 3 4 ALL

C

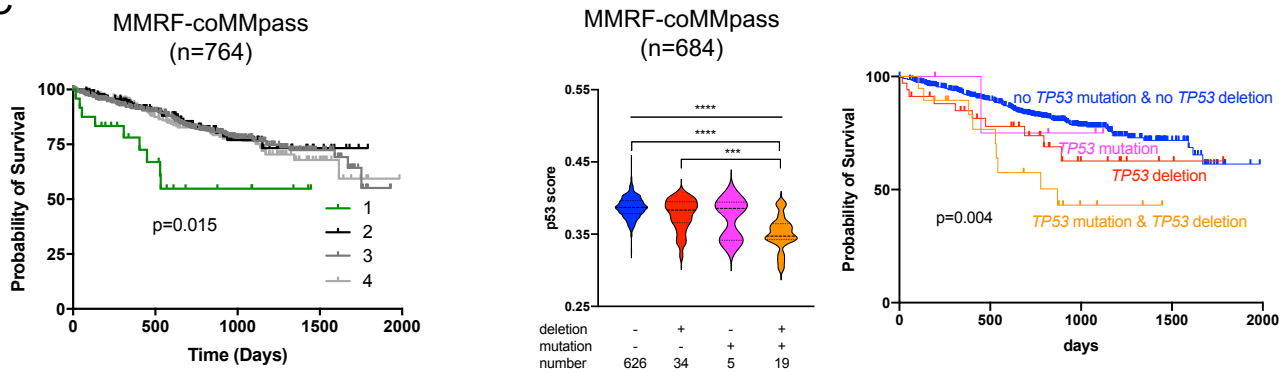
MMRF-coMMpass
(n=764)
Probability of Survival
p=0.015
1
2
3
4
Time (Days)
MMRF-coMMpass
(n=684)
p53 score
****
****
***
deletion - + - +
mutation - - + +
number 626 34 5 19
Probability of Survival
no TP53 mutation & no TP53 deletion
TP53 mutation
TP53 deletion
TP53 mutation & TP53 deletion
p=0.004
days

Figure 3

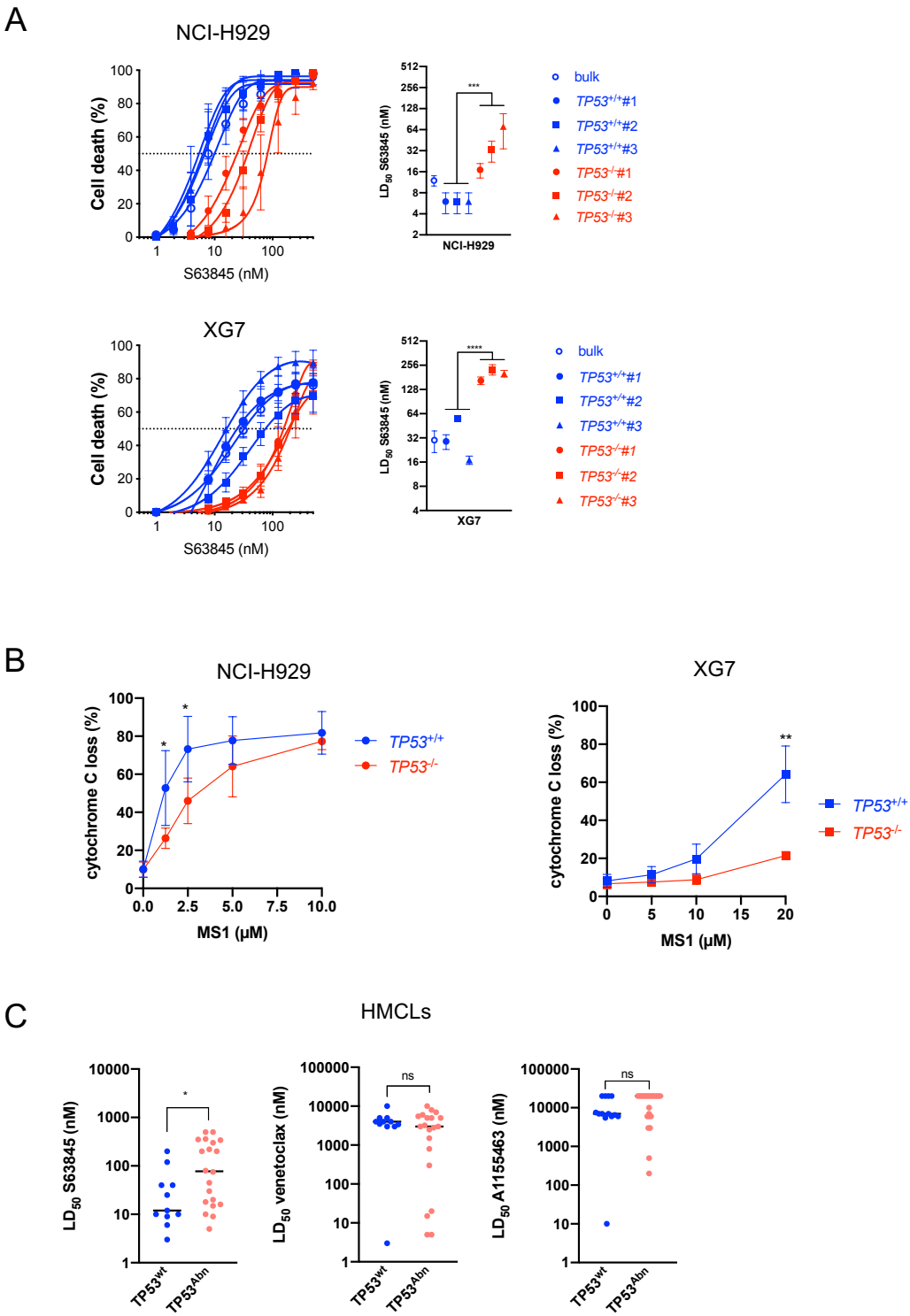
A
NCI-H929
Cell death (%)
S63845 (nM)
LD50 S63845 (nM)
NCI-H929
bulk
TP53+/+#1
TP53+/+#2
TP53+/+#3
TP53-/-#1
TP53-/-#2
TP53-/-#3
XG7
B
NCI-H929
cytochrome C loss (%)
MS1 (μM)
XG7
C
HMCLs
LD50 S63845 (nM)
LD50 venetoclax (nM)
LD50 A1155463 (nM)
TP53wt
TP53Abn
ns

Figure 4

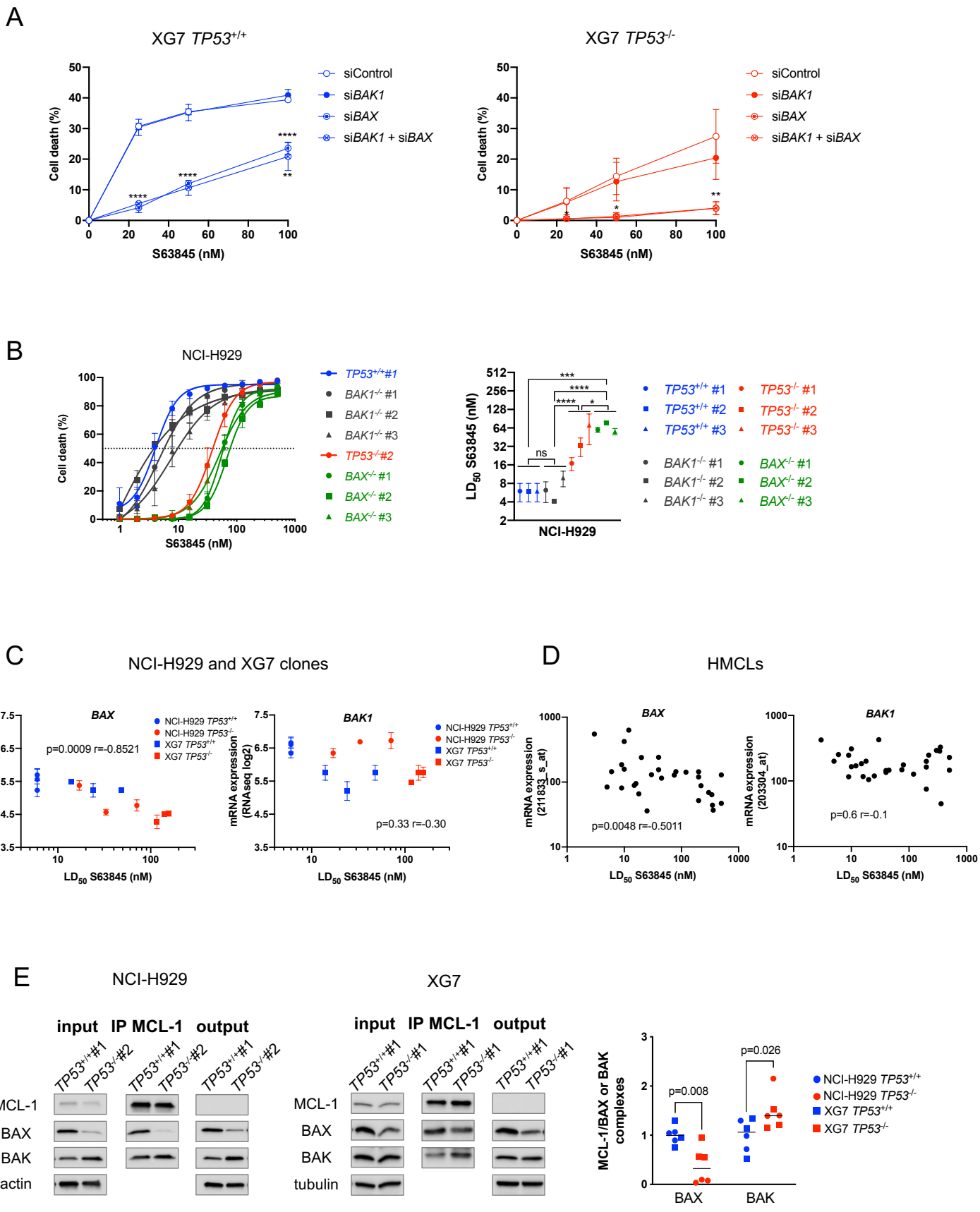
A
XG7 TP53+/+
XG7 TP53-/-
Cell death (%)
S63845 (nM)
siControl
siBAK1
siBAX
siBAK1 + siBAX
B
NCI-H929
TP53+/+#1
BAK1-/- #1
BAK1-/- #2
BAK1-/- #3
TP53-/-#2
BAX-/- #1
BAX-/- #2
BAX-/- #3
LD50 S63845 (nM)
ns
C
NCI-H929 and XG7 clones
BAX
BAK1
mRNA expression (RNAseq log2)
p=0.0009 r=-0.8521
p=0.33 r=-0.30
D
HMCLs
mRNA expression (211833_s_at)
mRNA expression (203304_at)
p=0.0048 r=-0.5011
p=0.6 r=-0.1
E
NCI-H929
XG7
input IP MCL-1 output
MCL-1
BAX
BAK
actin
tubulin
MCL-1/BAX or BAK complexes
p=0.008
p=0.026
NCI-H929 TP53+/+
NCI-H929 TP53-/-
XG7 TP53+/+
XG7 TP53-/-

Figure 5

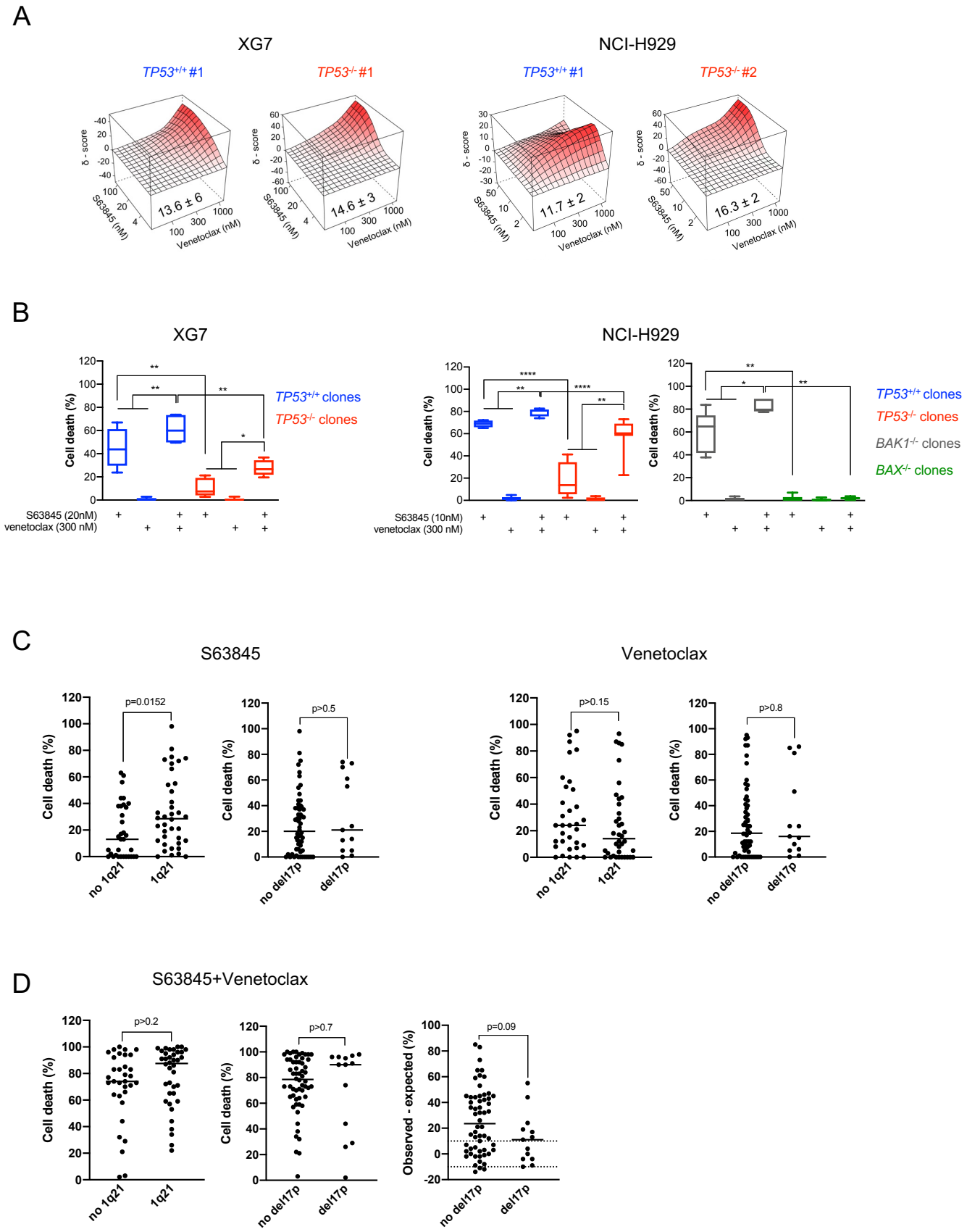
A
XG7
NCI-H929
TP53+/+ #1
TP53-/- #1
TP53+/+ #1
TP53-/- #2
δ - score
S63845 (nM)
Venetoclax (nM)
13.6 ± 6
14.6 ± 3
11.7 ± 2
16.3 ± 2
B
XG7
NCI-H929
Cell death (%)
TP53+/+ clones
TP53-/- clones
BAK1-/- clones
BAX-/- clones
S63845 (20nM)
venetoclax (300 nM)
S63845 (10nM)
venetoclax (300 nM)
C
S63845
Venetoclax
p=0.0152
p>0.5
p>0.15
p>0.8
no 1q21
1q21
no del17p
del17p
D
S63845+Venetoclax
p>0.2
p>0.7
p=0.09
Observed - expected (%)

Figure 6

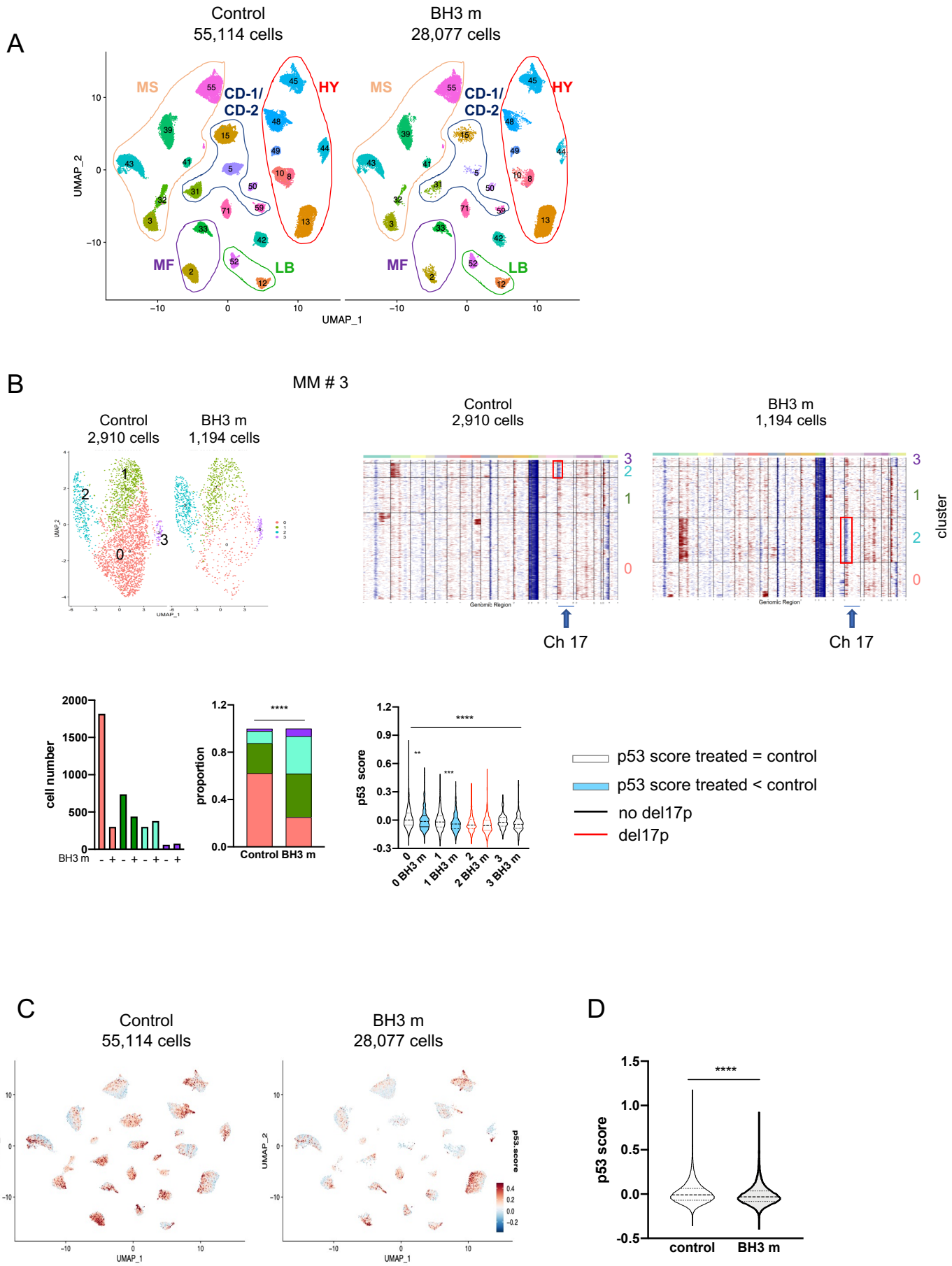
A
Control
55,114 cells
BH3 m
28,077 cells
MS
CD-1/
CD-2
HY
MF
LB
UMAP_2
UMAP_1
B
MM # 3
Control
2,910 cells
BH3 m
1,194 cells
Genomic Region
Ch 17
cluster
cell number
BH3 m
proportion
Control BH3 m
p53 score
0 BH3 m
1 BH3 m
2 BH3 m
3 BH3 m
p53 score treated = control
p53 score treated < control
no del17p
del17p
C
Control
55,114 cells
BH3 m
28,077 cells
p53.score
D
p53 score
control
BH3 m

A p53 score derived from *TP53* CRISPR/Cas9 HMCLs predicts survival and reveals major role of BAX in BH3 mimetics response

Supplemental information.

This document contains supplemental Materials and Methods, legends to 10 supplemental Tables and 12 supplemental Figures, 6 supplemental references.

Supplemental Materials and Methods

Reagents and antibodies

BH3 mimetics S63845, Venetoclax and A1155463 were purchased from Chemietek (Indiana Polis, ID, USA), and Selleck Chemicals (Houston, TX, USA). Anti-CD138-PE monoclonal antibody came from Beckman Coulter (Villepinte, France), and Annexin V-APC from Immunotools (Friesoythe, Germany). Anti-cytochrome-C mAb came from BD Bioscience (Le Pont de Claix, France). Anti-MCL1 and anti-BCLXL Abs were purchased from Santa Cruz Biotechnology (Heidelberg, Germany). Anti-BAK mAb and anti-BAX pAb came from Cell Signaling (Ozyme, Saint-Cyr l'Ecole, France), anti-BIM and anti-ACTIN from Millipore (Molsheim, France), anti-BCL2 from BD Transduction Laboratories (Le Pont de Claix, France), and anti-p53 was purchased from Oncogene Science (Life Technologies, Paris, France).

Survival analysis

Time-to-event survival curves were estimated with the use of the Kaplan-Meier method. Patients were divided into four groups based on the signature score (NbClust package and K-means methods). Probabilities of OS were compared in groups using the log-rank test and Cox proportional-hazard regression (Prism, GraphPad software).

Whole transcriptome sequencing

3'seq-RNA Profiling protocol (DGE-Seq) was performed according to Charpentier et al[1]. The mRNA poly(A) tails were tagged with universal adapters, well-specific barcodes and unique molecular identifiers (UMIs) during template-switching reverse transcriptase. Barcoded cDNAs from multiple samples were then pooled, amplified and labeled using a transposon-fragmentation approach, which enriches for 3'ends of cDNA. A library of 350–800 bp length was run on Illumina NovaSeq 6000 using NovaSeq 6000 SP Reagent Kit 100 cycles (ref #20027464). Raw fastq pairs used for analysis matched the following criteria: the 16 bases of the first read corresponded to 6 bases for a designed well-specific barcode and 10 bases for a unique molecular identifier (UMI). The second read (58 bases) corresponded to the captured poly(A) RNAs sequence. We performed demultiplexing of these fastq pairs according to the sample sheet to generate one single-end fastq for all samples. Sequence alignments were performed with mRNA and mitochondrial genomic sequences (both available on UCSC). DGE profiles were generated by parsing the alignment files (.bam) and counting for each sample the number of unique UMIs associated with each RefSeq genes. Reads aligned on multiple genes, containing more than one mismatch with the reference sequence or reads containing a polyA pattern were discarded. Finally, a matrix containing the expression of all genes on all samples was produced. The absolute abundance of mRNAs expression values was used for determining gene expression

analysis. Normalization was performed by using DESeq2, normalized counts were transformed with vst (variance stabilized transformation) function from DESeq library. Differentially expressed genes were identified using edgeR.

Single-cell RNA-sequencing.

Control and BH3 mimetics treated bone marrow mononuclear cells were successively depleted of dead cells (dead cell removal kit) and erythroid cells (CD235a-conjugated beads) by immunomagnetic sorting (Miltenyi Biotec, Paris, France). A total of 15,000 cells (with a viability superior to 80%) were loaded per lane on the 10X Chromium device and processed for complementary DNA synthesis and library preparation according to manufacturer's protocol using 3 'v2/v3 or v3.1 chemistry (10X Genomics, Paris, France). Libraries were sequenced on NovaSeq 6000 to a mean depth of 45,000 reads/cell as paired-end, 28bp Read 1, 90bp Read 2 (GenoA, UMS Biocore, SFR Bonamy, Nantes).

Sample demultiplexing and genome alignment were performed using the Cell Ranger Software Suite (v3.0.2, 10X Genomics) and refdata-cellranger-GRCh38 3.0.0, respectively. Data analysis was performed using the R package Seurat (v.4.3.0). For each samples, the SoupX (version 1.5.2) package was used to remove cell-free mRNA contamination. Cells that have a total count of UMI below 1000, less than 600 expressed genes, or with high percentage of mitochondrial reads (three standard deviation above the median) which were mainly cells entering apoptosis were removed. An additional quality control step was performed to remove potential doublets, by using scds (v.1.6.0) and scDblFinder (v.1.4.0) R package.

Myeloma cells were identified by positive and negative selections. Normal bone marrow cells were identified and excluded (singleR v.1.4.1, downsampled late 2020 version of the Single-Cell Tumor Immune Atlas, TICAtlas_downsampled_1000.rds, available at https://doi.org/10.5281/zenodo.4263972) and cells having a plasma cell profile (with 5% or more UMI mapping to immunoglobin genes) were selected. In order to exclude normal remaining cells, we calculated two scores per cell based on gene expression using the AddModuleScore function (T/NK signature : *IL32, CD69, CCL5, CD52, BTG1, S100A4, RPS27, TMSB10, RPL31, ACTB, KLRB1, GZMK, CD3D, IL7R, NKG7*, and a light chain signature : *IGKC, IGLC1, IGLC2, IGLC3, IGLC4, IGLC5, IGLC6, IGLC7*): thresholds were determined to exclude these cells (two MAD above the median for NK/T signature, and three MAD below the median for the light chain signature). To exclude remaining normal plasma cells, we merged control and BH3 mimetics treated samples with plasma cells from normal bone marrow samples (merge function) and excluded "myeloma cells" that clustered with plasma cells. Then we identified highly variable genes (FindVariableFeature, nfeatures=2000, excluding immunoglobulin genes), and scaled the expression matrix with ScaleData function. Principal component analysis (PCA) was performed using the RunPCA function. We used the first 30 principal components to perform

unsupervised clustering analysis. We excluded cells clustering with normal cells for a resolution of 0.05, and manual curation was performed to exclude remaining cells having passed the lineage negative selection. The copy number variation profiles were inferred from scRNA-seq data, using inferCNV of the Trinity CTAT Project, https://github.com/broadinstitute/ inferCNV (v.1.9.1, default parameters for 10x Genomics data, cluster_by_groups=TRUE) and compared to plasma cells from normal bone marrow samples.

Following individual sample analysis, we performed a dataset merge to all the samples into a single dataset. We identified genes with significant variation across the dataset (FindVariableFeature, nfeatures=2000, excluding immunoglobulin genes) and a PCA analysis was performed on the 30 principal components for unsupervised clustering analysis. Samples were classified according to the myeloma molecular classification established by Zhan et al [2]: a score was calculated for each cell based on the gene expression list for each molecular subgroup. Finally, UMAP was used to visualize cell clustering.

Legends to Supplemental Tables

Table S1. *TP53* genomic sequence in CRISPR/Cas9 clones

Sanger genomic sequencing was performed in CRISPR/Cas9 clones. NAN3 *TP53*$^{-/-}$ #1 and *TP53*$^{-/-}$ #2 are identical. sgRNA sequence was designed to target aa 157-158 to impair all p53 isoforms.

Table S2. Differentially expressed genes in clones and HMCLs in function of *TP53* status

Gene expression profile was determined by DGE-Seq (A-D) or microarray (E). Differentially expressed genes in clones were identified using edgeR in clones or LIMMA in 43 HMCLs (microarray).

A, B, C, D: Gene differentially expressed between *TP53*$^{+/+}$ and *TP53*$^{-/-}$ cells in NCI-H929 (A), and XG7 (B), and between *TP53*$^{-/mut}$ and *TP53*$^{-/-}$ cells in NAN3 (C) and JIM3 (D).

E: Gene differentially expressed in 43 HMCLs according to *TP53* status

TP53^{wt} HMCLs : AMO1, BCN, MDN, MM1S, NAN9, NAN11, NCI-H929, SBN, XG3, XG6, XG7, XG10, XG12, XG19, XG21, XG24; *TP53*^{Abn} HMCLs: ANBL6, JIM3, JJN3, Karpas620, KMM1, KMS11, KMS12PE, L363, LP1, NAN1, NAN3, NAN6, NAN7, NAN8, NAN10, OPM2, RPMI8226, SKMM2, U266, XG1, XG2, XG5, XG11, XG13, XG14, XG16, XG20

Table S3. Genes differentially regulated by nutlin3a in *TP53*$^{+/+}$ and *TP53*$^{-/-}$ cells

Clones were treated overnight with 2 μM (XG7) or 10 μM nutlin3a (NCI-H929) and RNASeq was determined using DGE-Seq in triplicate wells. Only genes with significant changes (FDR<0.05, logFC<-0.5 or >0.5) in NCI-H929 and XG7 clones were kept, genes regulated by nutlin3a in *TP53*$^{-/-}$ clones were excluded (regulated by MDM2 but not by p53). Genes in bold represent the 16 genes identified in the absence of nutlin3a, 13 of them being involved in p53 score (by contrast, *MTM7* which was upregulated in *TP53*$^{-/-}$ cells was not found regulated by nutlin3a). Five genes i.e., *EPS8L2, FHL2*, *SESN1*, *SULF2*, *TP53I3,* belonging to the Li-Fraumeni signature were differentially expressed between *TP53*$^{+/+}$ and *TP53*$^{-/-}$ clones cultured with nutlin3a (underlined in the Table).

Table S4. p53 score in HMCLs

Gene expression profile of HMCLs was performed using DGE-Seq or microarray. The score was calculated using 13 genes (DGE-Seq) or 12 genes (microarray, none probe set specific for *APOBEC3H* being available). Characteristics of HMCLs were previously reported[3,4].

Table S5. p53 score in cancer cell lines

The p53 score was calculated in 1,105 cancer cell lines characterized for gene expression profile, *TP53* deletion and sequencing (DepMap portal). Significance of the score was assessed in function of the presence of *TP53* hit (deletion, mutation) in all cell lines and according to cancer types.

del: deletion, mut: mutation, Sarc: sarcoma, Gli: glioma, Mel: melanoma, Leuk: leukemia, Ly: lymphoma, My: myeloma

Table S6. p53 score in MYRACLE patients

CD138+ myeloma cells were purified from BM or PB of patient with myeloma and gene expression profiling was performed using DGE-Seq. The 13-gene p53 score was calculated using singscore package in R. Del17p and *TP53* sequencing were determined by FISH and Sanger sequencing in RT-PCR cDNA products. *TP53* hit was considered when deletion and/or mutation involved the majority of cells.

MM multiple myeloma, sPCL secondary plasma cell leukemia, pPCL primary plasma cell leukemia. D diagnosis, P progression, R relapse

Table S7. LD_{50} values of melphalan, nutlin3a and BH3 mimetics in control and *TP53*$^{-/-}$ clones

LD_{50} values of melphalan, nutlin3a, BH3 mimetics specific of MCL1, BCL2 or BCL-XL were determined in clones by Annexin V staining using flow cytometry after 24h (S63845, venetoclax, A1155463) or 48h (melphalan, nutlin3a) of treatment.

Table S8. LD_{50} values of BH3 mimetics in HMCLs

LD_{50} values of S63845, venetoclax and A1155463 in HMCLs were determined by Annexin V staining using flow cytometry after 24h of treatment. Characteristics of HMCLs were previously reported[3–5].

Table S9. *BAK1* and *BAX* genomic sequences in CRISPR/Cas9 clones

Sanger genomic sequencing was performed in CRISPR/Cas9 clones.

Table S10. Characteristics of patient samples analyzed using scRNAseq

The characteristics of the 24 patient samples analyzed using scRNASeq technology are indicated.

Sanger *TP53* sequencing was performed on RT-PCR cDNA products. Cell death was determined by flow cytometry after 24h-culture with BH3 mimetics combination

D Diagnosis, R relapse, MC molecular classification, UN unclassified, dup duplication, amp amplification

Legends to Supplemental Figures

Figure S1 Expression of the 17 genes differentially expressed between *TP53*$^{+/+}$ and *TP53*$^{-/-}$ cells in both NCI-H929 and XG7

RNA profiling of all NCI-H929 and XG7 clones was performed in triplicate and duplicate respectively by DGE-Seq[1]. Statistical analysis was performed using the Mann-Whitney test. Cells were cultured overnight with or without nutlin3a (2 or 10 μM for XG7 and NCI-H929 cells, respectively) prior to RNA extraction. *p<0.05, ** p<0.01, *** p<0.001, **** p<0.0001

Figure S2 p53 score in HMCLs according to *TP53* status and 14q32 translocation and in 1,105 cancer cell lines

A, B: Expression profile was performed using microarray[3]. Score was calculated with 12 probe sets because of the lack of *APOBEC3H* specific probe set.

A: HMCLs were segregated according to *TP53* status, wildtype versus abnormal (mutation and lack of expression).

B: HMCLs were segregated according to myeloma genomic group MS - t(4;14)-, MF - t(14;16) or -t(14;20), CCND1 - t(11;14)-, other and *TP53* status (wildtype or abnormal)[3]. Statistical analysis was performed using the Mann-Whitney test.

C: p53 score in 1,105 cancer cell lines. Score was analyzed in function of the presence of *TP53* hit (deletion, mutation) in carcinoma (left), in sarcoma, glioma and melanoma (middle) or leukemia, lymphoma and myeloma (right). Statistical analysis was performed using Kruskal-Wallis test with Dunn's multiple comparison test. Only significant differences were reported on the figure.

D: p53 score was analyzed in 1,105 cell lines according to gender status i.e., in female, male and in female versus male cell lines. Statistical analyses were performed using the Kruskal-Wallis test with multiple comparisons or with the Mann-Whitney test.

*p<0.05, ** p<0.01, *** p<0.001, **** p<0.0001

Figure S3 p53 score in CASSIOPEA and MMRF-coMMpass cohorts

A: the 13-gene p53 score was calculated in samples from 139 patients of CASSIOPEA cohort and K-means method segregated samples into 4 groups (left panel). Graphs represent OS in group 1 versus the other 3, represent OS according to risk classification or presence of del17p.

B: the 13-gene p53 score was calculated in samples from 764 patients of MMRF-coMMpass cohort and K-means method segregated samples into 4 groups (left panel). Middle graph represents the distribution of samples with *TP53* deletion or mutation or both within the 4 groups. VAF thresholds were set up at <-0.5 for deletion and >0.35 for mutation. Right graph represents the percentage of samples with *TP53* deletion, *TP53* mutation or both in each group. ** p<0.01, **** p<0.0001

Figure S4 Expression of the 10 genes involved in Li-Fraumeni score in NCI-H929 and XG7 clones.

RNA profiling of all NCI-H929 and XG7 clones was performed in triplicate and duplicate DGE-Seq[1], respectively. Statistical analysis was performed using the Mann-Whitney test. Cells were cultured overnight with or without nutlin3a (2 or 10 μM for XG7 and NCI-H929 cells, respectively) prior to RNA extraction.

*p<0.05, ** p<0.01, *** p<0.001, **** p<0.0001

Figure S5 Lack of efficacy of Li-Fraumeni score to discriminate clones, 1,105 cancer cell lines and patient samples according to *TP53* status

A, B: Li-Fraumeni and the 13-gene p53 scores were calculated in NCI-H929 (A) and XG7 (B) clones in the presence or absence of nutlin3a (overnight treatment with 2 or 10 μM in XG7 and NCI-H929 clones, respectively).

C,D: Li-Fraumeni score was calculated in 1,105 cancer cell lines (C) and in 38 samples (D) from patients with myeloma (MYRACLE cohort, see Table 1) according to the presence of *TP53* deletion and/or mutation.

*p<0.05, ** p<0.01, *** p<0.001, **** p<0.0001

Figure S6 BCL2 family expression profile of clones and HMCLs according to *TP53* status.

A, B: BCL2 family profile in NCI-H929, XG7, JIM3 and NAN3 $TP53^{+/+}$, $TP53^{-/m}$ and $TP53^{-/-}$ cells (A) and HMCLs (B) was performed by western blotting. Blue, red and orange colours indicate $TP53^{+/+}$, $TP53^{-/-}$ and $TP53^{-/mut}$ cells, respectively. Graphs represent the quantification of BAX and BAK over actin. Statistical analysis was performed using the Wilcoxon paired-signed rank test in clones (A) and the Mann-Whitney test in HMCLs (B).

Figure S7 Lack of impact of *TP53* silencing on global mitochondrial priming in NCI-H929 and XG7

Global mitochondrial priming was measured in isogenic NCI-H929 (left panel) and XG7 (right panel) $TP53^{+/+}$ (blue) and $TP53^{-/-}$ (red) clones by cytochrome c release using BIM and BMF peptides. Graphs represent 3 to 4 independent experiments. Statistical analysis was performed using the Mann Whitney test.

Figure S8 Role of BAK and BAX in the response to S63845

A. BAK or BAX protein expression in *TP53*$^{+/+}$#1 and *TP53*$^{-/-}$#1 XG7 cells transfected with si*BAK1* or si*BAX*. Results were expressed as the % of BAK and BAX expression in *TP53*$^{+/+}$#1 or *TP53*$^{-/-}$#1 XG7 transfected with siCont. Results are the mean ± SEM of 3 independent experiments. A representative western blot is shown in the right panel.

B. Expression of MCL1, BAK and BAX was determined in NCI-H929 *BAK1*$^{-/-}$ or *BAX*$^{-/-}$ clones by using Western Blotting.

C. Immunoprecipitation of MCL1 in the presence of S63845 in *TP53*$^{+/+}$#1 and *TP53*$^{-/-}$#2 NCI-H929 clones. NCI-H929 clones were treated for 3 hours with the indicated concentrations of S63845. Cells were lysed in 1 % digitonin-containing buffer and lysates were pre-cleared with protein A conjugated to sepharose beads. For IP assay, 0.7 mg of protein lysate was incubated overnight with an agarose-conjugated mAb anti-MCL1 from Santa Cruz Biotechnology. A representative experiment out of 3 is shown.

Figure S9 Lack of correlation between S63845 response and BCL2 family members in clones and HMCLs

Graphs represent the expression of the indicated BCL2 members in clones (DGE-Seq) and HMCLs (microarray) in function of S63845 LD_{50}. Probe sets were chosen according to their representativity of gene expression[6]. Statistical analysis was performed using the Spearman test.

Figure S10 Impact of t(11;14) in the response to BH3 mimetics combination

A. Death response in 42 MM samples without t(11;14) to S63845, venetoclax or their combination in function of the presence of del17p or 1q21 gain. Del17p was considered when it involved at least 50% of cells.

B. Death response in 18 MM samples t(11;41) to S63845, venetoclax or their combination in function of the presence of del17p or 1q21 gain.

Statistical analysis was performed using the Mann Whitney test.

Figure S11 Molecular classification of patient samples

A_ UMAP representation of myeloma cells from the 24 control and treated patient samples.

B_ UMAP representation of molecular classification score expression of patient samples based on Zhan molecular classification CD-1, CD-2, MS, HY, MF, LB, PR [2].

C_ UMAP representation of *CCND1*, *CCND2*, *FGFR3*, *FRZB*, *MAF*, *MAF-A*, *MAF-B*, *NSD2* gene expression.

Figure S12. BH3 mimetics induced changes in p53 score at single cell level

For each sample, control and BH3 mimetics-treated conditions were merged to identify clusters and UMAP representation was split into control and BH3 mimetics treated (BH3 m) conditions (up left panel). The graphs represent the 13-gene p53 score in each cluster (up right panel), the number of cells per cluster per condition (low and left panel) and the relative proportion of clusters (low right panel). Statistical analyses were performed using the Mann-Whitney test (paired clusters) or the Kruskal Wallis test (all clusters).

* p<0.05, ** p<0.01 , *** p<0.001, **** p<0.0001

Supplemental References

1. Charpentier E, Cornec M, Dumont S, et al. 3' RNA sequencing for robust and low-cost gene expression profiling. Protocol Exchange; 2021.
2. Zhan F, Huang Y, Colla S, et al. The molecular classification of multiple myeloma. *Blood*. 2006;108(6):2020–2028.
3. Moreaux J, Klein B, Bataille R, et al. A high-risk signature for patients with multiple myeloma established from the molecular classification of human myeloma cell lines. *Haematologica*. 2011;96(4):574–582.
4. Gomez-Bougie P, Maiga S, Tessoulin B, et al. BH3-mimetic toolkit guides the respective use of BCL2 and MCL1 BH3-mimetics in myeloma treatment. *Blood*. 2018;132(25):2656–2669.
5. Tessoulin B, Moreau-Aubry A, Descamps G, et al. Whole-exon sequencing of human myeloma cell lines shows mutations related to myeloma patients at relapse with major hits in the DNA regulation and repair pathways. *J Hematol Oncol*. 2018;11(1):137.
6. Tessoulin B, Papin A, Gomez-Bougie P, et al. BCL2-Family Dysregulation in B-Cell Malignancies: From Gene Expression Regulation to a Targeted Therapy Biomarker. *Front Oncol*. 2018;8:645.

Table S1. *TP53* genomic sequence in CRISPR/Cas9 clones

Clones	TP53 sequence	Location
NCI-H929 *TP53*$^{-/-}$#1	del8 (CGCGTCCG) + mut 1 (C>A)	del17:7,675,144-137 + mut17:7,675,148
	del27 (ACCCGCGTCCGCGCCATGGCCATCTAC) + ins 7 (CTTCTCC)	del17:7,675,149-124 + ins17:7,675,143-137
NCI-H929 *TP53*$^{-/-}$#2	del6 (TCCGCG) + del1 (C)	del17:7,675,142-137 + del17:7,675,157
	del7 (CCCGCGT)	del17:7,675,148-142
NCI-H929 *TP53*$^{-/-}$#3	ins1 (C)	ins17:7,675,139
	del17 (CCGGCACCCGCGTCCGC)	del17:7,675,154-138
XG7 *TP53*$^{-/-}$#1	del35 (CCGcgtccgcgccatggccatctacaagcagtCAC) + ins 1 (A)	del17:7,675,147-113 + ins17:7,675,147
	del8 (CGCGTCCG)	del17:7,675,146-139
XG7 *TP53*$^{-/-}$#2	del1686	
	del1686	
XG7 *TP53*$^{-/-}$#3	del8 (CGTCCGCG)	del17:7,675,144-137
	del8 (CGCGTCCG)	del17:7,675,146-139
NAN3 *TP53*$^{-/-}$#1	Monoallelic, ins1 (C)	ins17:7,675,140
NAN3 *TP53*$^{-/-}$#2	Monoallelic, ins1 (C)	ins17:7,675,140
NAN3 *TP53*$^{-/-}$#3	Monoallelic, ins1 (A)	ins17:7,675,142
JIM3 *TP53*$^{-/-}$#1	Monoallelic, del19 (CGGCACCCGCGTCCGCGCC)	del17:7,675,153-135
JIM3 *TP53*$^{-/-}$#2	Monoallelic, ins1 (C)	ins17:7,675,140
JIM3 *TP53*$^{-/-}$#3	Monoallelic, del8 (GTCCGCGC)	del17:7,675,143-136

Table S2. Differentially expressed genes in clones and HMCLs in function of *TP53* status
A. Gene differentially expressed in bulk *TP53*$^{+/+}$ cells and *TP53*$^{-/-}$ NCI-H929 clones

Down in *TP53*$^{-/-}$ clones	logFC	logCPM	PValue	FDR	regulation by p53
TP53	-3.501793728	3.231802957	1.61E-13	4.85E-10	
RPS27L	-1.676069199	8.337512154	7.09E-20	8.53E-16	early direct
CDKN1A	-3.784290017	4.086839461	8.76E-19	5.27E-15	early direct
DDB2	-2.17107005	4.639060343	4.12E-14	1.65E-10	early direct
FDXR	-2.248829737	2.818261774	5.36E-09	6.44E-06	early direct
APOBEC3C	-0.862526069	7.093881105	1.06E-08	1.16E-05	early direct
PHLDA3	-4.102949025	1.376719419	1.46E-08	1.46E-05	early direct
TNFRSF10B	-1.98964005	2.582373755	6.74E-07	0.000430895	early direct
EDA2R	-2.648651798	1.802449608	5.64E-06	0.002424831	early direct
BAX	-1.068609819	3.853008079	5.65E-06	0.002424831	early direct
MDM2	-1.998252535	6.948461139	1.03E-05	0.003416992	early direct
PTP4A1	-0.671149495	5.682103156	2.88E-05	0.008064268	early direct
RRM2B	-1.320444858	2.864096513	4.01E-05	0.010944719	early direct
POLH	-0.903880183	3.454295596	0.000291856	0.04331717	early direct
TIGAR (C12orf5)	-0.948917027	4.504209265	1.08E-05	0.003416992	early direct
APOBEC3H	-3.597283587	2.627577025	1.87E-11	3.75E-08	late with proximal TP53 binding
STK38L	-1.140821257	4.021943068	1.09E-06	0.00056192	late with proximal TP53 binding
APOBEC3G	-0.853628892	5.225853902	6.13E-06	0.002542547	late with proximal TP53 binding
APOBR	-2.067729689	1.721069341	8.72E-06	0.00326966	late with proximal TP53 binding
RPL22L1	-0.542601493	7.380154014	2.49E-05	0.00729496	late with proximal TP53 binding
LMNA	-0.61378733	6.235432831	2.88E-05	0.008064268	late with proximal TP53 binding
TRIAP1	-0.951615786	6.389473396	0.000125342	0.02554008	late with proximal TP53 binding
TIMM21	-0.620198757	7.235329333	0.000159567	0.029065295	late with proximal TP53 binding
S100A6	-0.879651731	8.561757883	3.36E-07	0.00025217	late without proximal TP53 binding
TUBB2A	-1.239448789	3.010425336	7.11E-05	0.016765792	late without proximal TP53 binding
LSM6	-0.461421345	7.406761797	8.80E-05	0.01987576	late without proximal TP53 binding
PDLIM1	-0.743778013	5.12044413	0.000148689	0.028220337	late without proximal TP53 binding
AURKA	-0.414561514	7.127280396	0.000150233	0.028220337	late without proximal TP53 binding
CDC45	-0.44364268	6.294974958	0.000191984	0.033941631	late without proximal TP53 binding
TNFSF9	-3.063086543	0.638115832	0.000264329	0.041269601	late without proximal TP53 binding
CAPG	-0.989241459	3.405322834	0.000273515	0.041622696	late without proximal TP53 binding
ARL4C	-2.340945304	2.71279237	2.10E-08	1.94E-05	late without proximal TP53 binding /translational
NES	-1.71030906	5.136189125	6.39E-06	0.002559933	late without proximal TP53 binding /translational
SH3BGRL3	-0.405291072	8.856497103	4.65E-05	0.012161221	late without proximal TP53 binding /translational
PYGB	-0.633532177	5.417758867	5.23E-05	0.013052689	late without proximal TP53 binding /translational
TUBB2B	-2.226330496	1.630200007	0.000208289	0.035772187	late without proximal TP53 binding /translational
APOBEC3B	-0.943830713	4.669574781	8.98E-06	0.00326966	translational
SEC11C	-0.407799292	9.391983595	0.000114823	0.024217531	translational
CCL5	-1.254657076	2.425753233	0.000253503	0.04118404	translational
RPL23AP7	-1.001055954	3.28005583	0.000332373	0.048141962	translational
FCRLA	-2.187629507	4.029532537	7.47E-13	1.79E-09	x

BTLA	-5.098294254	1.440544165	7.13E-10	1.22E-06	x
IRAG2	-2.344252116	3.867316499	3.06E-09	4.09E-06	x
MEI1	-1.73568358	3.309650861	4.64E-08	3.98E-05	x
EAF2	-1.125723072	5.778939696	7.20E-08	5.77E-05	x
NCKAP1L	-1.263688144	4.016029672	6.81E-07	0.000430895	x
BUB3	-0.561912513	8.312443066	8.41E-07	0.000481534	x
MSL3	-0.923775332	4.824948873	1.12E-06	0.00056192	x
RAC2	-0.636273989	7.470940852	1.12E-06	0.00056192	x
CD28	-0.728839953	6.061608102	4.16E-06	0.001924469	x
RIPOR2	-2.480093368	1.671929083	8.18E-06	0.003172272	x
HCLS1	-0.586472138	7.085115457	9.31E-06	0.003291823	x
MEF2C	-0.536414394	6.778929899	1.10E-05	0.003416992	x
BTK	-0.939010585	4.11545813	1.46E-05	0.004380148	x
PLAAT2	-0.514949966	8.104802019	4.28E-05	0.011436129	x
GPRC5D	-0.961509133	5.163130893	5.32E-05	0.013052689	x
LINC02245	-2.64523867	1.131900671	5.87E-05	0.014110824	x
CCDC88B	-1.52191491	2.381180039	8.93E-05	0.01987576	x
C16orf87	-0.656361989	4.686909316	0.000106925	0.022954572	x
HOOK3	-0.512739752	6.730761425	0.000131351	0.026318295	x
PALM2AKAP2	-0.426598152	7.299917854	0.000148194	0.028220337	x
SEL1L3	-0.618102985	5.102635037	0.000158232	0.029065295	x
NKG7	-2.380728944	1.727655637	0.000172536	0.030958584	x
FCRL2	-1.417209568	2.158139749	0.00020456	0.035640821	x
PNOC	-0.901843094	3.492562857	0.000221281	0.036947719	x
LNCTAM34A	-4.846675868	0.338222114	0.000236898	0.039013538	x
NUDCD3	-0.631434858	5.11403732	0.000263481	0.041269601	x
IGLL5	-0.452187905	11.25528923	0.000259484	0.041269601	x
RAP1A	-0.491953241	5.918227173	0.000271254	0.041622696	x
PPP1R16B	-0.668533237	5.03215667	0.000291116	0.04331717	x
CRYBB1	-1.172099789	2.93047278	0.000306233	0.044896795	x
Up in *TP53*$^{-/-}$ clones	**logFC**	**logCPM**	**PValue**	**FDR**	**regulation by p53**
FGFR3	1.975827761	4.293019628	1.30E-09	1.96E-06	late without proximal TP53 binding
CDKN2C	0.551420942	7.008633521	4.14E-06	0.001924469	late without proximal TP53 binding
PTP4A3	1.762467894	3.35217198	1.11E-05	0.003416992	late without proximal TP53 binding
CD320	0.425068074	8.676835734	0.000105586	0.022954572	late without proximal TP53 binding
APC	1.28278445	3.158581021	0.000121612	0.025207149	late without proximal TP53 binding
CMTM7	1.368957625	3.693147933	9.81E-06	0.003370418	translational
MT1F	1.370678433	5.077448134	7.60E-07	0.000456999	translational
VCX	1.365234728	4.18060449	4.24E-07	0.000299536	x
BMP7	2.629695073	2.245277379	5.29E-05	0.013052689	x
MT1G	2.683923826	3.448855014	7.68E-05	0.017751155	x
MIR4435.2HG	0.481575847	6.226048318	0.000143357	0.028220337	x
TUBA4A	0.398364415	7.712928107	0.000215831	0.036545307	x

B. Gene differentially expressed in *TP53*$^{+/+}$ cells and *TP53*$^{-/-}$ XG7 clones

Down in *TP53*$^{-/-}$ clones	logFC	logCPM	PValue	FDR	regulation by p53
TP53	-2.94376044	3.244739525	8.60E-14	2.45E-10	
RPS27L	-1.465101169	9.345294869	1.36E-22	1.55E-18	early direct
DDB2	-1.858645628	5.242955175	4.13E-19	2.35E-15	early direct
MDM2	-1.841784614	6.752976254	1.05E-18	3.99E-15	early direct
PHLDA3	-2.492309058	3.206011505	2.70E-12	4.39E-09	early direct
CDKN1A	-1.587534277	4.970879438	1.39E-11	1.76E-08	early direct
TM7SF3	-1.137638508	4.758151693	8.42E-10	8.00E-07	early direct
APOBEC3C	-0.646152177	6.769198748	6.06E-09	4.94E-06	early direct
RRM2B	-1.369010239	3.754302761	1.10E-08	8.36E-06	early direct
TNFRSF10B	-1.855029786	3.197052406	3.59E-08	2.56E-05	early direct
BAX	-1.151342589	3.606209899	1.66E-07	9.97E-05	early direct
EDA2R	-1.818458757	2.131150972	1.60E-06	0.000758412	early direct
TIGAR	-0.73666933	5.080089513	1.51E-06	0.000758412	early direct
RPS19	-0.374378409	13.26195075	3.96E-06	0.001734219	early direct
ZMAT3	-1.670662005	2.096164692	1.09E-05	0.003885987	early direct
CYFIP2	-1.049023734	3.738983223	2.78E-05	0.008125584	early direct
FDXR	-1.032794234	3.419578855	2.75E-05	0.008125584	early direct
CCNG1	-0.334911345	7.558404446	3.31E-05	0.008974604	early direct
PTP4A1	-0.556889995	5.022897412	0.000101102	0.021252894	early direct
APOBEC3H	-1.9636601	1.926484143	8.58E-06	0.003197793	late with proximal TP53 binding
PLXNB2	-3.425168709	2.482232748	2.96E-11	3.37E-08	late with proximal TP53 binding
PHPT1	-0.435364282	8.094844798	1.15E-06	0.000626404	late with proximal TP53 binding
F2R	-1.237839623	5.113924848	2.66E-13	6.06E-10	late without proximal TP53 binding
TNFSF9	-2.564190923	2.804710466	3.52E-11	3.65E-08	late without proximal TP53 binding
CD70	-0.829427722	5.843356643	3.14E-09	2.75E-06	late without proximal TP53 binding
VAMP8	-0.447937585	7.088147835	1.57E-06	0.000758412	late without proximal TP53 binding
PTP4A3	-0.565296122	5.541140277	5.55E-06	0.00230859	late without proximal TP53 binding
RPL13A	-0.328545239	10.11091478	5.67E-06	0.00230859	late without proximal TP53 binding
ARAP1	-1.067769202	3.206313043	1.90E-05	0.006188557	late without proximal TP53 binding
GAMT	-0.583617946	5.005327868	9.23E-05	0.020227022	late without proximal TP53 binding
OPTN	-0.579159212	4.780830926	9.49E-05	0.020407506	late without proximal TP53 binding
CAB39	-0.996717738	3.595996819	0.000102554	0.021252894	late without proximal TP53 binding
FUCA1	-1.333126727	2.646895478	0.000118718	0.022934741	late without proximal TP53 binding
PVT1	-1.248909232	2.57271666	0.000117602	0.022934741	late without proximal TP53 binding
CDIP1	-0.999225186	2.959288513	0.000148923	0.027920267	late without proximal TP53 binding
GSTM4	-0.798576998	3.705075597	0.000181755	0.032883141	late without proximal TP53 binding
GRK6	-1.114230456	2.993051653	0.000197515	0.032926152	late without proximal TP53 binding
SLC2A1	-0.755956199	3.980265794	0.000224778	0.035583651	late without proximal TP53 binding
HBEGF	-0.869640575	4.64895303	3.65E-07	0.000208198	translational
TGFBR3L	-2.579703346	1.552872421	4.48E-05	0.011615087	translational
NECTIN4	-1.244503762	5.204472649	2.46E-12	4.39E-09	x
IFNG	-0.774501189	4.83938164	5.00E-05	0.012673276	x

MACF1	-0.860286964	3.605089258	6.83E-05	0.015898674	x
TRPM8	-2.547574021	1.403034399	8.13E-05	0.018179647	x
WIPF1	-0.877532564	3.462574821	8.05E-05	0.018179647	x
TRAPPC8	-1.248166288	2.545364174	0.000110242	0.022044602	x
POU2AF1	-0.657695589	4.371844263	0.0001092	0.022044602	x
ENO3	-0.671890506	4.566283532	0.000198893	0.032926152	x
RHOBTB3	-0.573610775	5.978891822	0.000197101	0.032926152	x
TOP2B	-0.585969501	4.661310122	0.000209651	0.034137146	x
DGKG	-2.192178219	1.319649215	0.000279374	0.042457434	x
ABCB10	-0.845629134	3.917107531	0.000292043	0.043798725	x
Up in *TP53*$^{-/-}$ clones	**logFC**	**logCPM**	**PValue**	**FDR**	**regulation by p53**
NPM3	1.205019153	5.275362834	1.06E-11	1.52E-08	late without proximal TP53 binding
PRMT1	0.61157384	6.718120363	4.83E-08	3.24E-05	late without proximal TP53 binding
ISOC2	0.954656521	4.587782753	7.27E-08	4.61E-05	late without proximal TP53 binding
RDH13	1.051861654	4.165626516	1.21E-05	0.004112424	late without proximal TP53 binding
BCL2L12	0.703892714	4.845834028	2.78E-05	0.008125584	late without proximal TP53 binding
NDUFAB1	0.330178709	8.36579862	2.62E-05	0.008125584	late without proximal TP53 binding
NHP2	0.411794005	7.371697164	3.15E-05	0.008767474	late without proximal TP53 binding
PHB	0.331733675	8.223040514	5.94E-05	0.014441591	late without proximal TP53 binding
GRPEL1	0.394397076	8.031989428	6.14E-05	0.01457615	late without proximal TP53 binding
EIF5	0.307553421	7.919958447	0.00016441	0.030224832	late without proximal TP53 binding
TFAM	0.439044897	6.918496432	0.000196874	0.032926152	late without proximal TP53 binding
TMSB10	0.358375552	12.19052095	1.23E-05	0.004112424	late without proximal TP53 bindingl/translational
CMTM7	0.692108276	4.890000703	8.70E-06	0.003197793	translational
ZMAT2	0.610887923	5.528416993	3.78E-06	0.001723557	x
CSH1	5.183699381	0.883513338	6.85E-06	0.002692109	x
FAM3B	3.192948535	4.754717814	2.91E-05	0.008284631	x
ISG20	0.59029728	5.74306498	3.50E-05	0.009266358	x
RABEP1	0.777524394	4.361256966	5.96E-05	0.014441591	x
PAGE1	2.320534476	2.513811338	0.000149424	0.027920267	x
LENG1	0.643668024	4.358287842	0.000197326	0.032926152	x
SMIM4	0.401190601	5.962079602	0.000199325	0.032926152	x
EIF1AX	0.354917827	7.322905463	0.000214233	0.034392013	x
SPRR2D	2.077700175	1.455532849	0.000250095	0.038521333	x
CDA	1.624196836	2.34129003	0.000247827	0.038521333	x
BZW2	0.287218756	7.496520535	0.00030539	0.045205641	x

C. Gene differentially expressed in bulk *TP53*$^{-/mut}$ and *TP53*$^{-/-}$ JIM3 clones

Down in *TP53*$^{-/-}$ clones	logFC	logCPM	PValue	FDR	regulation by p53
TP53	-2.711567123	2.407157805	6.16E-09	7.24E-05	
MRPS26	-0.547165442	5.836367513	3.57E-05	0.034953198	late without proximal binding
MRPS34	-0.461797795	8.701644987	3.18E-06	0.0062339	late without proximal binding
TRAP1	-0.466130372	6.535735809	7.09E-05	0.059454106	late without proximal binding
INSC	-4.347038396	1.095077766	2.28E-07	0.00134116	x
RYR2	-3.661886341	1.004601308	1.56E-05	0.020352083	x
CCDC30	-2.031478928	2.136024214	8.65E-06	0.012707347	x
FES	-0.629824686	5.994227765	3.39E-05	0.034953198	x
ZNF207	-0.361812857	8.048464987	4.51E-05	0.04076773	x
Up in *TP53*$^{-/-}$ clones	**logFC**	**logCPM**	**PValue**	**FDR**	**regulation by p53**
MT2A	0.660808308	7.26829682	5.98E-06	0.010039066	translational
H2BC12	0.375459727	9.245734323	3.38E-05	0.034953198	x
H1.2	0.494862148	8.903377389	1.13E-06	0.002651942	x
DNAJC15	0.640127975	7.354968365	4.20E-07	0.001642677	x
H4C15	0.7509537	6.411083395	7.34E-07	0.002155476	x

D. Gene differentially expressed in bulk *TP53*$^{-/mut}$ and *TP53*$^{-/-}$ NAN3 clones

Down in *TP53*$^{-/-}$ clones	logFC	logCPM	PValue	FDR	regulation by p53
TP53	-3.079501832	2.431151916	9.97E-12	1.14E-07	
ICAM4	-3.665391984	0.89683443	2.49E-06	0.007141008	late with proximal binding
CD79B	-0.885456665	4.58275363	4.70E-06	0.010767353	translational
PARVG	-3.342722183	1.124281991	1.48E-06	0.005659577	x
Up in *TP53*$^{-/-}$ clones	**logFC**	**logCPM**	**PValue**	**FDR**	**regulation by p53**
C3orf14	0.604609873	6.520968103	1.11E-05	0.018839207	late without proximal binding
RIPOR2	1.008334359	5.440562553	2.60E-07	0.001490182	x
HBB	0.894297521	5.174830109	1.15E-05	0.018839207	x
SCN3A	2.4291372	2.521565229	2.20E-05	0.031491029	x
UNC13C	0.931640579	4.46769433	3.00E-05	0.038232446	x

E. Gene differentially expressed in HMCLs according to *TP53* status

Down in *TP53* abnormal HMCLs	logFC	AveExpr	P.Value	adj.P.Val	regulation by p53
MDM2	-3.633724513	5.162576728	4.78E-09	8.91E-05	early direct
FDXR	-2.338116717	7.874285435	3.33E-07	0.003101088	early direct
DDB2	-1.570834345	8.956423863	1.38E-06	0.008553507	early direct
PHLDA3	-2.079940364	3.536698496	6.67E-06	0.02483222	early direct
CDKN1A	-3.094532843	10.60484667	1.52E-05	0.047294991	early direct
Up in *TP53* abnormal HMCLs	**logFC**	**AveExpr**	**P.Value**	**adj.P.Val**	**regulation by p53**
CDKN2A	2.669332443	8.052466071	4.15E-06	0.019312658	x

Table S3. Genes differentially regulated by nutlin3a in *TP53*$^{+/+}$ and *TP53*$^{-/-}$ cells

	NCI-H929			XG7		
name	logFC	logCPM	pValue	logFC	logCPM	pValue
LCE1C	8.186184048	6.102325645	2.81E-22	2.719552407	1.507660396	0.001418
MDM2	5.539376587	9.681043386	3.8E-21	5.176850172	9.613365019	1.76E-41
LCE1B	8.06663017	5.740713244	9.04E-20	5.195104635	2.745697561	0.000000
RPS27L	3.379583897	9.859830129	1.07E-19	2.410513593	10.09567459	1.01E-29
APOBEC3H	5.563559848	5.181906532	3.35E-19	5.493350868	4.22675317	4.8E-27
FDXR	5.596792387	5.306155663	5.44E-18	3.972463563	5.737289398	2.81E-30
NECTIN4	7.890110664	4.125956755	0.000000	4.122166944	7.166595927	1.13E-35
TRIAP1	2.578125263	7.591876831	0.000000	1.743080725	7.126436252	2.67E-22
DDB2	3.459534545	5.746115628	0.000000	3.528444329	6.54966366	8.04E-33
LCE1E	8.284247813	4.208073522	0.000000	5.698627165	3.193437627	0.000000
LNCTAM34A	9.134135643	4.013429889	0.000000	5.008653774	2.58700571	0.000000
CDKN1A	7.819472702	7.996582496	0.000000	6.04104098	8.929117798	5.55E-32
APOBEC3C	2.813751226	8.7822062	0.000000	2.563938178	8.142532198	5.17E-30
TP53I3	6.018105769	6.50421779	0.000000	2.890777294	6.041756133	1.25E-18
GAMT	2.852995666	6.268838179	0.000000	1.661150433	5.56088038	0.000000
ZNF561.AS1	4.493761665	3.883484943	0.000000	3.647635793	3.046307562	0.000000
CPM	6.962200537	3.097931758	0.000000	3.808731954	2.071829579	0.000000
CA10	7.213754673	3.011465418	0.000000	6.671475816	1.889642544	0.000000
PRMT7	3.639756558	4.564811226	0.000000	2.183816173	4.704669582	0.000000
TIGAR	3.211791247	5.25652581	0.000000	2.359815019	6.052102506	9.12E-24
UBE2C	-2.85168962	6.912750088	0.000000	-2.147955399	6.176976237	0.000000
POLH	3.403888018	4.615720673	0.000000	1.896044603	4.56144615	0.000000
PHLDA3	9.555761099	3.302032503	0.000000	4.318996918	4.170660579	8.38E-23
DUSP14	2.352228054	5.490871973	0.000000	1.165935481	5.164290475	0.000000
TUBB	-2.016931742	10.16138172	0.000000	-0.725463389	10.58626691	0.000000
GDF15	7.860780883	2.625029042	0.000000	5.574293213	3.536843494	0.000000
GADD45A	4.147196046	5.765928988	0.000000	3.112676055	5.141318187	0.000000
CYSRT1	5.480347287	3.07206199	0.000000	5.758931784	2.557517071	0.000000
EI24	1.822738926	6.809161454	0.000000	0.58696498	4.427581981	0.000734
ISCU	2.110511481	6.561145895	0.000000	1.052046982	6.266897877	0.000000
CCNB1	-1.981662383	8.261207719	0.000000	-2.224075713	7.985703412	0.000000
PBK	-2.678507728	6.338219068	0.000000	-2.02351651	5.798968757	0.000006
CYRIA	4.589356574	3.423726582	0.000000	1.680595309	2.770716328	0.000000
BLOC1S2	2.258254639	5.417498393	0.000000	1.41777838	5.892168935	0.000000
ACTA2	7.59583506	2.362116264	0.000000	3.703571765	2.405386357	0.000000
TUBA1B	-1.794212103	10.22133141	0.000000	-1.020763986	10.9564581	0.000000
BAX	2.733470199	4.435001246	0.000000	2.010376014	4.131262732	0.000000
CDIP1	2.753755819	4.666836313	0.000000	1.282391357	3.46787024	0.000000
F2R	2.358775256	5.374276745	0.000000	2.207842214	5.762909309	1.09E-21
NADSYN1	2.564387809	4.474904182	0.000000	0.84712806	5.320915969	0.000000
BTG2	2.41380281	4.990454649	0.000000	2.95855251	4.507775216	0.000000
TP53	3.103855768	3.681593636	0.000000	2.674057947	3.425492552	0.000000
ANXA4	2.748300635	4.373784251	0.000000	1.981609706	5.916807146	1.54E-21
CKS1B	-1.665838342	9.680050577	0.000000	-1.81783949	9.030744033	0.000000
MAD2L1	-1.835279922	7.201205024	0.000000	-1.763755394	6.386200976	6.38E-20
TUBA4A	-2.244862161	6.798386659	0.000000	-1.316127793	6.988166301	0.000000
PXT1	6.72991531	2.501570298	0.000000	6.770580171	4.459053843	2.43E-25
RRM2B	3.021895125	3.63383109	0.000000	3.152383715	5.016896574	1.06E-24
CD28	1.83911418	6.392910938	0.000000	0.539189697	6.353084094	0.000000
NDUFAF8	1.528740699	7.149821412	0.000000	1.320195467	6.973057971	0.000000
LCE1F	7.252414408	2.011354337	0.000000	4.214234333	0.542233309	0.000471
LINC02303	8.915064123	2.600870864	0.000000	4.811147009	0.772671565	0.000022
SKA1	-2.552572325	5.681178553	0.000000	-2.420785255	5.381337092	1.6E-20
CCDC57	2.447729885	4.821778766	0.000000	1.282684295	3.875909777	0.000000
GINS2	-1.857105034	6.569508772	0.000000	-0.679103529	5.392724534	0.000000
TNC	4.694013206	4.470204656	0.000000	5.037000322	4.203569148	0.000000
PHPT1	1.47614539	9.264156976	0.000000	1.339805882	8.700685234	0.000000
AMZ2	1.788447131	6.375777567	0.000000	1.604917987	6.58830497	1.5E-20

NDC80	-2.489376071	5.574178003	0.000000	-2.047455141	4.851536721	0.000000
RHOC	1.689066817	6.907435546	0.000000	1.573358255	6.291449582	1.07E-19
ASCC3	2.073766524	4.766011984	0.000000	1.769783483	5.046382101	0.000000
NUSAP1	-2.011083478	6.66207871	0.000000	-1.124999494	6.873065723	0.000000
BLVRB	2.201484026	5.375407402	0.000000	0.830884352	6.690075216	0.000000
CCDC90B	1.935442339	6.177774332	0.000000	1.897607341	6.81948534	4.21E-23
LINC00537	2.94993145	3.841288333	0.000000	1.975190575	2.917312781	0.000000
MINCR	3.171870707	3.410207829	0.000000	1.07600144	5.731866839	0.000000
KIF2C	-2.247684655	5.597737601	0.000000	-2.140528353	5.597887261	0.000000
NEAT1	3.113190241	5.650214993	0.000000	0.654921087	5.83849782	0.000000
CACYBP	-1.451210044	8.310194698	0.000000	-0.970326912	9.664998963	0.000000
PXDN	5.374129327	1.868077998	0.000000	1.3101927	4.377699641	0.000000
COL6A2	2.391776486	4.172310714	0.000000	0.734352012	3.470609134	0.002406
YPEL5	1.766262053	5.101037358	0.000000	0.96270566	4.170221346	0.000000
TMEM68	1.483624461	5.933435587	0.000000	1.34201627	5.515526237	0.000000
SORL1	5.116744719	2.166619955	0.000000	1.704775994	1.02636054	0.008835
XPNPEP1	1.526035072	6.245559208	0.000000	1.415189291	7.233322297	3.61E-20
TNFSF9	5.229961371	2.318864506	0.000000	2.986136382	3.557797444	0.000000
CDC20	-2.286234202	5.427306156	0.000000	-2.572750248	5.786092215	2.17E-23
WDR1	1.490055993	5.878391049	0.000000	0.587243619	5.449644445	0.000000
CYFIP2	2.585465739	4.795420269	0.000000	2.163091146	4.528127326	0.000000
CCNB2	-1.65920599	6.522849175	0.000000	-1.367473735	5.886429184	0.000000
PGF	6.408928373	1.864678526	0.000000	5.224425958	2.486756088	0.000000
RRM2	-2.175135273	5.912380166	0.000000	-1.295509041	6.566052227	0.000000
EPS8L2	2.87342253	3.276976204	0.000000	3.658017032	1.592244072	0.000000
PLK1	-2.166484554	5.308797555	0.000000	-2.513574039	5.412693642	2.05E-20
ASTN2	3.023863288	3.058418858	0.000000	2.12101775	2.995233686	0.000000
RFC5	-2.040090128	5.274132457	0.000000	-0.703848456	5.379244886	0.000002
HMGB2	-1.669930493	9.462601893	0.000000	-1.463816483	9.727129897	0.000111
LMNA	2.028816442	6.358941539	0.000000	0.864396697	6.382508378	0.000000
RPS19	1.192831925	14.37932388	0.000000	0.876063793	13.51711739	0.000000
NUF2	-2.257967015	5.330478421	0.000000	-1.866092953	5.725148166	0.000000
GPX1	1.4577454	6.212142334	0.000000	1.254188717	4.925954936	0.000000
CHEK1	-1.959437103	5.697955363	0.000000	-0.67649611	4.024870552	0.000924
MYO9B	2.493950664	3.303639391	0.000000	1.24311582	3.527286164	0.000001
CSKMT	1.730752992	5.673368205	0.000000	0.520361672	5.524688561	0.000000
EDA2R	4.012989165	2.547278117	0.000000	3.765839927	3.147430342	0.000000
CYP4F3	8.079461201	1.831797656	0.000000	5.770670949	2.55240988	0.000000
GABPB1.AS1	2.330530478	3.65329349	0.000000	0.869183755	2.641971384	0.008538
LOC283710	3.909544345	2.603277023	0.000000	1.10603994	3.639811363	0.000326
MCM10	-2.785131136	4.688912618	0.000000	-1.924994912	4.83246742	0.000000
TNFRSF10B	2.7451281	3.337067432	0.000000	2.823710558	3.9407073	0.000034
DINOL	6.103703718	1.551365224	0.000000	5.098089962	0.907563353	0.000001
CDCA8	-1.689864003	5.84062689	0.000000	-2.154069542	5.474165828	0.000000
FBXO22	1.683268805	5.100044583	0.000000	1.210233977	4.941738201	0.000000
CDC6	-1.584927004	6.075519975	0.000000	-0.667433647	5.713348673	0.000001
KPNA2	-1.212786419	7.640815756	0.000000	-1.703503793	7.753981146	3.15E-22
UBE2T	-1.481471292	6.972312126	0.000000	-0.794838822	7.481221593	0.000000
BUB1	-1.938893058	6.069441158	0.000000	-1.623204216	6.42830303	8.84E-20
CDK1	-1.55608725	6.272645002	0.000000	-0.889547352	7.588597098	0.000000
SORBS1	4.508668334	1.733231967	0.000000	2.294498655	1.277158537	0.000283
INKA2	3.683711093	2.472339078	0.000000	3.626635587	1.934302978	0.000000
CEBPZOS	1.64375243	5.119858759	0.000000	0.89834088	5.655717715	0.000000
HMGN2	-1.249078716	9.093103546	0.000000	-0.612947386	8.43141924	0.000000
AURKA	-1.540048765	6.229293916	0.000000	-1.257652351	5.793805637	0.000000
C6orf52	2.635513215	3.264932586	0.000000	0.865762262	2.82317957	0.002590
EEF1E1	-1.267899088	7.256369836	0.000000	-0.527041631	7.080242735	0.000006
TTK	-2.951830933	4.460062629	0.000000	-2.098891451	4.623491432	0.000000
PRKAB2	2.596280301	3.320161278	0.000000	1.751625838	3.880957409	0.000000
PINCR	6.40426355	1.325756651	0.000000	3.689860614	1.118525135	0.000002
ARF4.AS1	2.674939093	3.658032345	0.000000	1.045397983	2.561997699	0.000784
HSDL2	1.949888287	4.566429826	0.000000	1.188824519	5.598346019	0.000000
CBX3	-1.170332929	7.92586775	0.000000	-0.650080589	8.498172385	0.000000

Table S3-2

CENPN	-1.339509533	7.015007195	0.000000	-1.269034031	5.595149582	0.000000
CLSPN	-2.494409228	4.933807657	0.000000	-0.959858758	5.518941934	0.000000
C6orf226	2.492285115	3.243781104	0.000000	1.77975854	1.245010398	0.001728
CKS2	-1.20798693	8.582922519	0.000000	-1.337292561	9.137706293	1.74E-19
H2AZ1	-1.268213715	10.49270337	0.000000	-1.093627016	9.89305833	0.000000
GBE1	2.365324032	3.544954935	0.000000	1.19176898	4.951424926	0.000000
FABP5	-1.046459604	9.324740061	0.000000	-0.57925968	9.335208805	0.000000
PHF19	-1.470873696	6.019647905	0.000000	-0.593559013	8.105768509	0.000000
HJURP	-2.211629774	4.747865814	0.000000	-2.046217945	3.725307977	0.000000
CHAF1A	-2.851433468	4.262621281	0.000000	-0.665442662	4.008608828	0.000813
BLNK	2.105540266	3.904258019	0.000000	2.481914557	3.621040343	0.000000
DHFR	-1.531979852	6.261322215	0.000000	-0.90219534	6.185102654	0.000000
UBE2S	-1.793830693	6.136031744	0.000000	-2.099298889	7.09136113	0.000013
NORAD	1.497126643	5.217402706	0.000000	0.750708316	4.728490263	0.000020
XPC	2.552720584	3.834625477	0.000000	2.306600849	4.779637897	4.44E-19
PURPL	3.16763793	5.574825401	0.000000	1.694304391	3.083600112	0.000000
POLR3K	-1.065778401	8.057843881	0.000000	-0.630144998	7.852272693	0.000000
AURKB	-1.595954467	6.642422893	0.000000	-1.791970589	6.31365772	0.000000
TMPO	-2.050511503	5.0134611	0.000000	-0.793385562	5.489419722	0.000000
PVT1	3.410885071	2.97673831	0.000000	2.134389656	3.072493196	0.000000
TK1	-1.389129986	6.413747018	0.000000	-1.332145283	6.699139493	0.000000
FAS	4.098497294	2.081947932	0.000000	1.531935071	4.420022057	0.000000
BIRC5	-1.596502686	5.880106463	0.000000	-2.009106914	6.0908844	0.000000
PTP4A1	1.49127727	5.051042135	0.000000	1.047443552	5.366670071	0.000000
S100A11	1.15811391	10.97531246	0.000000	0.515647466	11.25302246	0.000000
FUCA1	3.831758819	3.874659966	0.000000	3.658372369	4.494690328	0.000000
DUT	-1.87402639	5.971903351	0.000000	-0.580289306	6.626847681	0.001263
DTL	-2.482769565	4.503172102	0.000000	-0.502169962	4.880912004	0.003997
MAGEA4	0.991230662	8.389619264	0.000000	0.665503295	8.308339464	0.000000
KANK3	5.924254651	1.468103472	0.000000	3.106607773	0.58130731	0.002361
BUB1B	-2.476331493	4.441569274	0.000000	-1.800511336	4.552633056	0.000000
TP53INP1	3.786159795	2.05259539	0.000000	1.944239466	3.220676293	0.000000
SUSD6	2.367368179	3.135814533	0.000000	1.098869918	3.302855726	0.000016
TUBA1C	-1.330297627	7.751985963	0.000000	-1.117258136	8.274130572	0.000000
DNAJC21	1.740006721	4.459283894	0.000000	0.638508959	4.13064862	0.001277
TYMSOS	3.604912364	4.554842376	0.000000	1.940958227	3.847252963	0.000000
FEN1	-1.140649153	6.883373268	0.000000	-0.616841321	6.975404986	0.000000
KNSTRN	-1.42637803	5.681886112	0.000000	-1.221793333	5.525518708	0.000000
NCAPD3	-1.685038517	5.171869401	0.0000000104	-0.615847135	3.798642113	0.005562
SYNCRIP	-1.28291262	7.109727568	0.0000000116	-0.653107384	7.982885302	0.000000
DLGAP5	-2.486353097	4.768856198	0.0000000125	-1.661655465	5.304273962	0.000000
AHCY	0.970945229	8.645335074	0.0000000134	0.569503098	8.480475006	0.000000
PRKX	3.370226727	2.496534399	0.0000000135	0.913905718	2.908927884	0.001435
CDCA5	-2.577384812	4.328013409	0.000000014	-1.866867971	4.074181939	0.000000
NUP35	-2.10427448	4.456830331	0.0000000163	-1.052784853	4.74307569	0.000000
PRC1	-2.005408596	5.252901998	0.000000017	-1.945541109	5.335529752	0.000000
PIDD1	4.102011131	1.869621709	0.0000000177	2.265573792	2.396370531	0.000000
HMGB1	-1.076877967	9.121544676	0.0000000186	-1.164203048	9.348742341	0.000000
NCAPH	-1.95243316	4.906197886	0.000000019	-2.319644879	5.265727153	0.000000
RFC3	-1.950491789	5.008154	0.0000000197	-1.314846031	4.311776826	0.000000
LOC100294145	1.543507569	4.665925483	0.0000000205	1.581547287	4.805692861	0.000000
LINC01480	3.01965377	9.942336441	0.0000000211	3.115707149	10.45159922	0.000000
LRP10	1.894603905	4.042846698	0.0000000214	1.385885884	3.503435174	0.000000
RAD51AP1	-1.864470695	4.707427175	0.0000000215	-1.199423811	3.971069109	0.000000
GRN	1.762873514	6.165241524	0.0000000238	0.698342691	5.449373741	0.000004
SRA1	1.101908813	6.275540123	0.0000000244	0.640010192	6.358236908	0.000000
SLC30A1	2.155967266	3.162123611	0.000000025	0.887242551	4.16584092	0.000554
EXO1	-3.26039137	3.830360366	0.0000000314	-2.124416076	4.055686743	0.000000
LOC105371855	7.396044359	1.263139547	0.0000000323	5.155094449	0.938585197	0.000009
RANBP1	-1.383567285	5.886932164	0.0000000346	-0.653893566	6.654144295	0.000000
ATAD2	-1.954870946	4.410504899	0.0000000392	-0.896973155	4.63996931	0.000001
CKAP2L	-3.672572313	3.686273009	0.0000000398	-2.136275484	3.511905091	0.000000
SLC35D1	2.097867846	3.318058771	0.0000000399	1.343701104	2.99833161	0.000001

Table S3-3

EMG1	-1.251422152	6.512878845	0.0000000421	-0.559954277	6.721427363	0.000000
FAM13C	5.982145332	1.057460616	0.0000000434	3.313574007	0.939124172	0.000228
PRKAB1	2.235350466	3.127182666	0.0000000455	0.811027076	3.149719829	0.002197
DKC1	-1.055830807	7.144546171	0.0000000457	-0.601740421	6.839812214	0.000000
SESN1	3.145771679	2.532602077	0.0000000518	4.127612618	3.537807227	7.76E-20
ARAP1	2.470995408	3.178415263	0.000000054	1.129233123	3.574706266	0.000012
BTBD10	1.704155395	4.398699828	0.000000057	0.918797909	4.449543572	0.000001
LOC105371267	7.231234011	1.151021643	0.0000000663	5.045885909	0.876803876	0.000008
TPX2	-1.586589411	5.192889812	0.0000000667	-1.176791653	5.476012986	0.000000
LRR1	-1.215211606	5.945075817	0.0000000671	-1.095991792	5.509414903	0.000000
CEP85L	2.572671305	2.513108224	0.0000000677	1.884460137	2.894573735	0.000000
MTFR2	-2.493466076	4.061689209	0.000000069	-2.0327843	4.130504408	0.000000
NUP85	-1.518137829	4.995926457	0.0000000716	-0.522102856	5.241854104	0.000237
C4orf46	-1.562652505	5.12532928	0.000000075	-1.243272669	5.295403944	0.000000
CADM1	1.535082864	5.108637319	0.0000000765	0.563875384	4.258158415	0.001351
DBF4	-1.582324484	4.887437638	0.0000000808	-1.208143724	5.088297864	0.000000
FCRL5	2.21668008	3.096705307	0.0000000828	1.106797156	3.032521977	0.000099
CENPF	-1.837441937	5.599927562	0.0000000847	-1.617125557	5.1482027	0.000000
RACGAP1	-1.632088045	4.9155921	0.0000000937	-2.035079806	4.576151755	0.000000
MKNK2	1.541700145	4.317752794	0.0000000964	0.893647307	3.516954354	0.000074
STMN1	-0.885381207	7.498190089	0.0000000969	-0.537912169	7.68045552	0.000000
UGT2B17	4.636231998	1.828179776	0.000000107	3.219263908	0.622075887	0.001855
LOC100129291	3.3076313	2.406246401	0.000000109	2.464464502	1.481453722	0.007420
PLXNB2	3.436453722	4.119073125	0.00000011	5.508777622	3.845564619	0.000000
CCDC58	-1.329570456	6.061741665	0.000000112	-0.797409126	5.548470064	0.000000
E2F7	2.550288158	2.442386733	0.000000118	1.482922159	2.506484276	0.000080
COQ8A	1.731206474	3.863061951	0.000000122	1.125238321	3.955706346	0.000001
VRK1	-1.160903323	6.117912163	0.000000129	-1.155397074	6.406620374	0.000000
HDAC4.AS1	3.349149796	1.958851528	0.000000135	2.128975337	0.967695608	0.005648
SPC25	-2.081798374	4.570472804	0.000000143	-1.978802099	4.157906893	0.000000
SNHG8	1.118391188	7.195778683	0.000000147	0.774037294	6.536155114	0.000000
DDX59.AS1	5.744391742	0.898967245	0.000000153	1.444990872	1.270971964	0.009029
RETSAT	1.847076791	3.981697467	0.000000159	1.023780876	4.796457621	0.000000
GSS	1.384387974	4.966835742	0.000000161	1.058398281	5.339192799	0.000000
KIF23	-2.084464296	4.466485492	0.000000165	-2.34735293	3.92707452	0.000000
RABGGTA	1.159443652	5.632269128	0.000000166	0.545253794	4.890528399	0.000950
ORC1	-1.898806266	4.412009593	0.000000173	-1.215454003	4.340456556	0.000000
SMC4	-1.267987715	6.437246496	0.000000181	-1.232228017	6.764070389	0.000000
CCT5	-0.818649374	9.501795274	0.000000183	-0.610591923	9.084904933	0.000000
CDC23	-1.669008457	4.637250056	0.00000019	-0.845446926	4.45640956	0.000009
LSM6	-0.988548077	6.784064744	0.000000191	-0.518691834	7.14506993	0.000001
TAF3	1.566967903	4.150612787	0.000000192	0.900598992	4.587562799	0.000002
ANP32E	-1.343111488	7.744340497	0.000000193	-1.118494914	8.278693813	0.000000
MT1X	-0.949991403	7.141496305	0.000000195	-0.984331416	5.68270677	0.000000
PTGES3	-0.918966188	7.033664434	0.000000218	-0.771707067	7.897349088	0.000000
NCAPG	-2.460315832	3.670017899	0.00000023	-1.940122441	4.005544389	0.000000
PTPRE	2.469748758	3.073814144	0.00000023	1.748402219	1.608088997	0.000209
HMMR	-1.536668449	5.196065734	0.000000232	-1.157169309	5.856925691	0.000000
CENPK	-2.017766811	4.674471692	0.000000247	-0.67198703	4.529968478	0.000127
TRAIP	-2.236460404	4.585023505	0.000000254	-1.854040899	4.444523221	0.000000
C6orf58	4.622878349	1.303015821	0.000000263	3.211681365	0.621246426	0.001351
ZFAND2A.DT	2.663226051	2.148386609	0.000000276	1.737760811	1.394582782	0.006641
MRPL12	-1.03390565	6.148601248	0.000000277	-0.552009743	6.17655177	0.000015
TUBB4B	-1.028290852	6.823038208	0.000000281	-1.334190461	6.286387195	0.000000
EIF4E	-1.013792876	7.028990544	0.000000302	-0.588425632	5.910819168	0.000015
WFS1	2.148726899	3.218172492	0.000000304	0.815127753	2.760411387	0.007692
PCNP	0.938361645	6.819782544	0.000000313	0.78217667	7.051276475	0.000000
KIF20B	-1.581509911	5.009767055	0.00000033	-1.934721542	5.267801464	9.35E-18
HYLS1	-1.422085771	5.280391584	0.000000369	-0.73912498	3.854911183	0.000536
EXOSC8	-1.078972882	6.449627202	0.000000372	-0.830445873	6.401777271	0.000000
RPL13A	0.942831036	11.60144403	0.000000374	1.023732857	10.5087205	0.000000
MYO6	1.476892255	4.124353417	0.000000375	1.207486642	3.941606687	0.000000
SORCS2	5.189724006	0.969204942	0.000000378	2.807596686	0.73537935	0.001383

SPDL1	-1.589962692	4.72929148	0.000000386	-0.985201448	4.55002232	0.0000004
NOLC1	-0.911234518	7.663521295	0.000000388	-0.658190133	7.757632765	0.0000000129
RPS18	0.853535254	13.27613202	0.000000389	0.529499901	13.15921551	0.0000000832
MAEL	5.303479369	1.295208976	0.00000039	5.46171035	1.091971694	0.000000201
CDC25C	-2.329553177	3.817226191	0.000000393	-1.59579927	3.324861053	0.0000000941
DTYMK	-1.480543803	5.024511282	0.000000404	-0.548957508	4.737746357	0.001548694
MAGOH	-0.927528253	7.133241475	0.000000405	-0.755409585	7.327152186	0.000000
TOP2A	-2.301244562	5.455575306	0.000000428	-1.705093486	5.575229479	0.0000000
ZMAT3	3.702693463	1.733042832	0.000000429	3.289626321	3.427865485	0.000000
TRAPPC6A	1.428104001	4.49148834	0.000000435	1.181228428	3.680267051	0.00000281
PIK3CG	2.689442281	2.092915118	0.000000437	0.530162161	4.50642341	0.004304376
GPR87	6.844565128	0.90617297	0.000000449	6.187776738	3.319071111	0.0000000
PADI4	4.209513801	1.39055407	0.000000474	6.246576368	2.983205811	3.01E-18
SHCBP1	-2.1961202	4.651151303	0.000000487	-2.042378679	4.413624307	0.0000000956
IRF4	-1.106906916	6.317139382	0.000000509	-0.930181601	7.366204445	0.0000128
RNF126	-1.532068064	4.920462322	0.000000528	-0.559830271	4.695274456	0.000473369
EID2B	2.562991307	2.243026589	0.000000544	1.675225306	2.033888473	0.000178439
GM2A	1.403863856	4.863813651	0.000000549	1.784814254	6.192917251	0.000000
LAMC1	2.354391908	2.582643675	0.000000568	1.223502711	2.284660152	0.00122292
KEL	6.887837361	0.912949393	0.000000582	4.953326583	1.469057095	0.00000000
MKI67	-1.814984819	5.001129369	0.000000598	-2.091118489	5.580011275	0.0000175
EBNA1BP2	-0.943074173	6.493767903	0.0000006	-0.90658514	7.049602138	0.000000
TRA2B	-1.149619386	5.805195108	0.000000612	-0.547144648	6.493164851	0.00000191
SNRPD1	-0.806112094	9.057964134	0.000000687	-0.529828664	9.483289824	0.000000222
MND1	-1.427542062	5.279101736	0.000000697	-1.379243603	5.50742847	0.000000
FAM136A	-0.895102609	6.863837998	0.000000703	-0.600651443	6.603311154	0.000000515
LOC105370203	2.384846634	2.67310086	0.00000071	1.833296951	2.517921756	0.000000655
SH2D2A	1.779625598	3.398877859	0.000000725	1.838951712	2.19454099	0.0000108
SGO2	-1.928279392	4.191657597	0.000000737	-1.81574806	4.924362621	0.000000
RAC2	0.930941645	7.638982483	0.00000076	0.512124518	7.474215155	0.00000124
CHAC2	-1.486003556	5.325611458	0.000000768	-0.51440345	5.868220558	0.0000683
RPL23AP82	1.815097704	3.005604715	0.000000772	1.566915904	3.505272885	0.0000000217
ESCO2	-2.193342679	4.117225651	0.000000806	-1.765866794	3.756858096	0.0000000274
DRAM1	3.875584768	2.441214753	0.000000817	3.495695482	2.654112536	0.000000
JPT1	-0.874801956	7.419866957	0.000000831	-0.930799445	8.010444668	0.000000
GEMIN7	-0.955530022	6.179388541	0.000000838	-0.587020239	6.108864054	0.00000271
ASPM	-2.173436607	3.787499312	0.000000856	-2.342206147	4.180686001	0.00000000
HDGF	-1.087928413	6.019574932	0.000000866	-0.760783037	6.030167208	0.0000318
CUL9	2.076422867	2.847968753	0.00000101	1.318231316	3.142948109	0.0000276
CENPX	-1.009558518	6.032952091	0.00000102	-0.523948687	7.16502344	0.001171859
NEK2	-2.535977789	3.588911347	0.00000104	-1.754900641	2.831223612	0.000000845
OSBPL3	2.091350706	2.380496607	0.00000112	1.326112554	3.446259679	0.000000266
CDKN3	-1.568606112	6.313540286	0.00000113	-1.735260441	4.600647444	0.000818793
TRIP6	1.696477862	4.187185905	0.00000115	1.097521754	3.588341735	0.00000541
SPAG5	-1.447685864	4.986856901	0.00000121	-1.670832031	4.863937012	0.000000
GINS3	-2.553283729	3.723271164	0.00000122	-0.593116603	4.048402791	0.003143024
FASTKD3	-1.298236373	4.974771555	0.00000123	-0.744000082	4.493833236	0.0000648
CDCA3	-1.832972488	5.281293726	0.00000133	-2.39570387	5.326632628	0.000000
BRMS1L	1.743239017	3.177348145	0.00000135	1.287225544	2.529882051	0.0000716
CD320	-0.929611002	7.565433307	0.00000143	-0.586483158	7.092260218	0.00000338
MRPL41	-1.019280222	6.918773223	0.00000143	-0.571157556	5.918975156	0.0000223
ITGAL	1.01363748	5.074105656	0.00000143	0.622964904	3.729966504	0.0042741
MAGED2	1.06516418	5.577288215	0.00000144	0.831044488	5.286579494	0.0000000394
HNRNPA2B1	-0.702692833	9.492993629	0.00000148	-0.521354181	10.20260606	0.000000185
AMZ2P1	1.7279478	3.246545967	0.00000149	0.942269617	4.818999229	0.000000055
DUSP10	1.807303067	3.241645376	0.00000149	0.692926637	3.084136487	0.009421234
TRIP13	-1.588326189	4.767311656	0.00000154	-1.925046465	3.746117595	0.0000000
ALDH1L1	4.564244428	2.000356149	0.00000166	3.128808181	1.87179445	0.0000000
CDCA2	-2.12645563	3.974890139	0.00000167	-2.529687073	4.009483136	0.000000
SOX4	2.565476109	5.850342155	0.00000167	0.751347592	5.508225563	0.000000567
NOP56	-0.796008662	7.213724321	0.00000176	-0.506264743	7.96227646	0.000000628
MELK	-1.901598632	4.514299001	0.00000185	-1.063055939	4.633675643	0.0000000606
CENPL	-1.445186662	4.385393314	0.00000185	-1.441469722	3.60836926	0.000000247

ECI2	-1.008301214	5.769312946	0.00000198	-0.904010078	5.617788423	0.0000000017
MATN1	7.695283877	1.538352716	0.000002	5.670081684	2.470368016	0.000000
PAK1IP1	-1.051107922	5.551879035	0.000002	-0.522980897	5.939255059	0.0000232
TMEM126B	-1.008529548	6.413961048	0.0000022	-0.668066036	6.176731587	0.000000769
ATP6AP2	0.927328518	5.876072185	0.00000227	0.522057964	5.977003645	0.0000426
TCP1	-0.908268848	6.534862819	0.00000229	-0.876680177	7.512481261	0.000000
TCERG1L.AS1	6.658610381	0.812628868	0.00000234	4.948850773	0.840023569	0.00000866
PFDN2	-0.857587126	6.984675462	0.00000237	-0.657959339	7.433664801	0.0000000175
CCS	1.632494112	3.425409396	0.00000242	0.660477147	3.207239198	0.007654609
ATXN3	1.110790248	4.738363961	0.00000243	0.796958738	4.475910095	0.0000147
GTSE1	-1.915341781	4.093797401	0.00000248	-2.376841598	3.934951438	0.000000
PEX3	-1.217274837	5.01321586	0.00000256	-0.58753568	5.049613607	0.000277361
TNFRSF10A	1.645606577	3.467342652	0.0000026	1.125433085	3.082865697	0.003140302
NUP54	-1.527425505	4.555542503	0.0000028	-0.678852683	5.108888196	0.00000792
CMC2	-0.828422455	6.774577402	0.000003	-0.896482657	6.424704296	0.0000000
NOP16	-0.806986519	7.852244593	0.00000309	-0.813141591	7.967313221	0.0000000
CCDC85B	-1.318759356	5.425732508	0.00000315	-0.665647567	5.244869949	0.00000632
OTUD5	1.524571698	3.756661893	0.0000032	0.89476955	8.775243189	0.006038458
EGFLAM	5.304115097	0.673823393	0.00000324	4.538240818	0.661380435	0.000161031
LOC101928659	3.104216157	1.829284555	0.00000334	1.186996057	1.967448911	0.003182751
MRPS34	-0.789672493	7.152881731	0.00000339	-0.722448481	7.671491337	0.0000000021
LOC102723373	6.523016521	0.724548577	0.00000341	7.410635921	2.47837517	0.000000198
RAP2B	1.983658509	4.496805504	0.00000353	0.812504316	4.645633971	0.002181283
KIF18A	-2.648740237	3.305263559	0.00000373	-1.64458901	3.338597972	0.0000000963
MRPL27	0.771549048	7.730181491	0.0000038	0.747832777	7.846401936	0.000000
EXOSC3	-1.441735203	4.399840971	0.00000386	-0.534035436	5.282300062	0.000238474
SIAE	1.844996016	2.665814743	0.0000039	1.169204969	2.400218192	0.001321294
NUPR1	2.763062054	1.773064805	0.00000407	6.117223586	1.491399808	0.0000000
POC1A	-1.289290278	4.876906341	0.00000425	-1.9079644	4.863497863	0.000000
ITPR2	2.097559357	2.43810104	0.00000427	1.583138146	3.831547042	0.0000000
SMC2	-1.389899077	5.677584315	0.00000429	-0.607873788	6.109099514	0.00000108
BDNF	3.728419324	1.101279166	0.00000445	2.238144198	0.870805076	0.004937136
PPM1D	2.148609869	2.449883796	0.0000045	1.6589122	2.946730194	0.000000171
SNHG15	-0.974623614	6.272330142	0.00000452	-0.529647626	6.141535317	0.000014
BTG1	1.476700537	5.282515937	0.0000046	1.685577511	4.001235622	0.00000000
CEP55	-3.193848357	3.53242408	0.00000462	-2.162308923	3.926899913	0.000000
MGAT3	1.697462467	3.014799231	0.00000466	2.5502764	1.525844866	0.0000153
CD70	2.282805885	2.422280124	0.00000499	1.579923173	6.173167743	7.43E-18
HSPE1	-0.668704825	9.892283948	0.00000499	-0.978582712	10.11614956	0.000000
ANKRD19P	2.260276702	2.34028093	0.00000513	1.995848026	1.343808226	0.000416984
CALM2	-1.214586655	9.791852801	0.00000535	-0.621571638	9.558149685	0.00000000
PYGB	1.295767756	5.103508455	0.00000538	0.722754395	3.506463811	0.001401866
PTBP3	1.408230963	4.20158286	0.0000055	1.05648828	4.592821733	0.0000000504
SIRT2	1.439292297	4.037338904	0.00000564	0.712654628	3.852372351	0.000931566
CENPQ	-2.068092766	3.345005034	0.0000058	-1.430261384	3.386875932	0.000000249
PLA2G4A	-2.41895631	3.3152932	0.00000594	-3.780417062	0.535139599	0.004916714
MYBPHL	6.378107689	0.631602123	0.00000595	5.353286085	1.033473871	0.000000262
GLTP	1.521012768	3.744216286	0.00000595	0.701329479	3.671118362	0.002148833
RCBTB2	1.73214863	4.722281336	0.0000061	0.787503974	6.636588619	0.007238639
NIP7	-1.249751594	5.608839813	0.00000628	-0.514330662	5.694140786	0.000236136
KIF20A	-1.440440513	4.642319056	0.0000063	-2.565464002	4.274344941	0.000000
WWP1	1.700514141	2.943517827	0.00000636	0.938732188	3.28849979	0.000157438
BCLAF1	-1.025297552	6.021241471	0.00000664	-0.741084539	6.702484837	0.0000000
MPHOSPH6	-1.103098181	5.672991711	0.0000067	-0.562333328	5.473989959	0.000113329
FANCI	-1.362299415	4.634556028	0.00000696	-0.837247718	5.037538651	0.000000542
RAD1	-1.403585333	6.39923427	0.00000697	-0.624529539	5.665107836	0.0000102
CENPM	-1.162906372	4.971049003	0.00000703	-0.71096544	5.467794116	0.0000031
F8	2.746785739	1.92895207	0.00000703	2.096569491	1.568981186	0.000059
LBR	-1.247714622	5.077097847	0.00000706	-1.061292514	5.704643574	0.000000
FARSA	-0.91920055	6.503374857	0.00000725	-0.506063473	6.389439274	0.0000131
KIF4A	-2.146162741	3.646273969	0.0000073	-1.385432696	4.014069985	0.00000094
ITGB1BP1	-1.271966035	5.106643044	0.00000744	-0.640205341	6.310987824	0.000000128
SELENOH	0.816294352	6.125219742	0.0000075	0.544835316	6.85833288	0.0000253

PYHIN1	3.793529177	1.036443695	0.00000761	6.486885478	3.190421355	0.000000
CDC45	-2.514976645	5.740492086	0.00000789	-1.299498632	5.818217669	0.000000
RTL8A	1.035084424	4.864741578	0.00000804	0.887732982	4.228909702	0.00000567
LINC00324	3.068236802	2.436960128	0.00000812	1.942987439	1.323648402	0.000749979
TM7SF2	1.972551278	3.032669321	0.00000816	1.133395488	3.965814867	0.00000313
TMEM44.AS1	1.921178349	2.872755355	0.0000089	0.728972373	3.194768923	0.003376127
SUV39H2	-1.637555399	4.329676135	0.00000905	-1.176496409	4.402884777	0.0000000187
C22orf46	1.489853563	3.261149259	0.00000908	1.340819131	3.657839115	0.00000033
RBM8A	-0.641966696	9.752279136	0.00000913	-0.722251091	9.749353666	0.000000
AHSA1	-1.088752878	5.838270526	0.00000921	-0.707628616	6.493439262	0.000000
DEPDC1	-2.629170443	4.454766996	0.00000986	-1.853568499	3.494904206	0.0000000
CD47	-1.576345848	4.643326628	0.00000995	-0.564633142	4.703191592	0.000585946
BLM	-1.903063363	3.331648304	0.0000103	-1.417106963	3.841090372	0.0000000175
DNAJC5	1.796356968	2.41879031	0.0000103	1.096827419	2.377652308	0.001358768
FBXO5	-2.221212171	3.145521349	0.0000107	-1.587666734	4.453433773	0.000000
CENPE	-2.020710673	3.772830348	0.0000108	-1.382290479	3.798425527	0.0000000193
E2F2	-2.623417025	3.675151967	0.0000109	-0.797629481	3.254909968	0.00289017
ZNF337	2.259749454	2.121000128	0.0000112	1.116884327	2.990977153	0.0000437
FHL2	5.080971595	4.459198841	0.0000118	1.282959273	3.963464084	0.000000093
TMEM30A	1.307376305	3.867919319	0.0000122	0.720791399	4.638867928	0.0000378
RAD51	-2.346956871	3.271209884	0.0000124	-1.147252947	3.060275047	0.0000864
EXOSC7	-1.066452991	5.953084983	0.0000127	-0.61347994	6.282456824	0.00000222
PKMYT1	-3.031949706	3.135068073	0.0000129	-2.103997262	3.115633036	0.00000109
HES2	6.254965815	0.577954393	0.0000133	6.407825481	1.694332736	0.000000
ANLN	-2.464340614	3.150315853	0.0000133	-2.026112851	3.233769562	0.000000
LSP1	1.15685942	6.170639306	0.0000133	0.614350048	3.915002339	0.001952203
LINC02014	2.916970692	1.704575171	0.0000138	2.484052404	1.251670002	0.000186324
METTL27	2.913226791	1.50204843	0.0000141	2.260603813	1.372805733	0.0000802
SLIRP	-0.645210933	9.527659052	0.0000143	-0.694034416	9.483340251	0.000000
ORC6	-1.329603537	4.261206054	0.0000146	-1.631228081	4.946922781	0.000000
CGRRF1	1.061918626	4.551998383	0.000015	0.638714493	3.635624886	0.003797537
SGO1	-2.205697651	4.381249288	0.0000151	-1.781904228	4.395443938	0.000000
HSPA8	-1.685157611	10.94044427	0.0000157	-0.851908346	10.896115	0.000000
ERO1A	-1.539775198	3.986696643	0.0000162	-0.847952585	4.412715169	0.0000226
GTF2E2	-1.76767596	3.648041877	0.0000167	-0.63804645	4.482310875	0.000214916
KIF15	-3.111098619	2.863074645	0.0000179	-1.503740037	3.490373972	0.000000365
LOC100506302	1.242536021	3.586022658	0.0000193	0.504939112	4.380194897	0.005003501
ARHGDIB	1.133072065	6.6715148	0.0000194	0.64015613	5.706325104	0.000594841
AMD1	-1.033294069	5.266197533	0.0000201	-0.601494958	5.916512711	0.00000576
CST3	1.252443264	3.985217551	0.0000207	0.704284985	5.544103913	0.000000423
LACC1	3.170067707	1.294966757	0.0000213	2.427964975	1.223205792	0.000282083
CNFN	1.174894552	3.767021654	0.0000219	1.659830529	3.150052446	0.0000000555
CENPA	-2.576355125	3.25039711	0.000022	-2.574429705	3.053218095	0.000000
EMC9	-1.225406658	4.585429466	0.0000221	-0.872311878	2.775099708	0.003677484
NOL10	-1.23763961	4.483400825	0.0000225	-0.633885633	4.715076088	0.000153123
SNHG29	0.683946869	8.295117306	0.000023	0.797303338	7.153383912	0.000000
COL24A1	1.706047934	3.047656512	0.0000238	1.451455505	2.497630611	0.000334829
GAR1	-1.332532077	4.515672017	0.0000239	-1.377646983	4.427059245	0.00000
SKA3	-1.499764472	3.838021536	0.0000245	-1.402850394	3.834756376	0.0000000136
RAD21	-1.067834082	4.983755039	0.0000248	-1.067994848	4.787550568	0.0000000379
DLEU2	-1.568190589	4.412735428	0.0000255	-1.290095725	3.799405337	0.000000445
LINC02551	2.23121089	1.972535504	0.0000262	3.160180903	0.873249605	0.000507607
CCNK	1.586950328	2.882000643	0.0000265	0.951461711	2.908310967	0.00905463
DLAT	-1.375293895	4.284108605	0.0000274	-0.628073879	4.649791026	0.000126863
CUL7	1.899939902	2.490138016	0.0000276	0.898978641	2.336580054	0.005385527
TRIM7	1.683194263	3.091687671	0.0000277	0.994155458	2.5892732	0.001339256
RBM25	-0.792724834	6.115043916	0.0000278	-0.65950006	6.463218411	0.000000167
PRR3	-1.372603599	4.559339079	0.0000279	-0.576060437	3.736092947	0.010389044
CSNK1G1	1.972152649	2.200366767	0.000029	1.431043431	3.177434385	0.000000521
ZNF37A	1.335692028	3.905275464	0.0000301	0.620515538	4.448360276	0.00046755
KCNN3	3.056853886	6.706749671	0.0000305	4.656313997	5.211479857	0.000132946
CKAP5	-1.146795663	4.667023793	0.0000312	-0.940005356	5.35959882	0.000000176
ZNF79	3.126142507	1.555294949	0.0000313	1.71961047	2.456240636	0.00000185

CIP2A	-1.64932552	3.805448412	0.0000315	-2.250157609	4.21553921	0.000000
LYAR	-0.913398728	5.206223449	0.0000319	-1.245477807	6.164368678	0.000000
SLC29A1	-1.215667327	5.300277676	0.0000325	-0.684992187	5.446127022	0.00000156
VOPP1	0.938083279	5.914168142	0.0000352	0.561775765	5.668576948	0.0000583
RALY.AS1	1.227604439	3.568548956	0.0000354	1.101340446	3.411741077	0.0000186
MPHOSPH10	-0.821763217	6.034820476	0.0000362	-0.603658017	6.496298651	0.000000425
CCDC39	2.185256728	2.270203701	0.0000362	2.220472824	2.081767546	0.00000114
TEX30	-1.088362971	4.689073258	0.0000385	-0.542588845	5.862433417	0.0000403
RPL3	0.813208699	12.95316227	0.0000393	0.732984826	12.80509859	0.000000
ECT2	-1.873450221	3.414593444	0.0000404	-1.268809808	3.734843493	0.00000013
SOAT1	-1.557376192	3.968134015	0.0000408	-0.640777026	4.68856269	0.000125455
CD44	1.539437815	7.134190628	0.0000412	1.158821193	6.152948282	0.004402054
KIF14	-2.834735997	2.629247589	0.0000442	-2.055194251	2.99702534	0.00000108
GNL3	-0.594607869	7.298328025	0.0000442	-0.500603772	7.357500984	0.0000109
POLD2	-0.87306915	5.905106102	0.0000455	-0.542294677	6.579900997	0.00000698
UTP3	-0.6833809	6.539576326	0.0000463	-0.559375639	5.917714325	0.00000529
AZIN1	-0.912320243	5.905768054	0.0000464	-0.58555217	6.113074795	0.00000185
BBC3	3.549503426	0.913718248	0.0000479	3.235823583	0.904795216	0.000132649
SNRPG	-0.559329703	9.161967169	0.0000496	-0.580521051	9.493904518	0.000000
NSG1	3.879319675	0.744538678	0.0000504	3.242192382	1.145223254	0.0000847
GOLGA3	1.099945732	4.091587279	0.0000505	0.873188456	3.369427129	0.001269005
PPY	6.066553578	0.475878017	0.0000517	4.579827868	1.2502536	0.000000197
ANAPC16	0.625305327	7.50145304	0.0000518	0.615187183	7.217504017	0.0000000613
E2F8	-3.296636765	2.54980633	0.0000525	-1.846930413	2.978444817	0.0000000611
FRMD8	1.305598499	3.538358429	0.0000529	0.503125108	4.729573585	0.006907838
PRPF38B	-1.466084905	3.99945126	0.0000537	-0.59138215	4.473868578	0.000931612
EEF1AKMT4	-0.681703325	7.007053192	0.000054	-0.556891032	6.160859082	0.00000566
MYOM2	1.641328175	2.429439665	0.0000541	2.425255413	1.462845806	0.00000949
CNOT9	-1.019531165	5.048069376	0.0000547	-0.564422331	5.492412235	0.000316605
RN7SK	3.90164466	5.92367602	0.0000586	1.165896726	3.981306391	0.0000114
TM7SF3	1.382924451	3.018023968	0.0000603	2.326490472	5.700027226	1.61E-24
LYST	1.572766604	2.624454317	0.0000611	0.616552191	3.557549782	0.005282072
NOP58	-0.662355613	8.032068247	0.000063	-0.554318654	8.42888485	0.0000000827
LEO1	-0.820903832	5.591789467	0.0000648	-0.533407633	5.784411584	0.0000459
PLK4	-2.293261661	3.014564266	0.0000649	-1.381026289	2.483157858	0.000250143
CCNG1	1.093156185	6.887687765	0.000065	0.971523913	7.890470421	0.000000
DDIAS	-1.655794751	3.347385811	0.0000657	-2.199932219	3.76325069	0.000000
ZNF322	1.711471856	2.710502303	0.000066	1.283363781	3.197945578	0.000000951
SNHG17	-0.829867254	5.49883275	0.0000674	-0.7960971	4.721169221	0.00000423
MAK16	-1.013600764	5.48128561	0.0000686	-0.566202492	5.280609307	0.0000669
SPRYD4	0.835404047	5.412431565	0.0000709	0.964253886	5.018251004	0.0000000288
RNF25	-1.733659114	3.303834148	0.0000712	-0.608999086	3.56438515	0.005992963
PLAC8	1.604519812	4.912467511	0.0000717	2.250783582	5.598630239	0.000000
TROAP	-0.738578724	6.51859023	0.0000771	-0.958163846	5.342848714	0.0000000048
DENND6B	1.403641097	5.511345159	0.0000796	2.010832348	1.893722978	0.0000124
GINS1	-1.538500409	3.460443851	0.0000799	-1.067030236	3.97629525	0.00000106
MRPS15	-0.69974871	5.99051901	0.0000827	-0.625036911	6.529922111	0.000000152
LOC257396	1.326978327	3.115471504	0.0000844	1.40556377	2.445409221	0.0000317
ID3	2.421726876	5.613674173	0.0000844	0.692333338	3.262024384	0.005836706
NUP205	-1.673711965	3.59026758	0.0000852	-0.659001203	4.521560622	0.0000758
CDC123	-0.627910641	7.818466292	0.0000853	-0.584795432	7.876913958	0.000000191
PRADC1	-1.20127414	4.194330471	0.0000887	-0.763644513	4.519585719	0.0000532
ARSA	1.921867101	2.237017172	0.0000902	1.099693733	2.334545709	0.001411425
EML2	1.55967131	2.534527209	0.0000923	0.908157108	3.079109187	0.000945223
U2SURP	-0.608570289	6.70411765	0.0000967	-0.837483874	7.058219688	0.000000
RITA1	-1.635297184	3.453260199	0.0000992	-0.691347445	3.712586384	0.002437089
MRTO4	-0.637242826	6.955661002	0.000100159	-0.753413692	7.216768018	0.000000
PTRH1	1.306865358	3.258286701	0.000101821	0.807669508	3.907746023	0.0000847
LIN7A	5.690878488	0.352312743	0.000104821	3.947469949	1.255408063	0.000000827
TMEM131	1.374343116	2.868842368	0.000107997	0.869467976	3.33907387	0.005669119
ACTL6A	-0.804349426	5.545148428	0.000108474	-0.52256825	6.034582266	0.0000289
MYBL2	-0.884443036	5.29308156	0.000115336	-1.156984417	4.672102999	0.000000016
NASP	-0.999962282	6.398658463	0.000116061	-0.652131082	6.82538134	0.000000124

TRIM3	4.213721715	0.505876562	0.000117792	2.72450817	0.905311994	0.000395947
STEAP1B	-1.119356471	4.381723824	0.000118167	-0.760239998	2.954008454	0.006898434
WRAP53	-1.228724418	4.213968897	0.000119601	-1.190150762	4.476843735	0.000000
LSM12	-0.816745549	5.275196365	0.000121337	-0.527308702	5.895818773	0.0000842
IP6K2	0.771153136	4.89526957	0.000122005	0.717184251	5.583836556	0.000000522
NUP107	-0.822902145	4.956888003	0.000123655	-0.870055113	5.402694301	0.000000
GUSBP15	-6.135478552	1.886719023	0.00013197	-1.210206705	1.722787958	0.009570792
IER3	3.048214821	1.285587377	0.000132884	1.84795691	1.741150438	0.000264406
ATF3	2.524429809	2.859546525	0.000134685	1.562402616	2.20059332	0.0000765
SUZ12	-1.34495495	3.785669149	0.000140998	-0.956609166	3.943505879	0.0000373
PGRMC1	-1.469552048	3.814757706	0.000141793	-0.928410451	4.686050115	0.000000149
PCBP4	1.835075463	2.062749261	0.000149009	1.160805302	3.523252087	0.00000847
IMMP1L	-1.204826529	4.526512074	0.000149563	-0.552469689	4.179373085	0.003299281
IFI27L2	0.533130409	7.053726303	0.000152634	0.516956865	7.417086846	0.00000867
SIVA1	-0.781851935	5.942824637	0.000154777	-0.686227548	7.015383889	0.000000
STON2	0.948239854	4.591051332	0.000157102	0.794432964	4.835990792	0.000443575
SEC11C	1.132001636	9.699191469	0.000160091	0.608424155	9.494070852	0.000000
TCF25	1.132586697	4.925184643	0.000160991	0.64302454	4.523268961	0.000665574
SLC38A1	-0.687694152	6.169571473	0.00016877	-0.794241158	6.489150045	0.0000000682
WDR18	-0.850142574	4.856113938	0.000172446	-0.702881924	5.437109784	0.00000578
LOC100506098	1.984851256	1.78755762	0.000174562	1.506964544	1.368960536	0.004665956
RPS9	0.689516426	9.899420775	0.000174647	0.556310214	10.02676173	0.000000169
PSMG1	-1.309179525	4.952781249	0.000175884	-0.746922617	5.395235159	0.000000399
CHCHD3	-0.915072789	4.721012762	0.000176139	-0.881964704	5.441491024	0.0000000157
ANKRD20A12P	2.919625169	1.219911279	0.000176609	1.967356599	1.861712775	0.000008
PHLDB3	1.670358144	2.288038888	0.000181221	1.341587771	1.435159849	0.007973705
MRPL4	-0.868927251	5.453251074	0.00018288	-0.982551564	5.413701223	0.0000000899
MIS18A	-1.509419407	3.684648229	0.000186489	-1.41780828	3.687748221	0.00000009
SUGCT	4.097513607	3.138128524	0.000187843	4.225169937	2.180526238	0.000000
SCAND1	0.623213892	6.030546133	0.00019623	0.684544681	4.711406591	0.000113747
SIL1	0.779512099	5.214856103	0.000201911	1.340904306	3.784057386	0.00000135
ZKSCAN1	1.089261777	3.454897936	0.000203813	0.658155898	3.845831796	0.002123473
COG4	0.804142553	4.785633679	0.000213129	0.582319871	4.65416025	0.000211729
NSF	0.889785594	4.868937691	0.000221555	0.785251904	4.838607044	0.0000117
AMOTL1	1.269327202	3.151474708	0.000227847	0.745137439	3.450966659	0.002008446
CIC	2.366308045	1.39035143	0.000228461	1.243786116	1.504014497	0.009653535
FAM227B	3.155758921	0.733198006	0.000232949	2.639580644	1.196005764	0.000107142
FAM41C	1.837428153	2.067355523	0.000236752	3.06712041	2.582973126	0.000000
GUF1	1.049850054	3.408819235	0.000238639	0.584964564	3.642676408	0.007697581
ARHGAP11A	-1.605621965	3.206320856	0.000244443	-1.830902752	4.107648562	0.000000
TMBIM1	1.529358005	2.562110726	0.000246847	1.100378038	3.168002908	0.0000483
GNL2	-0.705354277	6.251468699	0.00024821	-0.612920114	6.728946011	0.0000000854
HIPK3	1.218715996	3.402902706	0.00025087	0.991297797	3.180608252	0.000150222
GLOD4	-0.921711549	5.310190621	0.000261607	-0.521626861	5.800975657	0.000068
GAS6	1.767337976	1.991795481	0.000263961	0.904575307	3.028822024	0.000722758
CBWD1	-0.813176645	5.477644994	0.00026445	-0.503769193	5.047509706	0.00056389
LSM1	-0.660746901	5.859401054	0.000264548	-0.533253883	5.881664954	0.0000499
WDR12	-0.673605399	5.585583798	0.000265102	-0.662536454	6.278097058	0.000000113
SRSF7	-0.519963023	7.698434502	0.000271067	-0.780845057	8.263111769	0.000000
CCNF	-1.726564195	2.913127915	0.000279292	-1.289648179	3.295998926	0.0000057
RAB11B.AS1	1.20003487	2.988554607	0.000281329	1.709415426	2.558779641	0.00000085
C12orf29	-0.975519174	4.693034219	0.00028323	-0.680282638	5.468859082	0.0000024
DDR1	3.191695632	1.278452153	0.000284494	3.048060926	1.569755715	0.000000824
SPC24	-1.596752839	3.223368567	0.000287948	-1.209099059	3.245783349	0.0000132
PRR11	-1.27110087	4.396612806	0.000299174	-0.931802694	4.260640122	0.0000164
EIF2AK3.DT	2.600753073	1.242767394	0.000299814	2.380417486	0.769189126	0.004456589
HSD17B12	0.896314849	5.167280705	0.000306961	0.902467966	2.975265362	0.001089211
PERP	1.30253816	2.963858719	0.000312056	1.072922282	5.796146838	0.000000
ST3GAL4	-1.558677329	3.365927558	0.000313087	-1.092118236	2.427786043	0.002828825
TMCC1.AS1	0.954710435	4.018056725	0.00031346	0.970411598	3.285676213	0.001851081
PRPS1	-0.860255315	5.067532757	0.000322125	-0.732555829	5.641073227	0.0000000854
MIS12	-1.024370571	4.250113129	0.000327864	-0.681806482	4.528309154	0.0000772
ARL13B	-1.740939587	3.422127419	0.000329157	-0.823241751	3.748011145	0.000516872

RUVBL2	-0.61157822	5.960768554	0.000331327	-0.600942151	6.75355574	0.0000000938
ZNRD2	-0.545365848	7.403187238	0.000332342	-0.664236919	7.556079861	0.0000000262
POLR3G	-1.133095527	3.669657517	0.000341564	-1.103928381	4.777065933	0.000000391
ARVCF	3.684232016	0.504013997	0.000341594	2.916311265	0.771571572	0.000629088
PHB	-0.536144886	7.939145815	0.000344783	-0.605225118	7.947610244	0.0000000484
H4C5	-2.466493186	2.950939398	0.000359249	-1.276744557	2.959017393	0.0000935
RAD18	-0.964164474	4.346313686	0.000363771	-0.906456654	4.176838393	0.0000167
TSFM	-0.514210526	6.774230081	0.000367956	-0.630190811	7.025431654	0.0000000328
HILPDA	-0.978767265	4.178070898	0.000374645	-0.967927696	4.153396131	0.00000263
PDCD2L	-2.004225905	2.977327711	0.000381101	-1.228935189	3.617934055	0.00000135
RRS1	-1.689605871	3.741322186	0.000386928	-0.555775824	4.063878566	0.004332119
METTL8	1.136396412	3.515053765	0.000389111	0.554429174	3.81916692	0.005403248
NTHL1	-1.017497261	4.351638897	0.000389725	-0.755443965	4.281282358	0.000099
ZGRF1	-3.422385263	1.944194741	0.000395523	-1.991378575	1.442687594	0.000941601
DHX15	-0.619049757	5.863471518	0.000398148	-0.504294494	6.336555359	0.0000141
PRMT1	-0.600090118	6.484810302	0.000404774	-1.007763391	6.395491666	0.001612229
NUDC	-0.718883137	5.910415641	0.000405741	-0.745262745	6.156702848	0.000000232
CAPN3	2.483969698	1.29614236	0.000424136	1.117781435	2.219031732	0.005862486
TNPO1	-0.853995162	5.096219311	0.000427375	-0.614332912	5.435543325	0.00000837
ABCB6	1.073246259	3.672265697	0.000427788	0.631220983	4.656497742	0.000347068
KIAA1586	0.809567672	4.82989001	0.000438344	0.578082088	5.355008488	0.0000404
SAP30	-1.913842056	2.705943708	0.000441923	-1.07389432	2.738024941	0.000961454
KIF2A	-0.857208263	4.690926579	0.000446794	-0.5604356	6.052973905	0.00000394
ZNF540	3.949916528	0.400632077	0.000451102	2.465526433	1.114250339	0.000235144
ARMC2	1.319537403	4.062821228	0.000451798	1.579394298	1.32144713	0.002448114
MACF1	1.377153843	2.875183279	0.000453805	1.703579137	4.389808647	0.000000
SMARCA1	2.797710717	1.080125339	0.000464746	3.875391129	0.877465907	0.0000582
EEF2	0.739183574	8.521905776	0.000466929	0.69545861	8.474143316	0.000000
TRAF4	1.587119104	2.687149449	0.000490318	1.008625904	2.377392951	0.003144152
DCUN1D5	-0.916554129	4.793882078	0.000493906	-0.841643804	4.521815445	0.00000812
GRWD1	-0.782318706	5.565154231	0.00049593	-0.575681656	5.742444905	0.0000187
GADD45GIP1	-0.538348515	7.045465737	0.000499846	-0.587576318	6.358814432	0.000000965
SNAPC1	-1.955310012	2.750605005	0.000500289	-0.697127237	3.415701081	0.006781356
GAS5	0.774735166	10.86605686	0.000503518	0.846134783	9.547521922	0.000000
DNPEP	-0.838773913	5.117055864	0.000507559	-0.595924322	4.532276909	0.000634959
RNPS1	-0.707204804	5.337995291	0.000507835	-0.565626328	5.835755807	0.00000939
MED21	-1.347491904	4.496194048	0.000520378	-0.571404871	5.231738852	0.0000675
DEPDC1B	-1.965379899	3.248603759	0.000527498	-1.44357802	3.979455744	0.0000000102
PRELID1	-0.595944977	6.784995597	0.000531761	-0.734161078	7.306045955	0.00000
ZC3H6	1.390562075	2.41148898	0.00053903	1.097588049	2.377916452	0.002129565
PTDSS1	-0.989627784	4.13739243	0.000550302	-0.642376087	5.343501826	0.0000678
VANGL2	4.352182047	0.290563032	0.000559509	2.603985426	0.660185997	0.004727676
FKBPL	-1.104538978	3.780763966	0.00057444	-0.774831762	4.307084397	0.0000658
LINC00476	1.351513443	2.994684302	0.000599401	1.429553265	2.362780983	0.0000539
ATAD5	-1.376372964	3.338627652	0.000606446	-1.749769373	3.82758487	0.0000000059
C1orf112	-1.380380864	3.338805191	0.000614759	-1.04243944	3.092557833	0.000577492
RBM41	1.083560463	3.100657429	0.000627024	1.0670404	3.437100766	0.0000997
PPIH	-0.630605484	5.770909731	0.000633243	-0.930273633	5.913776973	0.00000003
NCAPD2	-0.939294937	4.217415168	0.000638291	-1.126248982	5.07250954	0.00000000
HS1BP3	1.356518128	2.301377188	0.000644377	1.41033444	2.443149911	0.0000311
RHNO1	-0.775563142	4.872575472	0.000662782	-0.584908083	4.593431536	0.000976649
SASS6	-1.671825953	2.990253111	0.000667849	-1.10559401	3.922553296	0.000001
SNHG30	-0.751825552	5.132260598	0.000685813	-0.712618067	4.571069048	0.0000594
RPUSD1	-1.153002487	3.689629304	0.000705454	-0.627063973	3.841640019	0.002318759
IFRD1	-1.317653068	3.376004681	0.000717543	-0.898063944	4.112509721	0.0000126
KRT17	5.146915955	0.168231916	0.000728825	4.024632898	3.186206241	0.000000
CCDC12	-0.657256306	5.547427385	0.000730711	-0.50143587	5.899020415	0.0000594
TNFRSF14	1.376831872	3.489502747	0.000732413	0.9539586	2.209045868	0.005902812
ABHD4	1.10668154	5.567843144	0.000771273	0.784386101	4.340706025	0.0000527
SLC25A44	-1.150002232	3.847398999	0.000780421	-0.571775086	4.364034805	0.001094061
KIAA1217	0.839476767	4.386568843	0.000789215	1.862524643	1.92630878	0.0000163
PCMT1	-0.621694631	5.988060923	0.000796136	-0.671010322	5.972114072	0.000000205
PLEKHG1	2.410283065	1.204042737	0.000802396	2.736463455	1.08885131	0.000104813

CHEK2	-1.049425867	4.413515513	0.000807654	-1.178761702	4.65022764	0.0000000
ABALON	2.047457441	1.36471733	0.000812071	1.327958148	1.483601796	0.009757754
GPNMB	1.125243343	3.471483807	0.000817702	1.016082599	3.502897511	0.0000263
CHORDC1	-0.652573078	6.399693817	0.000833222	-0.82017996	6.246729607	0.0000000
KATNBL1	-1.395373023	3.037006795	0.000881697	-0.539441788	3.775512344	0.007332834
SURF6	-1.199089875	3.8662006	0.000887635	-0.868215395	4.178299835	0.0000645
ADAMTS7	5.186127804	0.171552153	0.000890294	3.532353806	0.734873325	0.000234329
KCTD1	1.784449959	2.062250257	0.000895397	1.576516037	2.238853726	0.000039
TRAPPC4	-1.108810997	8.964530272	0.000901217	-0.515051209	6.8609307	0.00000429
PTRH2	-0.51887809	6.753329799	0.000913738	-0.581445331	6.557304052	0.0000016
TMEM19	1.036691489	4.228577166	0.000926877	0.822650009	3.931352231	0.00031984
ZWILCH	-0.838520115	4.592907272	0.000933075	-1.058073355	3.729453697	0.0000444
TMEM160	-0.537876494	6.022404054	0.00093411	-0.738608106	5.423583762	0.000000807
RRP15	-0.684383738	5.269777479	0.000953993	-0.815332933	5.231439427	0.000000765
UTP6	-0.661736905	5.93437599	0.000967816	-0.523773722	6.464289454	0.0000228
BRD8	-0.88016876	4.509019094	0.001001996	-0.582724539	4.814701823	0.000543622
NOP53	0.838183261	5.758011994	0.001037278	0.622703132	5.56228261	0.0000239
SACM1L	-0.999188848	3.931259813	0.001054463	-0.713838233	4.315895512	0.0000969
LOC107985911	0.972879654	3.345365838	0.001070004	0.625956825	3.323924866	0.006986183
HSPH1	-0.892514765	4.524772046	0.001091862	-0.668715634	5.120446811	0.0000125
MIDEAS	-1.837871034	2.639905962	0.001097863	-1.184167007	3.747813293	0.00000149
KNL1	-1.521433491	3.133066154	0.001158522	-1.665918828	3.879550079	0.000000
AAMP	-0.590204392	6.036037928	0.001189904	-0.523153952	5.915215744	0.0000673
TANC2	2.343021928	1.137019433	0.001190598	1.353760138	2.31438644	0.000275035
CCSER2	1.316901009	2.366853102	0.001207526	1.206665609	3.776370075	0.0000000926
MLH1	0.636830427	5.031843608	0.001207563	0.620964819	5.332912439	0.0000269
KIF11	-1.187175511	3.628952725	0.001220394	-1.41486705	3.724082395	0.00000166
TIMM23	-0.683451608	6.004636655	0.001234091	-0.511749187	6.788244697	0.00000201
VPS13B	1.050439413	3.254852945	0.001310774	0.844760949	3.852145893	0.0000432
KIFC1	-1.701108559	2.712600785	0.001318786	-1.734452332	3.105459318	0.000000205
TKFC	1.722397855	2.136259296	0.00132427	0.838743953	3.831426345	0.000113332
FOXO3	0.909081243	4.405822864	0.00136791	0.597546174	3.478159064	0.009002296
PSTK	-1.02757226	3.821698329	0.001391505	-0.583039889	3.567225589	0.010311197
CBX6	1.277125246	6.476994331	0.001395067	0.937870143	5.761313855	0.000119789
DCK	-2.416409107	4.22234031	0.001416729	-0.668515685	3.953197386	0.000753516
STIL	-2.034082585	2.577622381	0.001474312	-2.607974212	2.705069019	0.00000000
CYB5D1	-1.877853786	2.869971525	0.001489178	-0.620803033	3.591335087	0.003574345
ORC2	-1.08855149	4.04128392	0.001510272	-0.775517866	4.914674761	0.00000199
GNE	1.215181177	2.480840964	0.001516008	0.9157648	3.31054331	0.000229359
EBP	-0.517870186	7.15273344	0.0015372	-0.666483091	8.263863537	0.005461823
PPP2R3A	3.473192127	0.444221709	0.001537329	1.72158189	1.605042507	0.000357907
TCTA	0.855436941	3.809292421	0.001570559	0.671087711	3.554265883	0.002520156
MTBP	-2.557717731	2.418437924	0.001570828	-1.271549374	2.409974546	0.000466236
IDH1	-0.701429647	4.791318953	0.001603753	-0.750386986	6.028241826	0.00000017
ANAPC4	-1.309008835	2.972886506	0.001608898	-0.551545815	4.044335939	0.00578069
MED30	-1.312829707	3.530754463	0.001611189	-1.350197271	3.329186582	0.00000163
NOL11	-0.644995887	5.431662199	0.001632652	-0.503540731	5.872480201	0.000222395
G2E3	-0.959126778	4.250866761	0.001632909	-0.551652454	3.732397366	0.007555912
XPO1	-0.738047388	4.570997204	0.001637823	-0.899016607	5.008254791	0.000000196
HDAC1	-0.659849489	5.420214	0.001642551	-0.552336768	5.417462206	0.0000533
SMAD5	0.822370427	3.89706252	0.001643344	0.58320459	4.590082213	0.000788996
LINC00240	2.83900352	0.731274821	0.001743695	2.494826048	0.805490267	0.002920115
PSMG4	-0.728744954	4.588637085	0.001808754	-0.589573096	4.876993702	0.000186069
LOC101929626	3.716038532	0.341633898	0.001810655	2.957836787	1.198313606	0.0000338
MRPL38	-0.73358847	5.030977596	0.001876252	-0.513577937	5.49600346	0.000189505
H1.3	-1.956766481	4.234923785	0.001895839	-2.036076017	4.155299565	0.0000000127
HSP90AA1	-0.797345767	10.0698324	0.001916985	-0.691610013	9.953739778	0.0000000
CNOT7	-0.612412816	5.357116736	0.001923158	-0.542471271	5.579092917	0.0000444
SULF2	2.526382765	4.773079893	0.001933528	2.620103615	2.980587369	0.001109321
SMIM20	0.589113852	4.94262737	0.001941174	0.563841189	4.882050513	0.000258275
PPP4R3A	0.964646795	3.507197275	0.001943832	0.549988479	3.884143679	0.010046341
HHAT	1.878760041	1.491862763	0.001975415	3.390252992	1.226163554	0.0000066
GEMIN4	-1.212905016	3.513162252	0.002039449	-0.70431588	4.346851415	0.000096

LCP1	0.860509019	5.066897467	0.002039611	0.762713118	6.461959697	0.006318453
OIP5	-1.260349491	3.427485949	0.002046543	-1.124217589	3.072283437	0.0000517
H4C3	-1.945142337	8.332579712	0.002086029	-1.474709372	7.781885069	0.00000164
PPAN	-1.090748346	5.223049243	0.002119066	-0.757850369	4.653231917	0.0000353
DNTTIP2	-0.750748244	5.070886972	0.002143867	-0.654876098	5.569698882	0.00000198
XRCC2	-1.029406352	3.384228886	0.002164117	-1.279451757	3.185344299	0.00000905
OSGEP	-0.521500839	5.913472809	0.002249895	-0.77359416	4.873637526	0.00000346
JOSD2	0.905350116	3.205648757	0.00225939	0.644600507	3.772024184	0.001753013
PPP1R14B.AS1	1.264889368	2.290019129	0.002273774	0.994316004	2.104629613	0.006139177
PLK3	1.854058492	2.169069854	0.002287768	1.311130082	1.478847753	0.007799573
NLRX1	1.412712658	1.956495845	0.002303979	1.894633474	1.893262433	0.0000298
CES2	1.112919985	3.011807944	0.002340109	0.921026963	2.946569687	0.00088919
TMEM187	0.992954015	3.308207444	0.002350572	0.915754673	2.221174102	0.006283686
LOC102724532	1.361002792	2.400003272	0.002385642	0.984890476	3.256466403	0.000199242
CFAP20DC	2.316506426	1.108773532	0.002447593	0.641345671	3.390562864	0.005848049
SRSF2	-0.986195216	5.499422439	0.002492791	-0.899327485	6.341555228	0.0000000
EDN2	4.876378099	0.0998655	0.002530157	5.119130694	2.046383368	0.00000000
POLR1C	-0.610619101	6.05561972	0.002559334	-0.574238448	5.977493125	0.000206218
BCL2L12	-0.853058228	4.254624494	0.002580338	-1.850529489	4.254797356	0.00000000
ASF1B	-0.97407002	3.830844558	0.002596543	-0.549055096	3.673182044	0.009922012
DUSP12	-0.619847591	5.097125386	0.002626967	-0.543097401	5.824298536	0.0000211
R3HDM2	1.364685264	2.253806218	0.002631215	0.955920343	2.251807731	0.00513103
CYHR1	0.88539118	3.165091978	0.002635097	0.584433755	4.891338576	0.000263605
DIAPH3	-2.190558216	2.133295191	0.002676634	-1.064988664	2.88467101	0.000851997
NRSN2.AS1	1.59518546	2.107912699	0.002715477	1.780043248	2.668241838	0.000000474
ASB2	1.256961523	4.293395983	0.002721549	1.304738618	4.783635193	0.000910542
TAF1A	-1.816616102	2.406051273	0.002745768	-0.877988127	2.798873661	0.002840505
WDR59	1.107395541	2.508960225	0.002782916	0.881153087	2.702979345	0.006349827
NDC1	-0.745073879	4.586922616	0.002824049	-1.458482084	4.646013679	0.0000000
STX16	0.927128975	3.200148291	0.002861299	0.847961984	3.109942373	0.00365983
EEF1A1	0.755112453	13.30462845	0.002922377	0.603801774	13.8884966	0.0000000315
SNRNP25	-0.634606592	5.399569195	0.002940971	-0.77820653	5.751077428	0.0000000486
TRIT1	-1.232218644	3.579180327	0.002947249	-0.816074796	4.397059208	0.0000148
FANCD2	-0.928868135	4.112808529	0.002990841	-1.092054037	4.199350358	0.000000979
CENPJ	-0.891651639	4.160241667	0.003029986	-1.033364795	4.957673834	0.000000375
NSD1	1.737473289	4.497068907	0.003058814	0.981272807	3.820700148	0.0000272
SERTAD1	1.568897534	1.92501338	0.003070553	1.382136273	3.157165185	0.00000178
VPS13C	0.998812267	3.528603358	0.003127521	0.633154981	4.205284731	0.000918608
ITM2A	1.662637042	5.090765192	0.003131821	1.70671203	7.366930775	0.0000344
MAST4	2.625473259	0.767551585	0.003322246	1.138923156	1.716864948	0.010445524
LYRM9	1.814945697	1.263796043	0.003482493	2.730498301	0.906619667	0.000599876
TUBB3	2.979879533	0.443900793	0.003560212	0.623719276	4.36064283	0.000578304
UBA2	-0.870949302	3.734217233	0.003645388	-0.537120542	4.774031895	0.004944838
SDC1	0.662272958	5.075490763	0.003799392	0.69764337	3.956975862	0.000721519
NCK1	-0.792200214	4.505648311	0.003821875	-0.730868773	4.296207018	0.0000781
GLA	-0.609486039	5.057094419	0.003842085	-1.056536559	5.882731438	0.000000
PLCG2	0.873987027	3.349440422	0.00393118	1.141961937	2.065513321	0.003661904
EPOR	-1.38064884	2.634992137	0.003945812	-1.154583936	2.640355186	0.000485423
NOL7	-0.830022812	8.0467293	0.004009681	-0.67293419	8.408594	0.000118553
AKAP9	0.636511721	5.102942169	0.004011719	0.536457638	5.626700933	0.0000831
GTPBP3	-1.212557257	2.891995472	0.00401897	-0.991327665	2.603836934	0.002635961
SHMT1	-1.498303387	3.755599648	0.004046331	-0.549214826	6.239680028	0.00000702
PTCD3	-0.606460148	5.38133298	0.004051848	-0.578822371	5.931108259	0.00000826
ATAD3A	-1.121397744	3.447922923	0.004081759	-0.879288442	4.091854992	0.0000929
DTWD1	0.56673025	5.007650827	0.004105206	0.803211338	5.781413568	0.00000348
STIP1	-0.595170892	8.187040097	0.004116445	-0.90599857	7.887922412	0.000000
CDC25A	-1.665000892	2.314694698	0.004138998	-0.957273193	2.320595704	0.009296903
ELK3	-2.353316242	1.817084078	0.004197683	-0.698174415	3.333451733	0.007079012
CCNA2	-2.482989307	5.283682395	0.004221566	-2.147026133	3.927778352	0.000000057
COMTD1	0.646556414	4.034367267	0.004222811	0.712990487	4.863332617	0.00000659
MYADM	-1.448787044	2.704665583	0.004326186	-1.426576426	3.689987598	0.0000000297
ARHGEF39	-2.484511365	1.927970492	0.004370176	-1.147856205	2.51291291	0.000587452
H2AX	-0.886939416	3.817645676	0.004591543	-1.010351879	2.554117487	0.002449906

FAM98C	1.252139453	2.250903965	0.004771657	1.209720138	2.905972571	0.0000889
LOC100507291	1.581629285	1.626734672	0.004811093	1.988158916	1.74196646	0.0000377
CCDC112	-0.944477481	3.451794543	0.004878963	-0.851091969	3.913372122	0.0000838
LINC02315	1.08218361	2.861244529	0.004956569	0.910496989	3.489581219	0.000112422
SET	-0.528849315	7.107252074	0.004969787	-0.705667811	7.325301331	0.00000155
MTF2	-0.929201498	3.681125956	0.004989524	-0.62706152	3.60650731	0.006502732
DRAM2	0.577905849	4.903404193	0.005057644	0.590075313	4.390191381	0.000889081
MCUB	-1.607085115	3.085528194	0.005162759	-1.269581744	2.545198115	0.000492016
DCAF8	0.586042687	4.60982407	0.005204787	0.500746759	5.308093594	0.000245037
APH1A	-0.560301316	5.230610301	0.005223743	-0.560585716	5.633462871	0.0000194
SLC16A1	-0.95297639	4.053785221	0.005398804	-0.637193138	4.139753956	0.000970258
REEP4	-0.802508567	4.405844653	0.005415146	-1.715960487	2.926180826	0.00000293
TFB2M	-0.659102433	4.957155307	0.005436572	-0.567001746	5.33349629	0.0000468
MTRR	-0.72527645	5.063613063	0.005660432	-0.646685133	5.495909975	0.0000214
DNAJC2	-0.965588344	4.499824205	0.00567202	-0.810696552	4.995463852	0.000000562
CRTAP	0.696640562	4.202706937	0.00572141	0.71886627	4.488826863	0.0000667
KRAS	-0.982350658	3.330103771	0.005728683	-0.646045346	5.403746233	0.0000185
ZNF596	1.878850944	1.362860093	0.005788478	1.637647076	1.342580795	0.002320732
PAFAH1B3	-0.509455489	5.149959747	0.00588704	-0.811211788	5.76671637	0.00000000
TIMM50	-0.524008338	5.755541269	0.006080192	-0.554105147	6.094601748	0.00000911
LIN9	-1.060780344	2.979896952	0.006143676	-0.71121909	3.052006674	0.009743802
TRIM26	1.07594349	3.889017871	0.00638235	1.035557311	4.379292074	0.000000122
TSACC	1.465772065	1.937820438	0.006450426	2.139482413	1.504217275	0.0000386
TMEM80	0.999805565	2.746075497	0.006503904	1.102306781	3.064678227	0.000131107
RRP7A	-0.661915974	5.023748705	0.006671211	-0.51755175	5.331838571	0.000305566
GLIPR2	1.05426988	2.951368124	0.006942239	1.60669594	3.083507568	0.000000104
MANEA.DT	2.48194853	0.624970042	0.007028672	1.456151232	1.722183623	0.001342835
MIS18BP1	-0.918801524	3.302405795	0.007039914	-0.684410262	3.237893871	0.007569832
SART3	-0.780006308	4.217949625	0.007042272	-0.507663112	4.586874417	0.003220973
JADE1	-0.962686241	3.267373592	0.007107946	-0.819817079	2.646701377	0.009334686
SPATA20	1.366987515	2.398263112	0.007120632	1.065881336	2.494122086	0.000915801
PRKACA	1.234160771	2.178557055	0.007323268	0.852645123	2.393665031	0.009886584
BAGE	-1.219675564	3.124757188	0.007346743	-1.258096304	2.198574173	0.001535853
TSR1	-0.834734756	3.815942755	0.007400175	-0.637122196	5.055862285	0.0000365
ZSCAN16.AS1	0.696749117	4.20582126	0.007429577	0.656986871	4.835963352	0.0000258
ANKRD27	-1.354242468	2.4591562	0.007624258	-1.098921743	2.884490647	0.000298948
TTC28.AS1	0.960748756	3.788391058	0.007741041	0.780613465	4.349144644	0.0000149
HDAC2	-0.609525533	4.892458456	0.007750836	-0.50331915	5.820758202	0.000186721
GCSH	-0.717795249	4.687897019	0.007766927	-0.666464257	4.08416444	0.000877698
ZNF33A	0.615109657	4.849623233	0.007777561	0.624574976	5.555254655	0.00004
CA11	1.201237678	2.121559376	0.007814925	0.699085831	2.977734599	0.00878826
MED27	-0.545680577	5.769769132	0.007918304	-0.52531774	5.613280533	0.0000588
C1orf174	-0.7812078	4.479784797	0.007933818	-1.084774686	5.566408914	0.0000000000
GGH	-0.889902338	5.683677344	0.007995232	-0.833601119	5.952351997	0.0000000257
CISH	-2.951198721	1.595431966	0.008066999	-1.117479737	3.203664807	0.000133155
FAM89B	1.037054684	2.623344981	0.008085112	1.188577757	3.365032629	0.000003
TCIRG1	0.959495946	3.527063891	0.008198987	0.985799792	4.394758748	0.00000144
PHYH	0.750367364	3.333808957	0.008337429	0.892135573	3.280237856	0.000168035
GXYLT1	1.287353352	1.846461161	0.008376416	0.824150736	2.967456401	0.002404513
B3GAT3	0.695988261	3.825893548	0.008491758	0.702397473	4.265077043	0.000204384
CENPI	-1.917009844	2.24991826	0.008573173	-1.506080733	1.965141086	0.001098914
IGF2R	1.070374855	2.260501207	0.008693367	0.785880693	3.482410535	0.001573799
SLC2A8	0.761612151	3.739449766	0.008751467	0.678348795	4.650115371	0.000114911
HCCS	-0.764700544	3.87733666	0.008813181	-0.5171269	4.013818158	0.008922281
ODF2	-0.581436176	4.638835349	0.008846883	-0.591350884	4.716238679	0.0002292
LIX1L	-0.798418807	3.747188621	0.008991103	-0.606871331	4.448909513	0.001149049
ZFP62	1.108686404	2.422650546	0.009076726	0.790167616	3.210059011	0.001011662
NMNAT1	0.843464278	2.801111485	0.009151336	0.971359005	3.240250614	0.000948228
DSCC1	-1.352726378	2.641763436	0.0091605	-0.746389202	3.112205027	0.003924736
LINC02749	2.206653796	0.860477895	0.009583966	2.356250222	1.059017451	0.000755402
HAUS8	-0.716071373	4.225735185	0.009616647	-1.051621346	4.155743428	0.00000196
DPM1	-0.581276511	8.463387764	0.009715681	-0.520606335	7.439817454	0.00000132
EPG5	1.531075318	1.579432887	0.00988813	0.786462528	2.576168614	0.008179316

RRP1B	-0.665087068	4.417645722	0.010080236	-0.664250073	4.58777686	0.000222227
THAP11	-1.213465344	2.789403799	0.010387331	-1.128643346	3.124181305	0.000129471
COPRS	-1.161711792	2.857345916	0.011226602	-0.656468571	4.020515983	0.000861963
SRSF4	-0.860259859	3.644697683	0.011567244	-0.676053449	4.571392485	0.000102263
CYLD	0.798087685	3.52281812	0.011646269	0.772206054	3.081477137	0.002487893
GOLGB1	0.802128713	5.267916426	0.011848061	0.688653322	5.526591403	0.00000305
PARL	-0.680973198	4.034777019	0.012135321	-0.543826694	4.44905729	0.002278879
NOC4L	-0.71015039	4.346057174	0.012473109	-0.801119049	4.31658948	0.0000625
CHPT1	-1.940108991	1.934093006	0.012489877	-1.11521287	2.447038491	0.002744187
PITX1	-2.775044352	1.465603735	0.012541404	-0.734182767	3.038846846	0.005662198
POLR2B	-0.627446559	4.561333245	0.012599468	-0.718959136	5.364003188	0.00000122

Table S4. p53 score in HMCLs

HMCL	*TP53* Sequence	p53 expression	T() Group	Score (DGE-Seq)	Score (microarray)
AMO1	+/+	+ (53kD)	OTHER	0.28888	0.27575
BCN	+/+	+ (53kD)	MAF		0.21285
MDN	+/+	+ (53kD)	CCND1	0.21547	0.24141
MM1S	+/+	+ (53kD)	MAF	0.18426	0.19864
NAN11	+/-	+ (53kD)	MAF	0.22941	0.26673
NAN9	+/+	+ (53kD)	MS		0.30101
NCI-H929	+/+	+ (53kD)	MS	0.28664	0.24100
SBN	+/+	+ (53kD)	OTHER		0.28592
XG3	+/+	+ (53kD)	OTHER		0.27038
XG6	+/+	+ (53kD)	MAF		0.21568
XG7	+/+	+ (53kD)	MS	0.29164	0.27840
XG10	+/+	+ (53kD)	OTHER		0.23446
XG12	+/+	+ (53kD)	MAF		0.22550
XG19	+/+	+ (53kD)	MAF		0.20524
XG21	+/+	+ (53kD)	CCND1		0.33880
XG24	+/+	+ (53kD)	MS		0.24100

HMCL	*TP53* Sequence	p53 expression	T() Group	Score (DGE-Seq)	Score (microarray)
ANBL6	Q331*/-	+ (45kD)	MAF		0.16755
JIM3	R273C/-	+ (53kD)	MS	0.07496	0.14715
JJN3	-/-	-	MAF	0.11734	0.14681
KARSPAS620	C135Y/-	+ (53kD)	CCND1		0.18746
KMM1	C135F/S241F	+ (53kD)	OTHER	0.08203	0.15578
KMS11	-/-	-	MS		0.11309
KMS12PE	R337L/-	+ (53kD)	CCND1		0.17313
L363	S261T/-	+/- (53kD)	MAF	0.12944	0.18491
LP1	E286K/-	+ (53kD)	MS	0.07140	0.12070
NAN1	E180*/-	-	MAF		0.15098
NAN10	A161D/-	+ (53kD)	CCND1		0.19808
NAN3	R248Q/-	+ (53kD)	MS	0.11215	0.16061
NAN6	Del exon 7-9/-	+ (35kD)	MAF	0.07164	0.19310
NAN7	Del exon 11/-	+/- (53kD)	CCND1		0.15486
NAN8	D21Y/-	-	MS	0.07741	0.09782
OPM2	R175H/-	+ (53kD)	MS	0.12086	0.16431
RPMI8226	G285A/-	+ (53kD)	MAF		0.19435
SKMM2	G132T/-	+ (53kD)	CCND1		0.14687
U266	A161T/-	+ (53kD)	CCND1		0.12866
XG1	Y126N/-	+ (53kD)	CCND1		0.14147
XG2	C176Y/R213*	+ (53kD)	OTHER		0.14920
XG5	R282W/-	+ (53kD)	CCND1		0.16889
XG11	C135Y/-	+ (53kD)	CCND1	0.08392	0.15671
XG13	R248Q/-	+ (53kD)	MAF		0.12488
XG14	G266E/-	+ (53kD)	CCND1		0.15208
XG16	A220G/-	+ (53kD)	OTHER		0.16081
XG20	-/-	-	MS		0.12063

Table S5. 13-gene p53 score in 1,105 cancer cell lines

	TP53 status								p value					
	no del & no mut		del &no mut		no del & mut		del & mut		no deletion no mutation versus			deletion versus		mutation versus
	n	median	n	median	n	median	n	median	del	mut	del & mut	mut	del & mut	del & mut
Carcinoma	119	0.2637	39	0.1090	308	0.1529	169	0.1440	<0.0001	<0.0001	<0.0001	0.2283	0.0135	0.2816
Sarc, Gli, Mel	131	0.2774	35	0.2289	76	0.1445	35	0.1344	0.0161	<0.0001	<0.0001	0.0033	0.0028	>0.9999
Leuk, Ly, My	64	0.2489	14	0.1230	56	0.1514	59	0.1238	0.0012	<0.0001	<0.0001	>0.9999	0.48004	0.1627
All cell lines	314	0.2664	88	0.1984	440	0.1516	263	0.1358	<0.0001	<0.0001	<0.0001	0.0005	<0.0001	0.0203

Table S6. p53 score in MYRACLE patients

Disease	Stage	# sample	17p	*TP53*	p53 score
MM	D	3			0.286
MM	D	5			0.213
MM	D	9			0.219
MM	D	10	del17p		0.223
MM	D	13	del17p		0.224
MM	D	14	del17p		0.183
MM	D	15			0.243
MM	D	17			0.271
MM	D	18	del17p	H193R	0.163
MM	R	31			0.234
MM	P	33			0.261
MM	P	34			0.179
MM	R	35			0.258
MM	R	38			0.175
MM	R	39			0.253
MM	R	41	del17p		0.216
MM	R	42			0.226
MM	R	43			0.232
MM	R	51			0.224
MM	R	56			0.226
MM	R	58			0.216
MM	R	62	del17p		0.231
MM	R	63			0.264
MM	R	64			0.201
MM	R	65	del17p		0.212
MM	R	72			0.135
MM	R	73			0.199
MM	R	74			0.224
MM	R	75			0.235
MM	R	76			0.313
pPCL	D	77			0.283
sPCL	R	78	del17p	S211R	0.138
sPCL	R	79	del17p	del123-133	0.149
sPCL	R	80	del17p	M133T	0.163
sPCL	R	81	del17p	A158V	0.173
sPCL	R	82	del17p	V272M	0.198
sPCL	R	83			0.261
sPCL	R	84	del17p	R213STOP	0.104

Table S7. LD_{50} values of melphalan, nutlin3a and BH3 mimetics in control and *TP53*$^{-/-}$ clones

	Melphalan LD_{50} (μM)	Nutlin3a LD_{50} (μM)	S63845 LD_{50} (nM)	Venetoclax LD_{50} (μM)	A1155463 LD_{50} (μM)
NCI-H929 *TP53*$^{+/+}$#1	13±3	2.0±0.3	6±2	4.7±0.4	>10
NCI-H929 *TP53*$^{+/+}$#2	9±2	1.8±0.3	6±2	5.0±0.7	>10
NCI-H929 *TP53*$^{+/+}$#3	12±2	2.0±0.3	6±2	4.8±0.6	>10
NCI-H929 *TP53*$^{-/-}$#1	14±2	>10	17±4	5.3±0.4	>10
NCI-H929 *TP53*$^{-/-}$#2	15±3	>10	33±11	5.5±0.6	>10
NCI-H929 *TP53*$^{-/-}$#3	21±3	>10	71±37	5.1±0.1	>10
Fold TP53$^{-/-}$*/TP53*$^{+/+}$	*1.47*	*>5*	*6.7*	*1.10*	
XG7 *TP53*$^{+/+}$#1	15±4	1.8±0.3	24±11	8.0±0.5	>10
XG7 *TP53*$^{+/+}$#2	27±8	1.8±0.5	48±10	9.0±0.5	>10
XG7 *TP53*$^{+/+}$#3	14±3	1.8±0.5	14±4	8.0±0.5	>10
XG7 *TP53*$^{-/-}$#1	28±3	>10	140±30	12.0±2.5	>10
XG7 *TP53*$^{-/-}$#2	30±3	>10	117±29	9.0±0.5	>10
XG7 *TP53*$^{-/-}$#3	27±3	>10	157±11	9.0±0.5	>10
Fold TP53$^{-/-}$*/TP53*$^{+/+}$	*1.52*	*>5*	*4.8*	*1.20*	
JIM3 *TP53*$^{-/mut}$#1	47±5	>10	94±4	14±2	>10
JIM3 *TP53*$^{-/mut}$#2	49±2	>10	105±3	12±1	>10
JIM3 *TP53*$^{-/mut}$#3	48±3	>10	112±2	17±3	>10
JIM3 *TP53*$^{-/-}$#1	46±6	>10	80±6	9±1	>10
JIM3 *TP53*$^{-/-}$#2	46±5	>10	90±3	18±7	>10
JIM3 *TP53*$^{-/-}$#3	45±6	>10	57±3	17±7	>10
Fold TP53$^{-/-}$*/TP53*$^{-/mut}$	*0.95*	*1.0*	*0.72*	*0.95*	
NAN3 *TP53*$^{-/mut}$#1	13±2	>10	46±14	6±1	>10
NAN3 *TP53*$^{-/mut}$#2	17±2	>10	46±11	6±2	>10
NAN3 *TP53*$^{-/mut}$#3	12±3	>10	33±9	5±1	>10
NAN3 *TP53*$^{-/-}$#1	13±3	>10	28±5	5±1	>10
NAN3 *TP53*$^{-/-}$#2	13±3	>10	27±8	6±1	>10
NAN3 *TP53*$^{-/-}$#3	14±3	>10	37±8	6±1	>10
Fold TP53$^{-/-}$*/TP53*$^{-/mut}$	*0.95*	*1.0*	*0.73*	*1.0*	

Table S8. LD_{50} values of BH3 mimetics in HMCLs

	TP53 status	Sequence	Group	S63845 nM	Venetoclax nM	A1155463 nM
MDN	Wild type	+/+	CCND1	40	3	6000
BCN		+/+	MAF	120	4000	7000
MM1S		+/+	MAF	200	4000	10
NAN11		+/-	MAF	10	4000	5500
XG6		+/+	MAF	25	3000	7000
NAN9		+/+	MS	12	10000	>10000
NCI-H929		+/+	MS	6	5000	>10000
XG7		+/+	MS	40	5000	>5000
AMO1		+/+	OTHER	3	3000	>10000
XG10		+/+	OTHER	9	3400	7500
XG3		+/+	OTHER	10	3500	6500
KARSPAS620	Abnormal	C135Y/-	CCND1	500	5	3000
KMS12PE		R337L/-	CCND1	200	15	>10000
NAN10		A161D/-	CCND1	20	300	6000
NAN7		Del exon 11/-	CCND1	9	20	3000
U266		A161T/-	CCND1	340	8000	>10000
XG1		Y126N/-	CCND1	16	7000	>10000
XG11		C135Y/-	CCND1	200	2500	10000
XG5		R282W/-	CCND1	360	5	>10000
ANBL6		Q331*/-	MAF	500	5500	6000
JJN3		-/-	MAF	75	1500	>10000
L363		S261T/-	MAF	15	3000	>10000
NAN1		E180*/-	MAF	10	800	7000
NAN6		Del exon 7-9/-	MAF	5	2800	6000
JIM3		R273C/-	MS	300	10000	>10000
LP1		E286K/-	MS	220	6000	>10000
NAN3		R248Q/-	MS	45	5000	>10000
NAN8		D21Y/-	MS	350	3200	>10000
OPM2		R175H/-	MS	30	5000	>10000
KMM1		C135F, S241F	OTHER	80	5000	>10000
XG2		C176Y, R213*	OTHER	18	3000	>10000

Table S9. *BAK1* and *BAX* genomic sequences in CRISPR/Cas9 clones

Clones	Genomic sequence	Location
NCI-H929 *BAK1*$^{-/-}$#1	ins1(T)	chr6:33,574,144
	ins1(T)	chr6:33,574,144
NCI-H929 *BAK1*$^{-/-}$#2	ins1(T)	chr6:33,574,144
	ins1(T)	chr6:33,574,144
NCI-H929 *BAK1*$^{-/-}$#3	ins1(T)	chr6:33,574,144
	del 8(ACGTCTAC)	chr6:33,574,136 143
NCI-H929 *BAX*$^{-/-}$#1	complex insertion and deletion	chr19:48,956,286
	insertion and deletion	chr19:48,956,281
NCI-H929 *BAX*$^{-/-}$#2	ins1(T)	chr19:48,956,295
	ins1(T)	chr19:48,956,295
NCI-H929 *BAX*$^{-/-}$#3	del11 (GTCGCCCTTTT)	chr19:48,956,295-305
	insertion and deletion	chr19:48,956,294

Table S10. Characteristics of patient samples analyzed using scRNAseq

MM		FISH				scRNASeq			cDNA seq	BH3 m combo
#	stage	t(4,14)	t(11,14)	1q21	del17p13	MC	1q	del17p	*TP53*	cell death (%)
2	D			dup 88%		MF	1q gain		nd	94
3	D	t(4,14)	nd		nd	MS		del17p 10%	wt	73
5	D		t(11,14)	dup 72%		CD-1	1q gain		wt	99
8	D				del17p 79%	HY		del17p 90%	wt	44
10	D				del17p 96%	HY		del17p 100%	wt	74
12	D		nd	amp 100%		LB	1q gain		nd	89
13	D				del17p 88%	HY		del17p 100%	wt	2
15	D		t(11,14)	dup 88%		CD-1	1q gain		nd	59
31	D		t(11,14)	dup 100%		CD-1	1q gain		wt	95
32	D	t(4,14)		dup 88%	del17p 35%	MS	1q gain	del17p 30%	nd	84
33	R			dup 20% amp 76%		MF	1q gain		wt	38
39	R	t(4,14)		nd	nd	MS		del17p 10%	wt	64
41	R	t(4,14)		dup 34% amp 38%	del17p 50%	MS	1q gain	del17p 80%	wt	26
42	R			amp 98%		UN	1q gain		wt	70
43	R	t(4,14)		dup 8% amp 90%		MS	1q gain		wt	65
44	R			dup 26%		HY	1q gain		nd	77
45	R	nd	nd	nd		HY	1q gain		wt	22
48	R			dup 83% amp 13%		HY	1q gain		nd	73
49	R				del17p 71%	HY		del17p 65%	nd	29
50	R	nd				UN			nd	59
52	R			nd	nd	LB	1q gain		nd	53
55	R	t(4,14)		nd	nd	MS	1q gain		nd	57
59	R		t(11,14)		nd	CD-2			nd	63
71	R		nd	dup 39%		UN			nd	71

Figure S1. Expression of the 17 genes differentially expressed between *TP53*$^{+/+}$ and *TP53*$^{-/-}$ cells in both NCI-H929 and XG7.

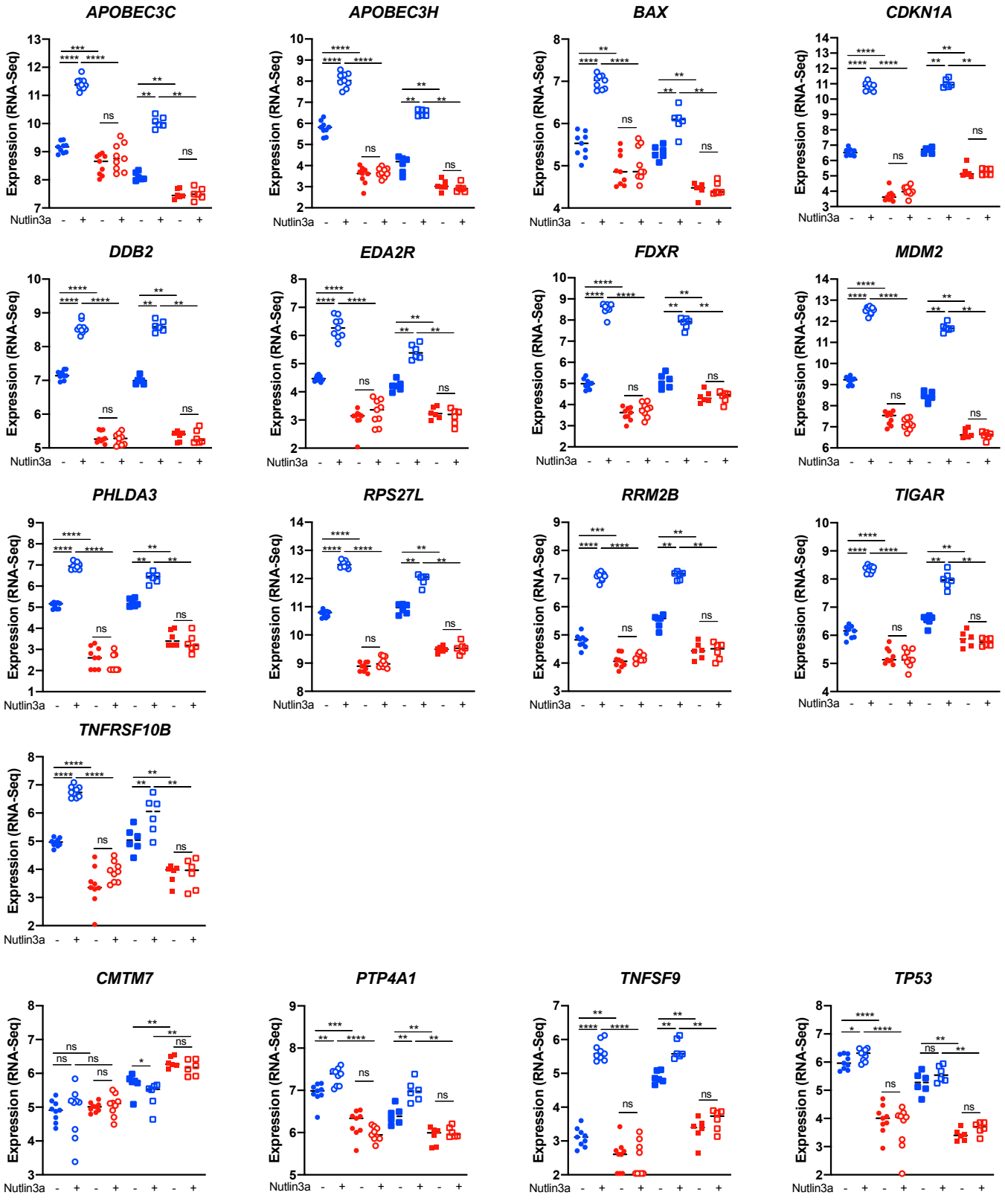

○ NCI-H929 — Clones *TP53*$^{+/+}$

□ XG7 — Clones *TP53*$^{-/-}$

Figure S2. p53 score in HMCLs according to *TP53* status and 14q32 translocation and in 1,105 cancer cell lines

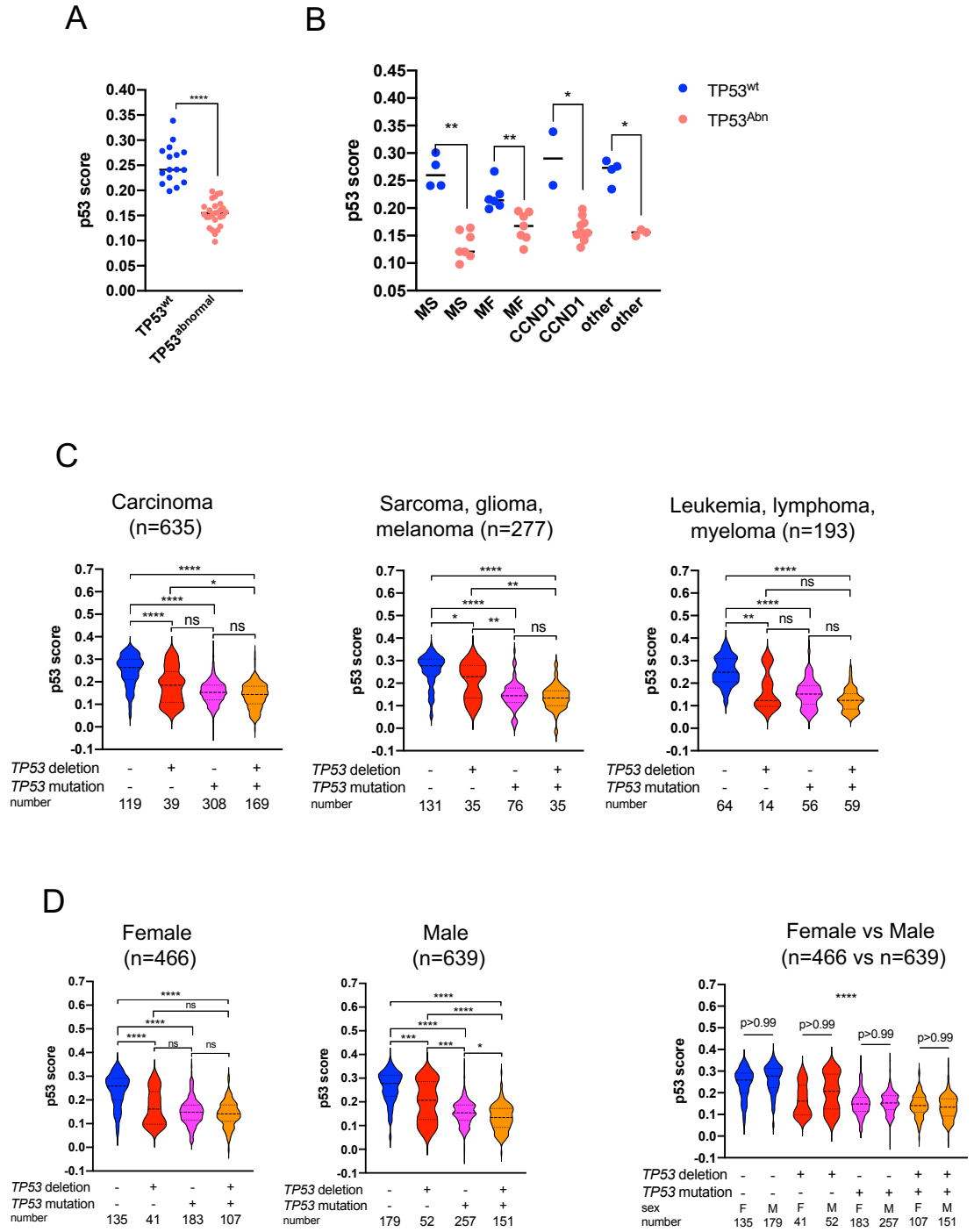

Figure S3. p53 score in CASSIOPEA and MMRF-coMMpass cohorts

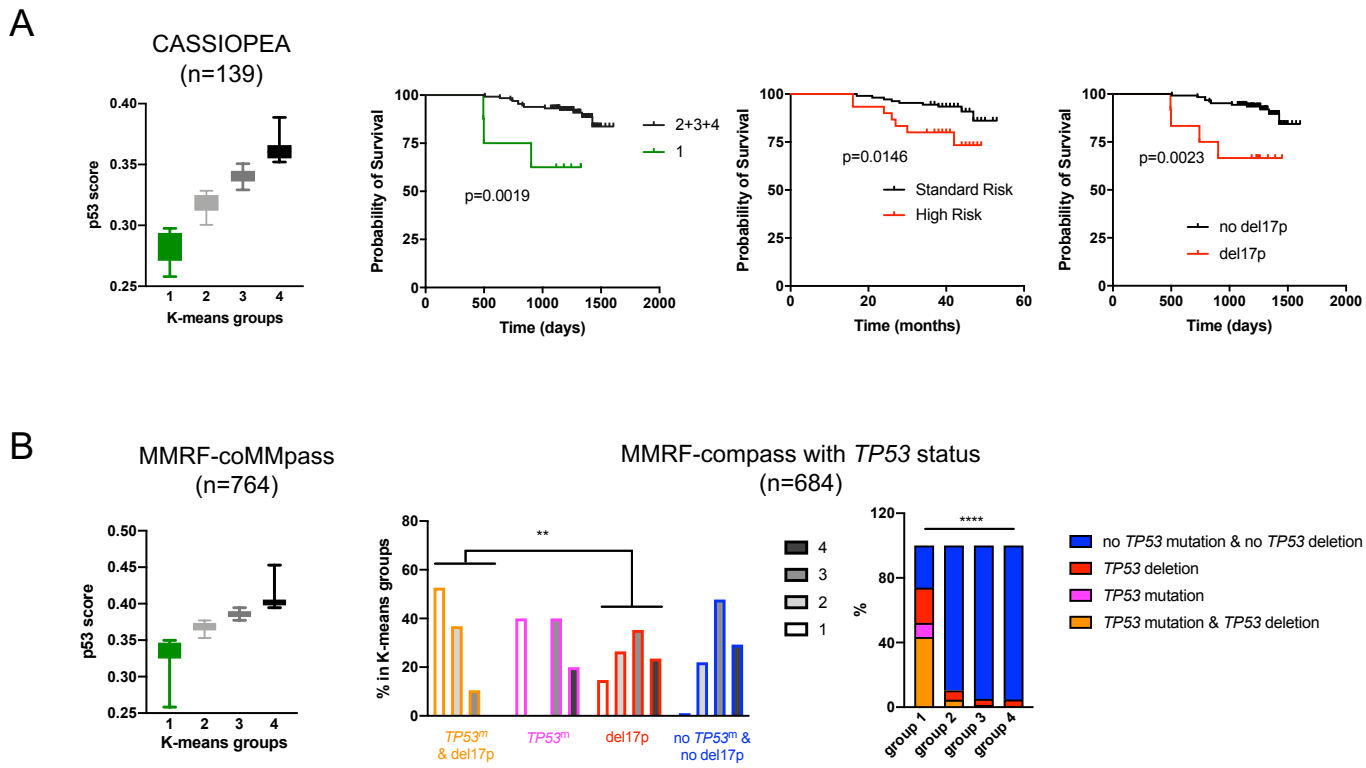

Figure S4. Expression of the 10 genes involved in Li-Fraumeni score in NCI-H929 and XG7 clones

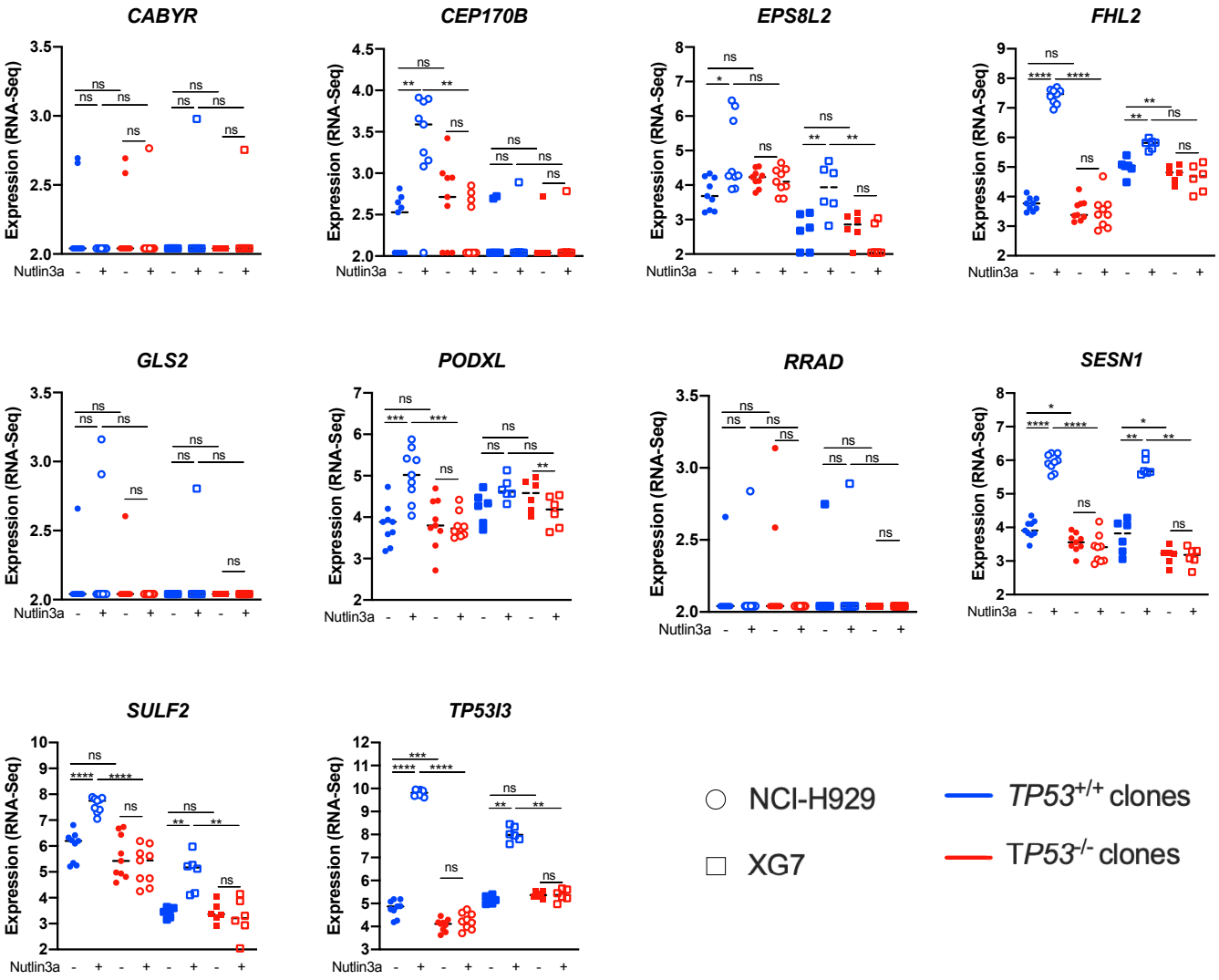

Figure S5. Lack of efficacy of Li-Fraumeni score to discriminate clones, 1,105 cancer cell lines and patient samples according to *TP53* status

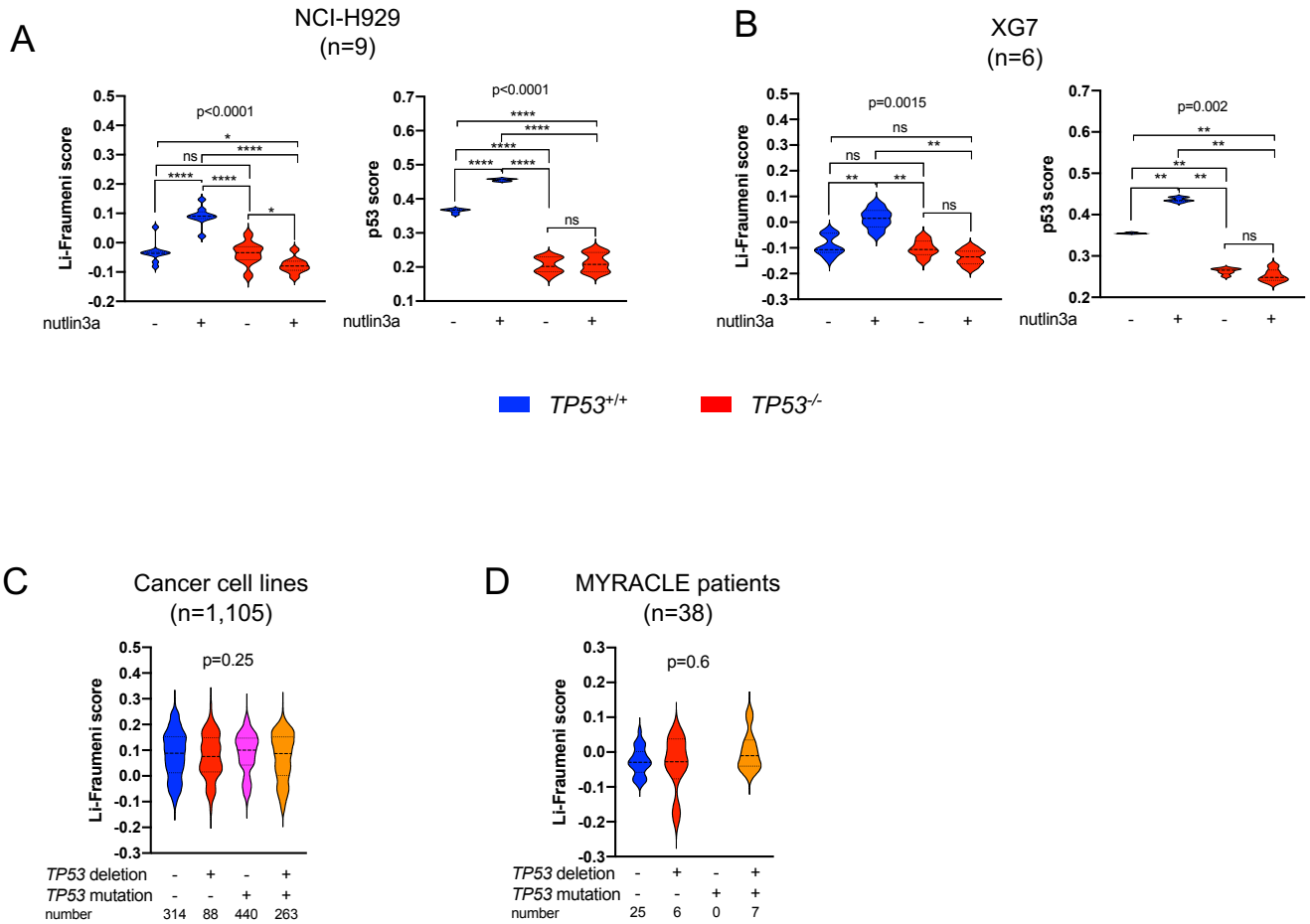

Figure S6. BCL2 family expression profile of clones and HMCLs according to *TP53* status.

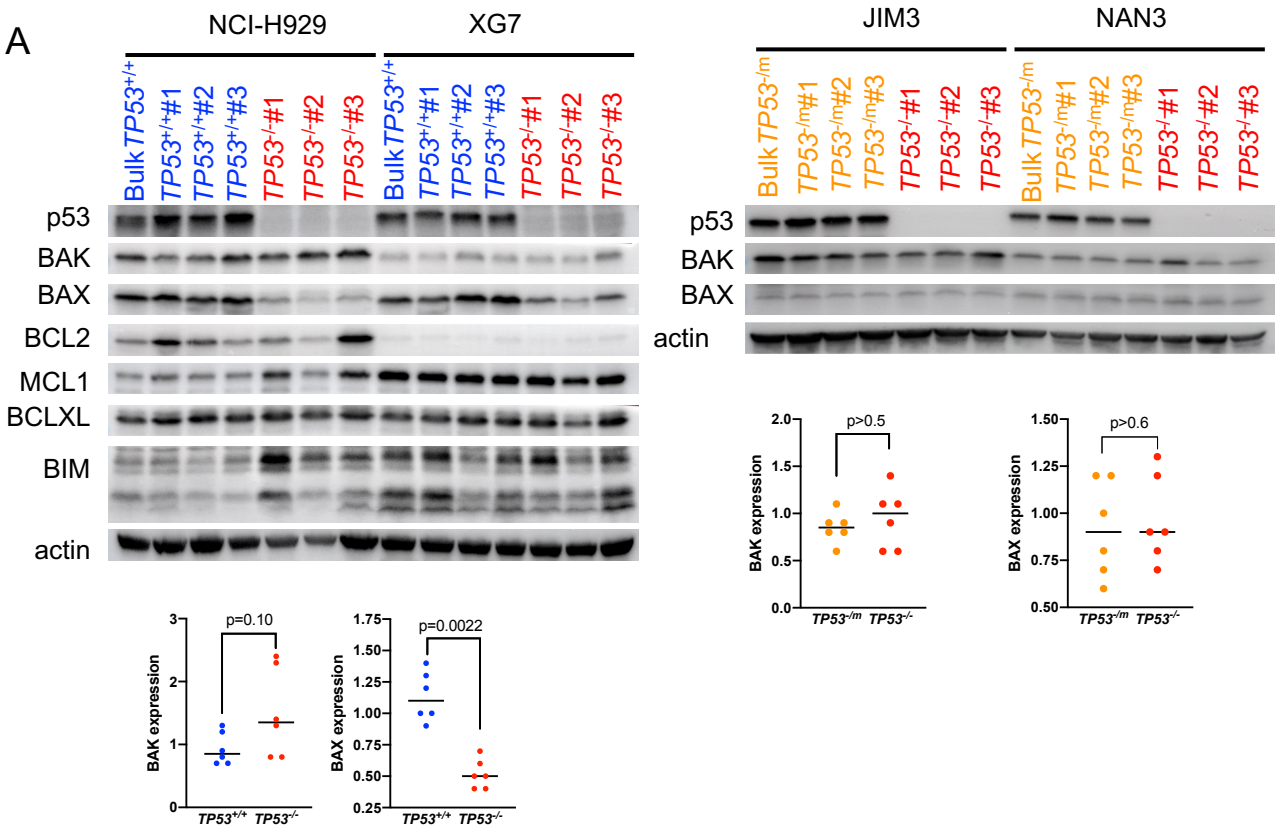

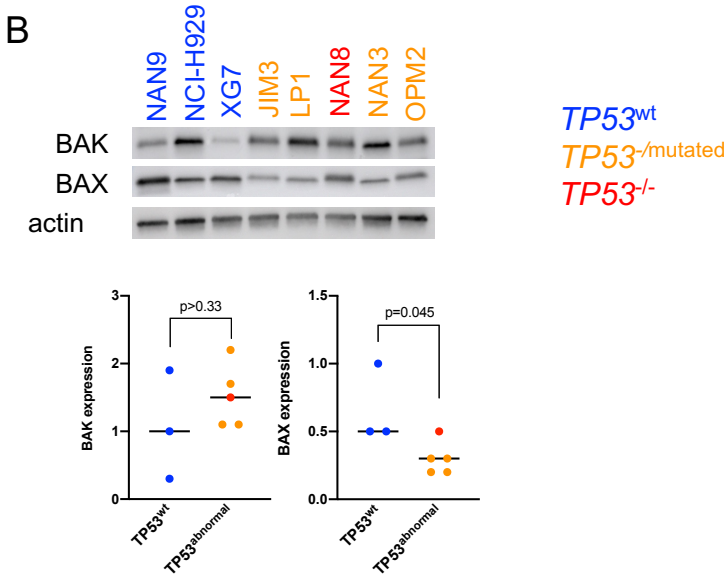

Figure S7 Lack of impact of *TP53* silencing on global mitochondrial priming in NCI-H929 and XG7

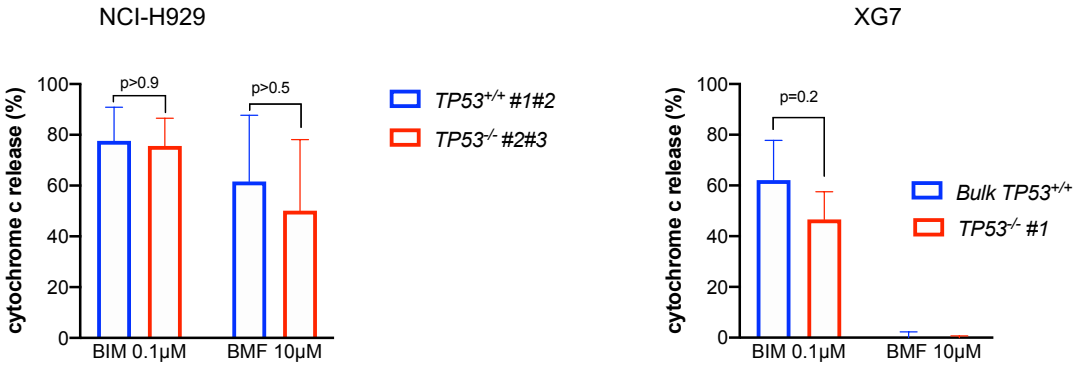

Figure S8. Role of BAK and BAX in the response to S63845

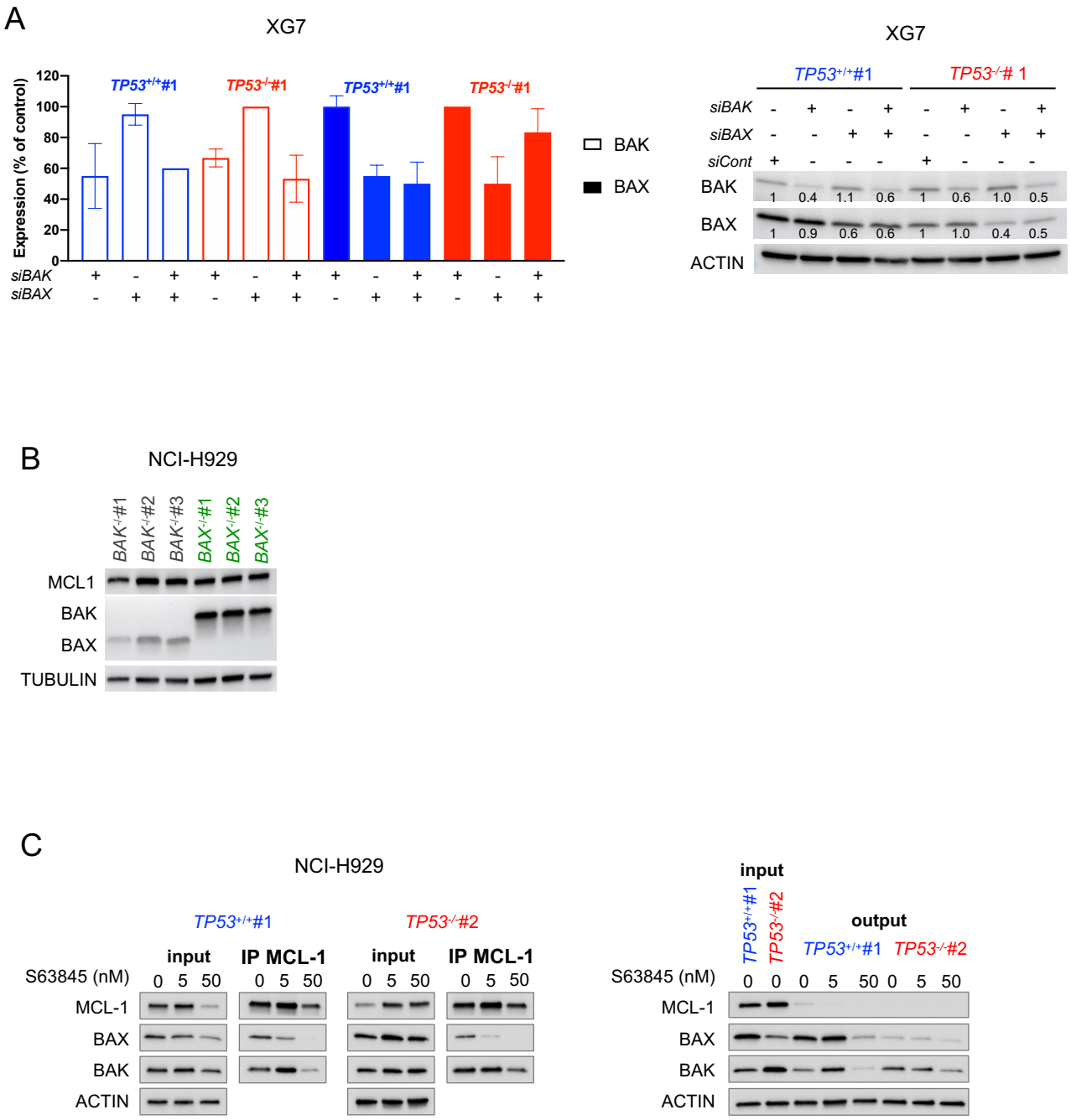

Figure S9. Lack of correlation between S63845 response and BCL2 family members in clones and HMCLs

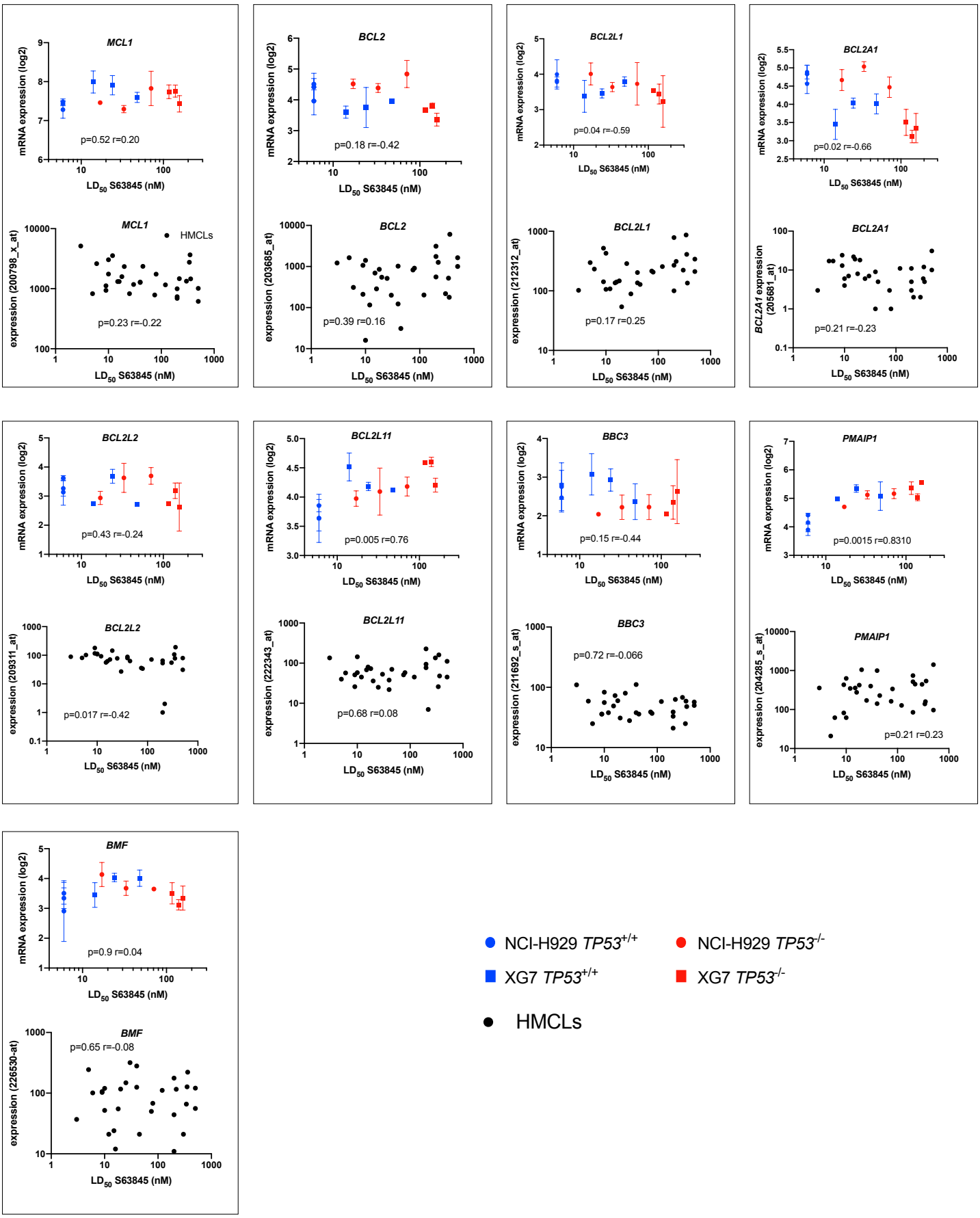

Figure S10. Impact of t(11;14) in the response to BH3 mimetics combination

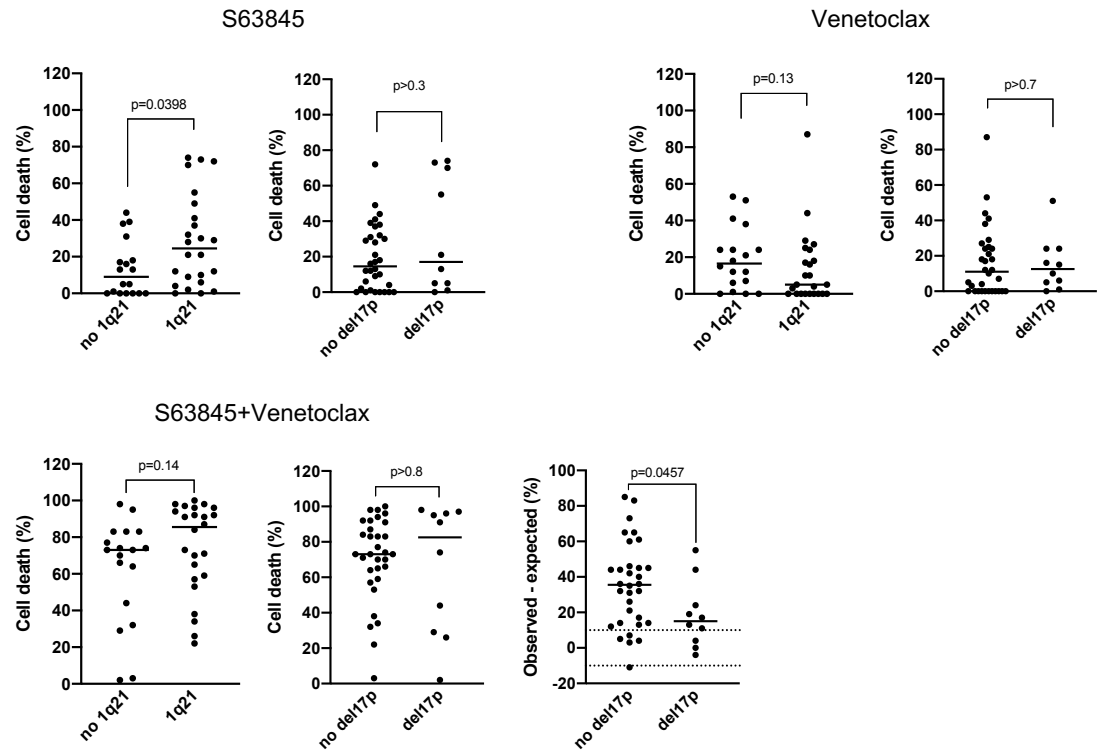

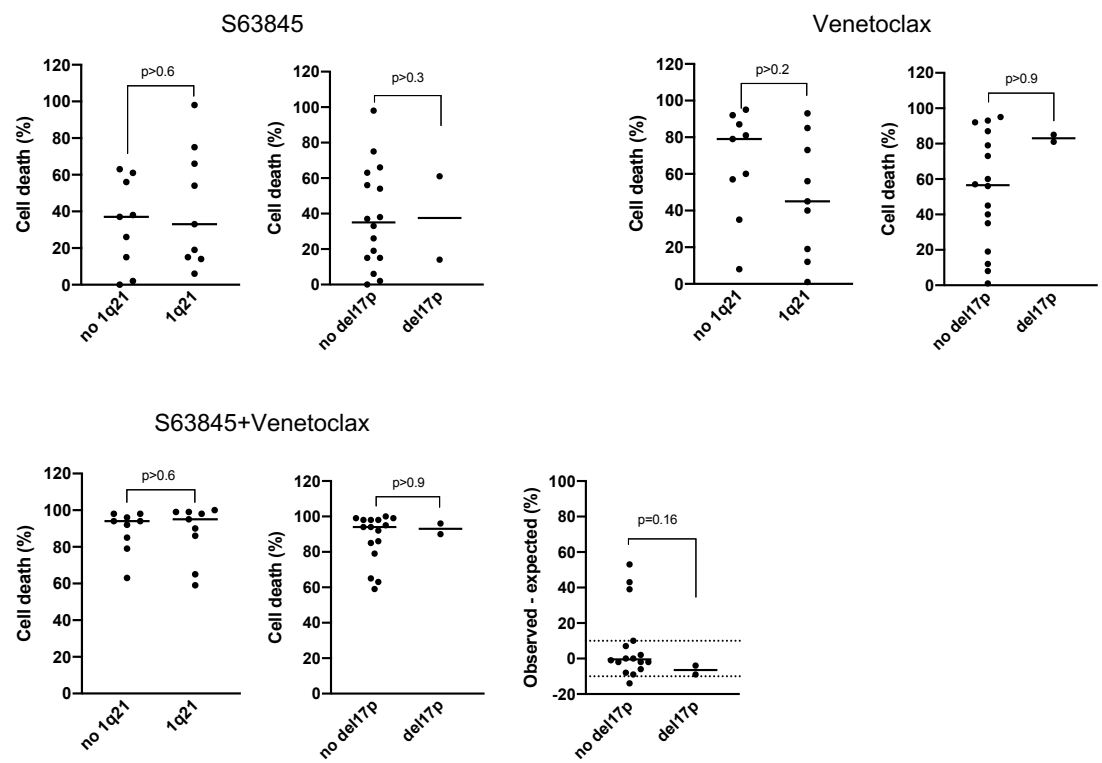

Figure S11. Molecular classification of patients' samples

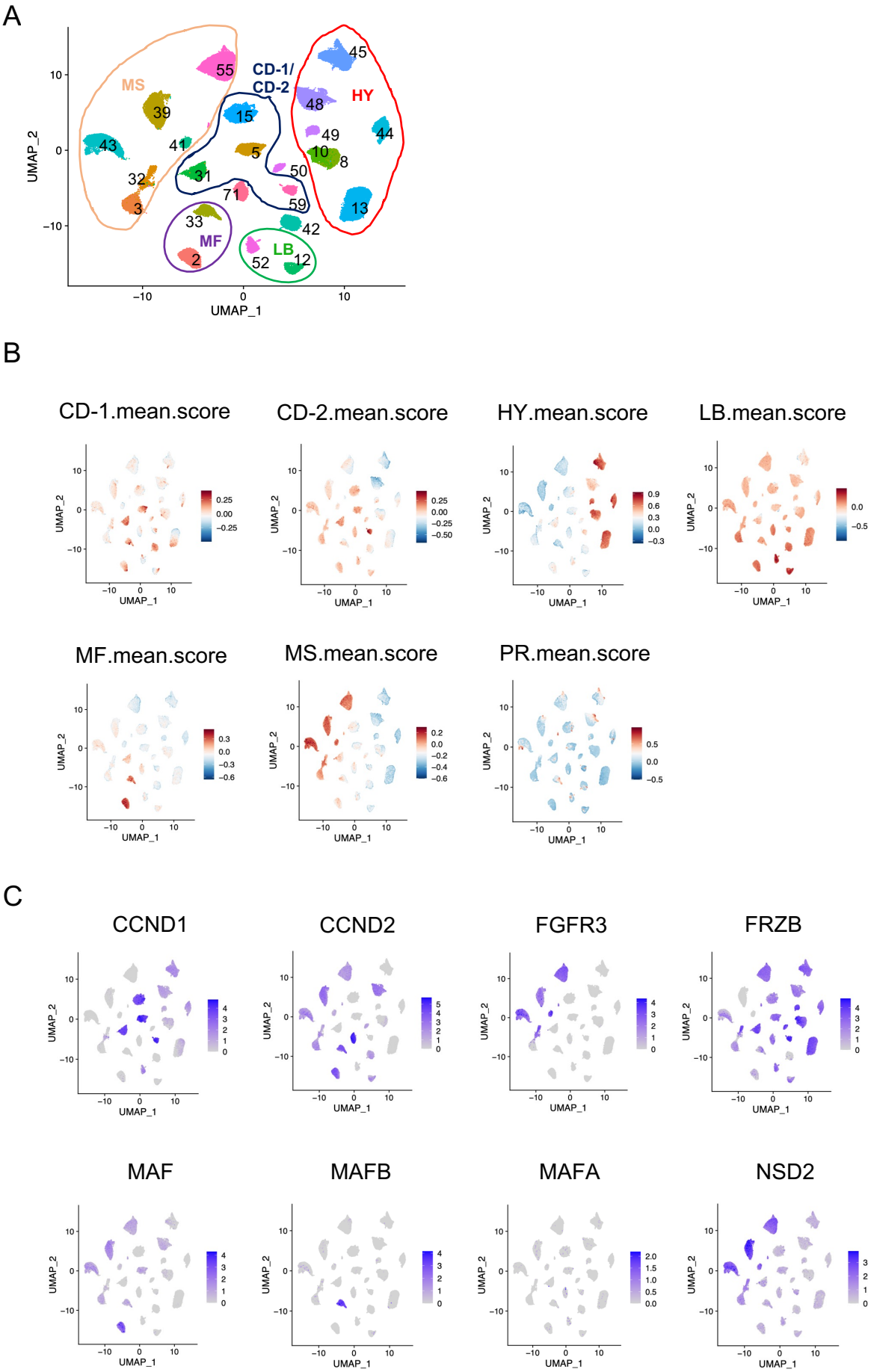

Figure S12. BH3 mimetics induced changes in p53 score at single cell level

Samples with p53 score changes in no del17p clusters

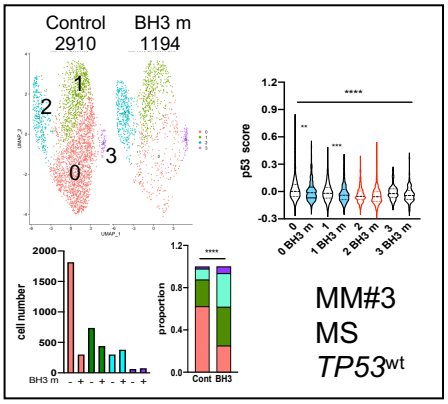

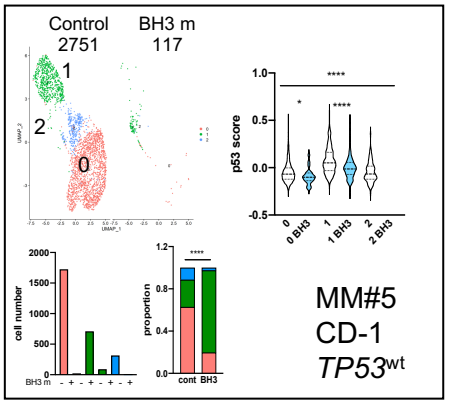

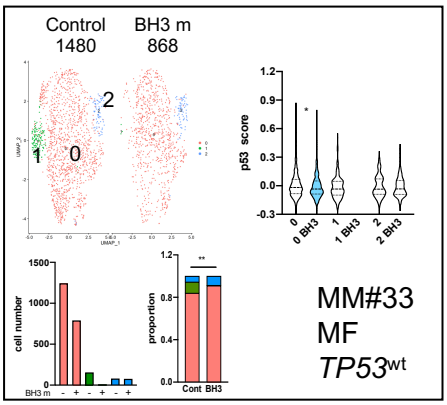

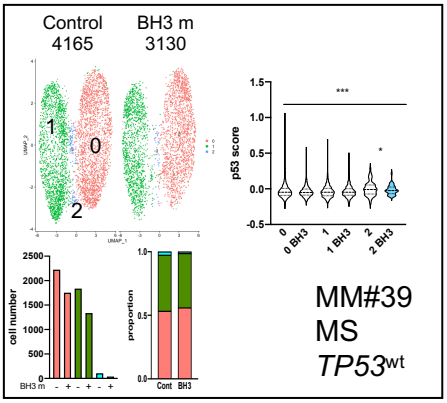

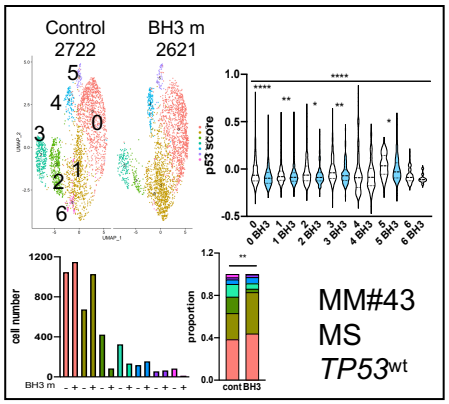

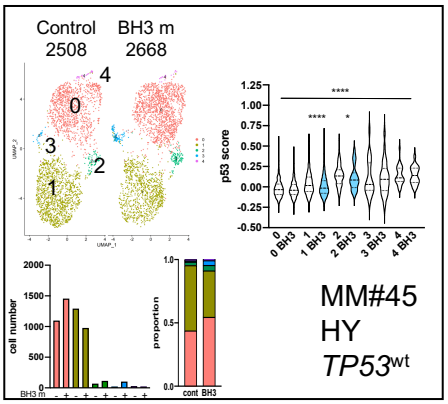

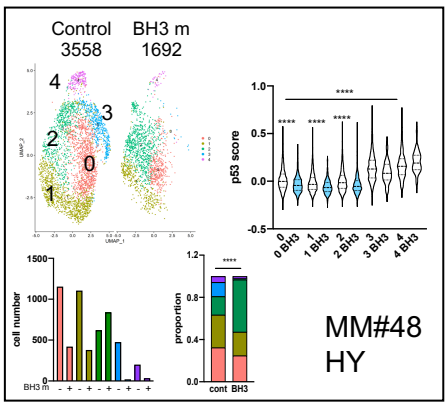

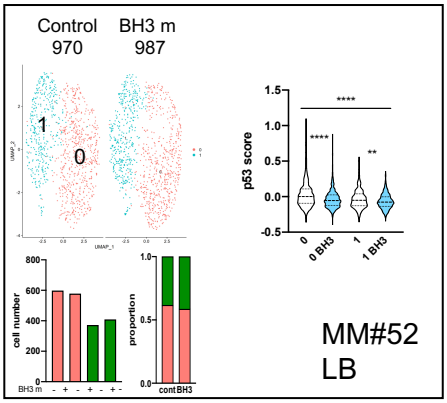

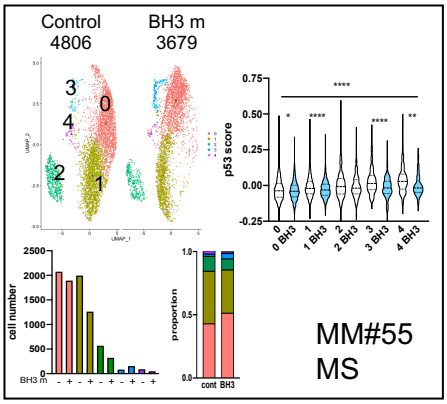

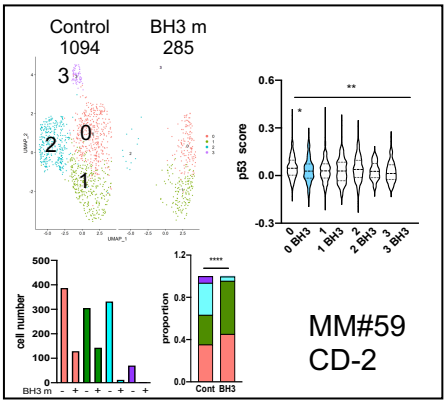

Violin plot legend

p53 score treated = control

p53 score treated < control

p53 score treated > control

no del17p

del17p

Figure S12. BH3 mimetics induced changes in p53 score at single cell level (p2)

Samples with p53 score changes in del17p clusters

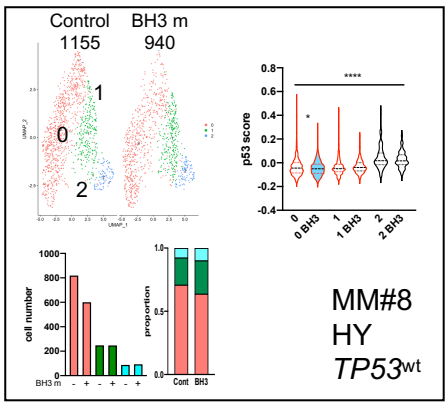

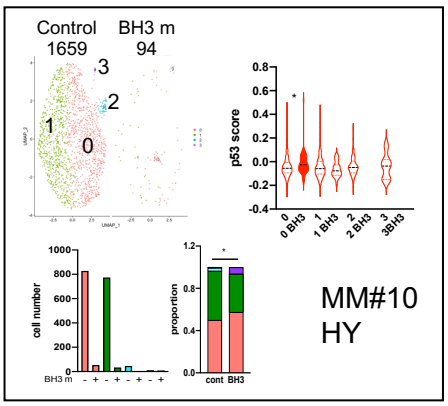

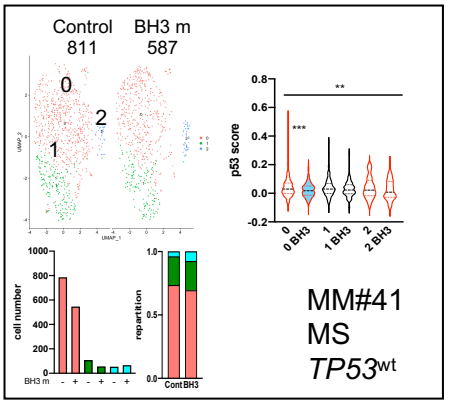

Violin plot legend

p53 score treated = control

p53 score treated < control

p53 score treated > control

no del17p

del17p

Figure S12. BH3 mimetics induced changes in p53 score at single cell level (p3)

Samples without p53 score changes

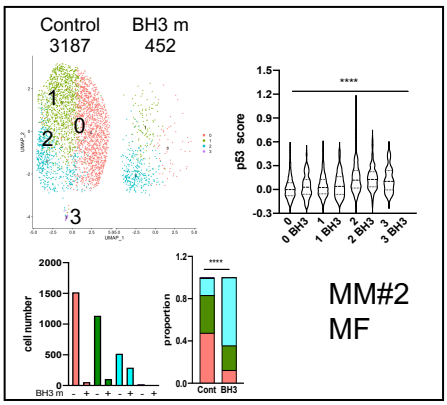

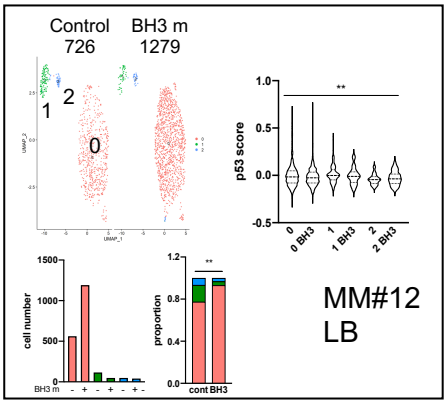

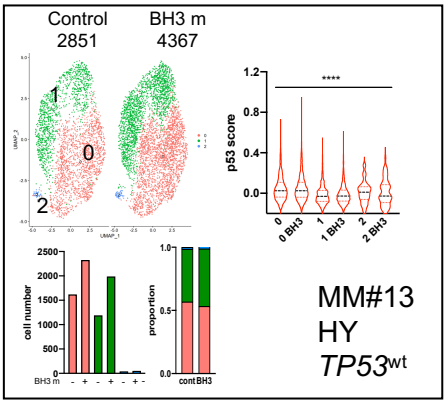

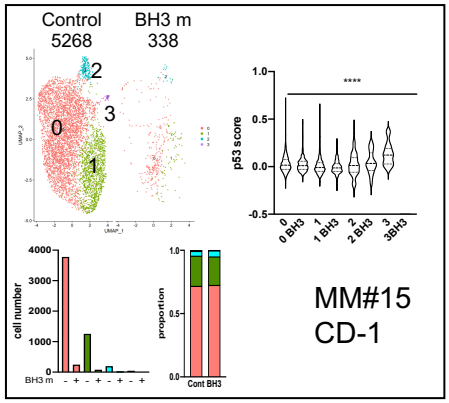

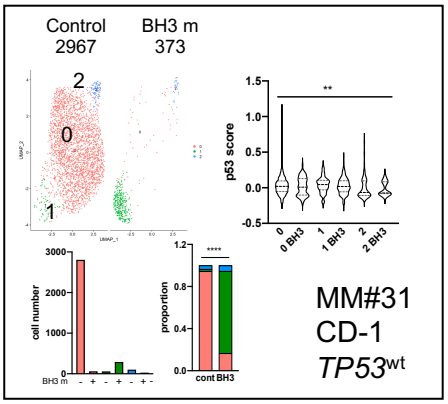

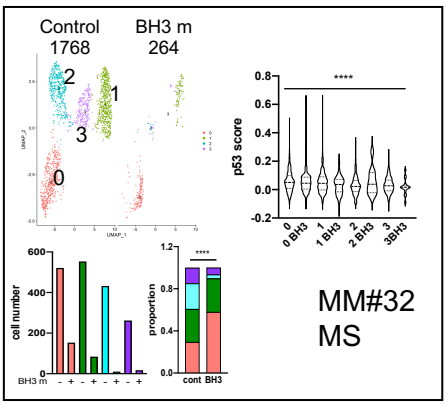

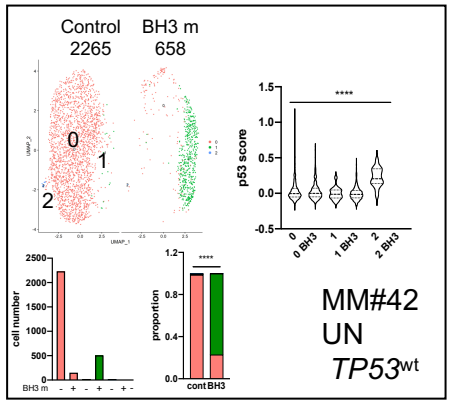

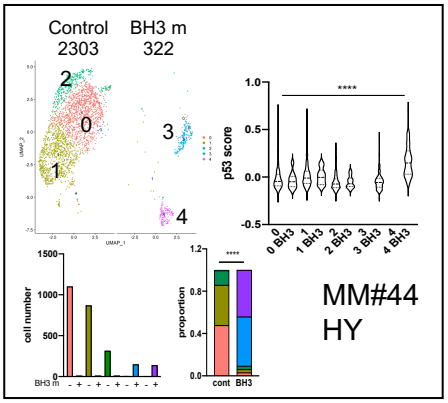

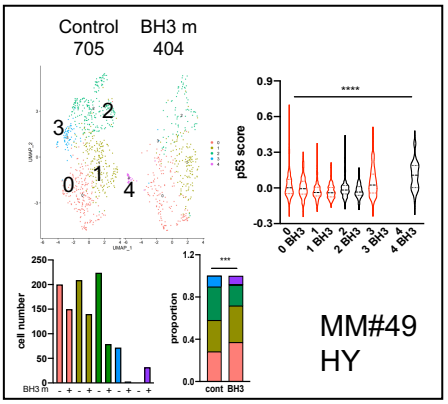

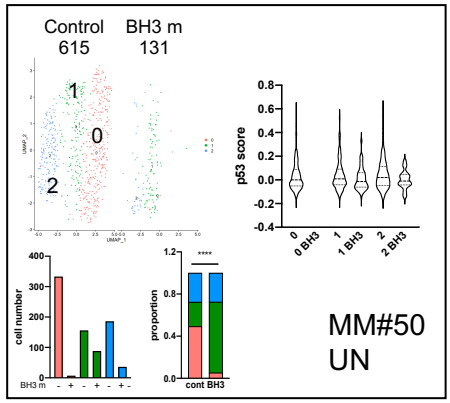

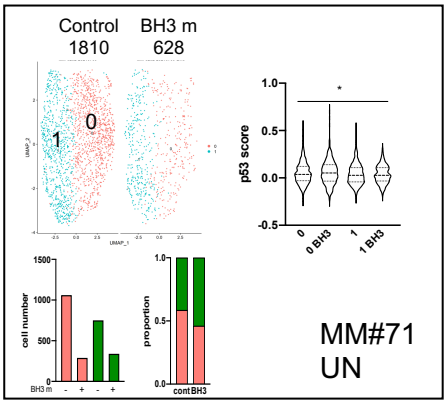

Violin plot legend

p53 score treated = control

p53 score treated < control

p53 score treated > control

no del17p

del17p